National Library of Canada

Acquisitions and Bibliographic Services Branch

395 Wellington Street
Ottawa, Ontario
K1A 0N4

Bibliothèque nationale du Canada

Direction des acquisitions et des services bibliographiques

395, rue Wellington
Ottawa (Ontario)
K1A 0N4

Your file Votre référence

Our file Notre référence

NOTICE

The quality of this microform is heavily dependent upon the quality of the original thesis submitted for microfilming. Every effort has been made to ensure the highest quality of reproduction possible.

If pages are missing, contact the university which granted the degree.

Some pages may have indistinct print especially if the original pages were typed with a poor typewriter ribbon or if the university sent us an inferior photocopy.

AVIS

La qualité de cette microforme dépend grandement de la qualité de la thèse soumise au microfilmage. Nous avons tout fait pour assurer une qualité supérieure de reproduction.

S'il manque des pages, veuillez communiquer avec l'université qui a conféré le grade.

La qualité d'impression de certaines pages peut laisser à désirer, surtout si les pages originales ont été dactylographiées à l'aide d'un ruban usé ou si l'université nous a fait parvenir une photocopie de qualité inférieure.

Canada

PETROLOGY AND GEOCHEMISTRY OF TIMISKAMING GROUP SEDIMENTARY ROCKS, KIRKLAND LAKE AREA, ABITIBI GREENSTONE BELT

MARC IAN LEGAULT

Thesis submitted to
the School of Graduate Studies and Research
in partial fulfillment of the requirements for the M.Sc.
degree in Geology

Ottawa-Carleton Geoscience Centre and
Université d'Ottawa/University of Ottawa

ISBN 0-315-89668-X

Canada

UNIVERSITÉ D'OTTAWA
UNIVERSITY OF OTTAWA

ABSTRACT

The Timiskaming Group is a late Archaean syn-tectonic lithological unit which lies unconformably on greenstone-belt volcanic rocks and consists of an alluvial-fluvial assemblage intercalated with alkalic volcanic rocks and a turbidite assemblage. The alluvial-fluvial assemblage is composed mostly of clast-supported conglomerates with interbedded cross-bedded arenites and lenses of argillite whereas the turbidite assemblage comprises interbedded graywackes and shales associated with minor matrix-supported conglomerates. Detailed study of these sedimentary rocks included measurements of K, U and Th contents using a γ-ray spectrometer, point counting of sandstones and conglomerates, and major, minor, and rare-earth element (REE) analysis.

Petrographic and geochemical studies have identified two distinct turbidite units: a turbidite north and a turbidite south of the Larder Lake - Cadillac Fault (LLCF). The fine-grained sedimentary rocks of the alluvial-fluvial assemblage and turbidite north unit have similar mineralogical and chemical compositions such as high SiO_2, U, Th and total REE. The turbidite south unit has high $Fe_2O_{3(tot.)}$, MgO, TiO_2, Cr and Ni.

Petrographic and geochemical examinations of clasts from the alluvial-fluvial assemblage indicate that the clasts are mostly igneous rocks with minor sedimentary rocks. Four major types of igneous clasts are recognized: calc-alkaline porphyries, trachytes, trondhjemites and tholeiitic basalts. Calc-alkaline porphyry clasts are related to diorite/quartz diorite intrusions that occur north of the LLCF. Trachytes and associated porphyry intrusions were derived from Timiskaming alkalic rocks. Trondhjemite clasts are similar to the marginal phases of the Round Lake batholith whereas the tholeiitic basalts are similar to underlying greenstone belt volcanic

rocks. The increase in tholeiitic basalt and porphyry clasts associated with the decrease of andesite clasts up the stratigraphic section suggest the alluvial-fluvial assemblage was mostly derived from a dissected arc.

Results indicate that the turbidite south unit is the oldest unit of the Timiskaming Group and the age of sedimentation is bracketed between 2685 Ma and 2700 Ma. It was derived from an undissected arc terrane uplifted during accretion. Sources for the turbidite south unit estimated from chemical compositions of shales are 12% rhyolite, 18% komatiite and 70% andesite. This setting is in contrast with the proposed setting for the alluvial-fluvial assemblage and turbidite north unit. They are inferred to have been derived from a dissected island arc after accretion, but before the unroofing of K-rich intrusions, which are presently extensively exposed. A source comprising 60% calc-alkaline porphyries, 20% trachytes and 20% tholeiitic basalts is estimated for the turbidite north unit from the chemical composition of shales. The different tectonic settings for the north and south units is consistent with the LLCF representing a suture zone. The distribution of trachyte clasts in the alluvial-fluvial assemblage only close to the LLCF suggests that displacement along the fault may have created conduits for alkaline magmas. Similar lithology of conglomerates north and south of the LLCF suggests that the alluvial-fluvial assemblage was deposited in a pull-apart basin after juxtaposition of two tectonic blocks along the fault between 2685 and 2677 Ma. The turbidite north unit may be of similar age or younger. The proximity of the source rocks suggest that only limited strike-slip movement occurred during and after deposition of the alluvial-fluvial assemblage.

SOMMAIRE

Le groupe du Timiskaming de la région de Kirkland Lake es t en discordance avec les roches volcaniques de la ceinture de roches vertes sous-jacente et comprend une unité alluvionnaire-fluviatile intercalée avec des roches volcaniques alcalines et une unité turbiditique. L'unité alluvionnaire-fluviatile est composée de conglomérats interdigités avec des grès à stratifications entre-croisés et des lentilles d'argilite tandis que l'unité turbiditique comprend des wackes et des shales interdigités avec des conglomérats mineurs. Une étude détaillée de ces roches sédimentaires comprenait l'analyse de K, U et Th à l'aide de la spectrométrie à rayons gamma, la pétrographie et le comptage de points des grès et des conglomérats, et l'analyse des éléments majeurs, mineurs et de terre rare. Les observations pétrographiques et chimiques ont identifiées deux séquences de turbidite distinctes: une unité turbiditique au nord et une au sud de la faille Larder Lake - Cadillac (FLLC). Les roches sédimentaires à grains fins des unités alluvionnaire-fluviatile et turbidite nord ont des compositions similaires et les deux sont caractérisées par des concentrations élevées de SiO_2, U, Th et éléments de terre rare. L'unité de turbidite sud a de hautes teneurs en $Fe_2O_{3(tot.)}$, MgO, TiO_2, Cr et Ni.

Nos observations pétrographiques et géochimiques sur les galets de l'unité alluvionnaire-fluviatile indiquent que la plupart des galets proviennent de roches ignées avec une faible contribution des roches sédimentaires. Quatre types majeurs de galets de roches ignées furent identifiés: porphyres calco-alcalins, roches volcaniques alcalines, trondhjémites et roches volcaniques tholéiitiques. Les galets de porphyre calco-alcalin sont reliés aux intrusions de diorite/diorite quartzeuze qui sont présents au nord de la FLLC. Les roches volcaniques alcalines et les intrusions porphyritiques associés proviennent des roches alcalines du Timiskaming. Les

galets de trondhjémite ressemblent à la phase marginale du batholite de Round Lake tandis que les roches volcaniques tholéiitiques sont semblables aux roches volcaniques de la ceinture de roches vertes sous-jacente. L'augmentation des galets de roches volcaniques tholéiitiques et de porphyres avec la diminution de galets d'andésite en montant la section stratigraphique suggèrent que l'unité alluvionnaire-fluviatile provient surtout d'un arc disséqué.

Les résultats indiquent que l'unité de turbidite sud est l'unité la plus vieille du groupe de Timiskaming (2685 à 2700 Ma) et qu'elle provient d'un arc non-disséqué qui fut soulevé pendant l'accrétion d'arcs. La source de l'unité sud est estimée à 12% rhyolite, 18% komatiite et 70% andésite d'après les compositions chimiques du shale. Cet environnement est très différent de celui proposé pour les unités alluvionnaire-fluviatile et turbidite nord. Ceux-ci proviendraient plutôt d'un arc insulaire disséqué après l'accrétion, mais avant l'érosion d'intrusions riche en K qui sont présentement exposés à travers la région. Une source comprenant 60% porphyres calco-alcalins, 20% trachytes et 20% basaltes tholéiitiques est indiquée pour l'unité de turbidite nord d'après les compositions chimiques du shale. Les différents environments de déposition pour les unités nord et sud sont en accord avec l'hypothèse que la FLLC représente une zone de collage. La distribution des galets alcalins dans l'unité alluvionnaire-fluviatile près de la FLLC seulement suggère que le déplacement de la faille aurait pu créer des conduits pour le magma alcalin. Des conglomérats semblables au nord et au sud de la FLLC suggèrent que l'unité alluvionnaire-fluviatile a été déposée dans un basin de transtension (pull-apart) après la juxtaposition de deux blocs tectoniques le long de la FLLC entre 2685 Ma et 2677 Ma; l'unité de turbidite nord est de la même âge ou un peu plus jeune. La proximité des sources indique que le décrochement pendant et après la déposition de l'unité alluvionnaire-fluviatile fut mineur.

ACKNOWLEDGEMENTS

The author wishes to thank a number of people for their interest and support throughout this study. I am indebted to Dr. Keiko Hattori of the University of Ottawa for proposing this project. Her enthusiasm for the project, valuable suggestions, and encouragement were instrumental in the completion of the thesis. The author is also grateful for her continuous financial support without which this study would not have been possible.

Thanks are also extended to Drs. J. Al Donaldson (Carleton University) and Keith Benn (University of Ottawa) who, as members of the advisory committee, supplied suggestions throughout the project. The author wishes also to extend his thanks to Dr. Wulf Mueller (Université du Québec à Chicoutimi) for collaboration and advice in the field. Brian Charbonneau (Geological Survey of Canada) is thanked for his permission to use the γ-ray spectrometer and for discussions on its applications.

Dr. J. Al Donaldson is thanked, along with Dr. Kent Condie (New Mexico Institute of Mining and Technology), for their reviews of Paper 1. Drs. Randy Rice (Carleton University) and J. Al Donaldson are thanked for their reviews of Paper 2.

Thin and polished sections were prepared with the skillful assistance of Jean-François Tardif. XRF analyses were completed by Ron Hartree (University of Ottawa) and Dr. Richard Rousseau (Geological Survey of Canada). REE determinations were done by John Loop (University of Ottawa; ICP-AES) and Dr. Greg Kennedy (Université de Montréal; INAA). Peter Jones (Carleton University) performed the microprobe analysis and Gilles St-Jean and Nathalie Morisset (University of Ottawa) determined C and O isotope ratios.

I would like to thank my fellow graduate students at the University of Ottawa for their helpful discussions and comments over the course of this study. Special thanks to Guy Levesque for his unpublished data and for our many discussions on the Kirkland Lake area.

To my parents, I express my gratitude for their continued support and encouragement throughout my many academic endeavours. I also thank my wife, Cheryl, for her patience and understanding as well as for giving me the opportunity to undertake this study.

I would like to dedicate this thesis to my children, Mélanie et Alexandre; may they find as much happiness and fulfilment in learning as I have in the past two years.

TABLE OF CONTENTS

	Page
ABSTRACT	i
SOMMAIRE	iii
ACKNOWLEDGEMENTS	v
TABLE OF CONTENTS	vii
LIST OF FIGURES	x
LIST OF TABLES	xii
LIST OF APPENDICES	xiii
GENERAL INTRODUCTION	1
PAPER 1 - Late Archaean geological development recorded in the Timiskaming Group sedimentary rocks, Kirkland Lake area, Abitibi greenstone belt	2
ABSTRACT	3
INTRODUCTION	4
ANALYTICAL METHODS	6
PETROGRAPHY	9
Conglomerate-sandstone unit	13
Turbidite unit	16
GEOCHEMISTRY	17
DISCUSSION	23
Provenance	25
Redefinition of turbidite south assemblage	33
Geological setting	34
Timing	37
Geological development of the area	39
Late Archaean upper crust	41

TABLE OF CONTENTS - continued

	Page
SUMMARY	41
ACKNOWLEDGEMENTS	42
REFERENCES	44
PAPER 2 - Provenance of igneous clasts in conglomerates of the Late Archaean Timiskaming Group, Kirkland Lake area, Abitibi greenstone belt	50
ABSTRACT	51
INTRODUCTION	52
GENERAL GEOLOGY	54
ANALYTICAL METHODS	55
CONGLOMERATES	61
IGNEOUS CLASTS	63
Porphyry clasts	63
Coarse-grained holocrystalline clasts	68
Volcanic clasts	68
DISCUSSION	69
Source rocks	70
Classification of clasts	70
Calc-alkaline porphyry clast source	70
Alkaline porphyry clast source	76
Coarse-grained holocrystalline clast source	77
Mafic and intermediate volcanic rock clast source	79
Implications for late Archaean development	79
Timing of sedimentation	82
Nature of LLCF	83
Tectonic setting	84
CONCLUSIONS	85

TABLE OF CONTENTS - continued

	Page
ACKNOWLEDGEMENTS	86
REFERENCES	88
APPENDICES	97

LIST OF FIGURES

Page

PAPER 1

Fig. 1. Geology of the Kirkland Lake area. 5

Fig. 2. Average clast compositions of CSU (a) and TSU (b). 14

Fig. 3. Classification of sandstones. 15

Fig. 4. eTh versus eU of sedimentary rocks. a - conglomerates, b - sandstones and c - siltstones. 19

Fig. 5. ($MgO+Fe_2O_3$) vs. SiO_2. 20

Fig. 6. Ti/Zr vs. Cr. 21

Fig. 7. Chondrite-normalized REE patterns for shales of TNU (a), CSU (b) and TSU (c). 22

Fig. 8. Ternary diagram showing weathering trends. 26

Fig. 9. Trace element discrimination diagram. 31

Fig. 10. REE patterns for model concentrations. 32

Fig. 11. Framework minerals discrimination diagram. 36

PAPER 2

Fig. 1. Geology of the Kirkland Lake area. 53

Fig. 2. Schematic cross-section of outcrop 3. 62

Fig. 3. $Na_2O + K_2O$ versus SiO_2. 64

Fig. 4. Amphibole classification. 65

Fig. 5. Classification of porphyry clasts. 67

LIST OF FIGURES - continued

	Page
Fig. 6. Larsen diagrams of calc-alkaline porphyry clasts and early intrusions.	72
Fig. 7. Spidergram of calc-alkaline porphyry clasts and late intrusions.	73
Fig. 8. Larsen diagrams of porphyry clasts and late porphyry intrusions.	74
Fig. 9. Composition of holocrystalline clasts and trondhjemite intrusions.	78
Fig. 10. Larsen diagrams of holocrystalline clasts and Round Lake batholith.	80

LIST OF TABLES

Page

PAPER 1

Table 1. Modal compositions of sandstones 7

Table 2. Gamma-ray spectrometry measurements 8

Table 3. Chemical compositions of sandstones and siltstones 10

Table 4. Trace and REE compositions of selected siltstones 12

Table 5. Modelling results for TSU shales 29

Table 6. Modelling results for TNU shales 30

PAPER 2

Table 1. Clast abundances of conglomerate beds 56

Table 2. Major and trace element concentrations of igneous clasts 58

Table 3. Average microprobe analyses of amphiboles 60

LIST OF APPENDICES

	Page
Appendix 1. Carbon and oxygen isotopic compositions of carbonate-bearing igneous clasts	97
Appendix 2. Field observations, gamma-ray spectrometry and magnetic susceptibility measurements, and collected samples	108
Appendix 3. Major and minor element concentrations of clasts and rocks which are not included in the manuscripts	131
Appendix 4. Average microprobe analyses of amphiboles and plagioclases which are not included in manuscripts	135
Appendix 5. Comparaison of gamma-ray spectrometry and instrumental neutron activation analysis (INAA) measurements	137

GENERAL INTRODUCTION

The late Archaean Timiskaming Group of the Kirkland Lake area lies unconformably over greenstone-belt volcanic rocks and is spatially associated with a large-scale deformation zone, the Larder Lake - Cadillac Fault. Various tectonic settings have been proposed for the deposition of the Timiskaming Group (e.g., Hyde, 1980; Dimroth et al., 1983; Hodgson and Hamilton, 1989; Card, 1990; Feng and Kerrich, 1990; Mueller and Donaldson, 1992). Detailed geochemical data on the shales, sandstones and conglomerate clasts should provide the constraints for the origin; this study presents the results of petrological and geochemical investigations of the different sedimentary facies comprising the Timiskaming Group.

The results of this study are presented in two papers. The first paper describes the petrography and geochemistry of the sandstones and shales of the alluvial-fluvial and turbidite assemblages. The results are discussed in terms of provenance, geological setting and timing of the Timiskaming Group as well as the implications on the geological development of the southern Abitibi belt in the late Archaean.

The second paper reports the petrography and geochemistry of igneous clasts from the alluvial-fluvial assemblage of the Timiskaming Group. Probable source rocks for these clasts are identified and occurrences on both sides of the LLCF are examined. Results are used to constrain the geological development of the area in the late Archaean. Proposals are made on the timing of sedimentation and tectono-sedimentary setting for the deposition of the alluvial-fluvial assemblage.

LATE ARCHAEAN GEOLOGICAL DEVELOPMENT RECORDED IN THE TIMISKAMING GROUP SEDIMENTARY ROCKS, KIRKLAND LAKE AREA, ABITIBI GREENSTONE BELT, CANADA

Marc I. Legault and Keiko Hattori

Ottawa-Carleton Geoscience Centre and Department of Geology,

University of Ottawa, Ottawa, Ontario, Canada, K1N 6N5

Submitted to Precambrian Geology, March 1993

Revised in August, 1993.

ABSTRACT

Sedimentary rocks of the Timiskaming Group have been classified into a conglomerate-sandstone unit (CSU) and a turbidite unit (TU). Turbidite sequences north and south of the Larder Lake-Cadillac Fault (LLCF) are significantly different. The turbidite south unit (TSU) has elevated concentrations of $Fe_2O_{3(tot)}$, MgO, TiO_2, Cr and Ni, whereas the turbidite north unit (TNU) has compositions similar to arenites of the CSU and has high SiO_2, U, Th and total REE.

The source of the TSU is estimated from chemical modelling and clast populations to be 12% rhyolite, 18% komatiite and 70% calc-alkaline andesite, mostly derived from an undissected volcanic arc terrane. It is proposed that the TSU formed in a foreland basin during uplift of calc-alkaline volcanic rocks and obduction of oceanic crust in response to deformation related to accretion. Sources for the CSU and the TNU were very similar, comprising 60% calc-alkaline porphyries, 20% alkaline trachytes and 20% tholeiitic basalts. The TNU was either contemporaneous with or postdated the CSU, and their depositions probably followed juxtaposition of two tectonic blocks along the LLCF. The source terrane for the CSU and TNU was a dissected arc which had exposed subvolcanic calc-alkaline intrusions. The sedimentation of CSU and TNU, however, predated the unroofing of K-rich intrusions, which are presently extensively exposed.

Abundant andesitic rocks in the TSU and the decrease in their abundances in the TNU and CSU indicates that andesites were once extensively exposed, but most were removed by erosion in late Archaean time.

INTRODUCTION

The Timiskaming Group, the youngest Archaean lithological unit in the Superior Province, is composed of sedimentary rocks with or without interlayered alkalic volcanic rocks. It is defined as a unit that unconformably overlies greenstone-belt metavolcanic rocks (e.g., Shegelski, 1980; David and Lajoie, 1989; Mueller et al., 1991). The present study pertains to the Kirkland Lake area in the Abitibi greenstone belt, the type locality for Timiskaming rocks (Hewitt, 1963; Fig. 1).

It is well recognized that the Timiskaming Group is a syn-tectonic assemblage that recorded information relevant to the late Archaean cratonization of the Superior Province, but the depositional setting for the rocks has been in debate. Proposed geological settings for the Timiskaming Group include sedimentation during the final stages of island arc volcanism before accretion (e.g., Dimroth et al., 1983), a molasse-type deposit related to large scale oblique thrusting along the Larder Lake - Cadillac Fault (LLCF)(e.g., Hodgson and Hamilton, 1989) or a pull-apart basin formed by strike-slip movement of the LLCF (e.g., Thurston and Chivers, 1990; Card, 1990). In addition, the relationships of the different facies of the Timiskaming Group are also in debate. Many workers considered the different units as different facies formed in a single sedimentary basin (e.g., Hewitt, 1963; Hyde, 1980) that were later juxtaposed by thrusts (Hamilton and Hodgson, 1984). Jensen (1985a, 1985b) proposed that the sedimentary rocks south of the LLCF belonged to the greenstone-belt volcanic sequence, Larder Lake Group, based mainly on their distribution. Corfu et al. (1991) and Jackson and Fyon (1991) suggested that the turbidite unit (TU; Hearst Assemblage) was formed earlier than the conglomerate - sandstone unit (CSU; Timiskaming Assemblage).

This paper presents petrological and geochemical data for conglomerates, sandstones and

Figure 1. Geological map of the Kirkland Lake area, showing sample locations (CSU - 1, 2, 3, 15, 19, 31, 32, 36, 37, 39, 43, 52, 58; TNU - 16, 21, 23, 24, 25, 29, 33, 34, 44, 45, 50, 53, 54, 55, 56; TSU - 26, 27, 28, 30, 40, 46, 47, 48, 49, 59; older sediments - 36, 38). Modified from Hyde (1978). Subdivision of sedimentary rocks of the Timiskaming Group is based on our field observations. Inset: location of the study area within the Abitibi greenstone belt.

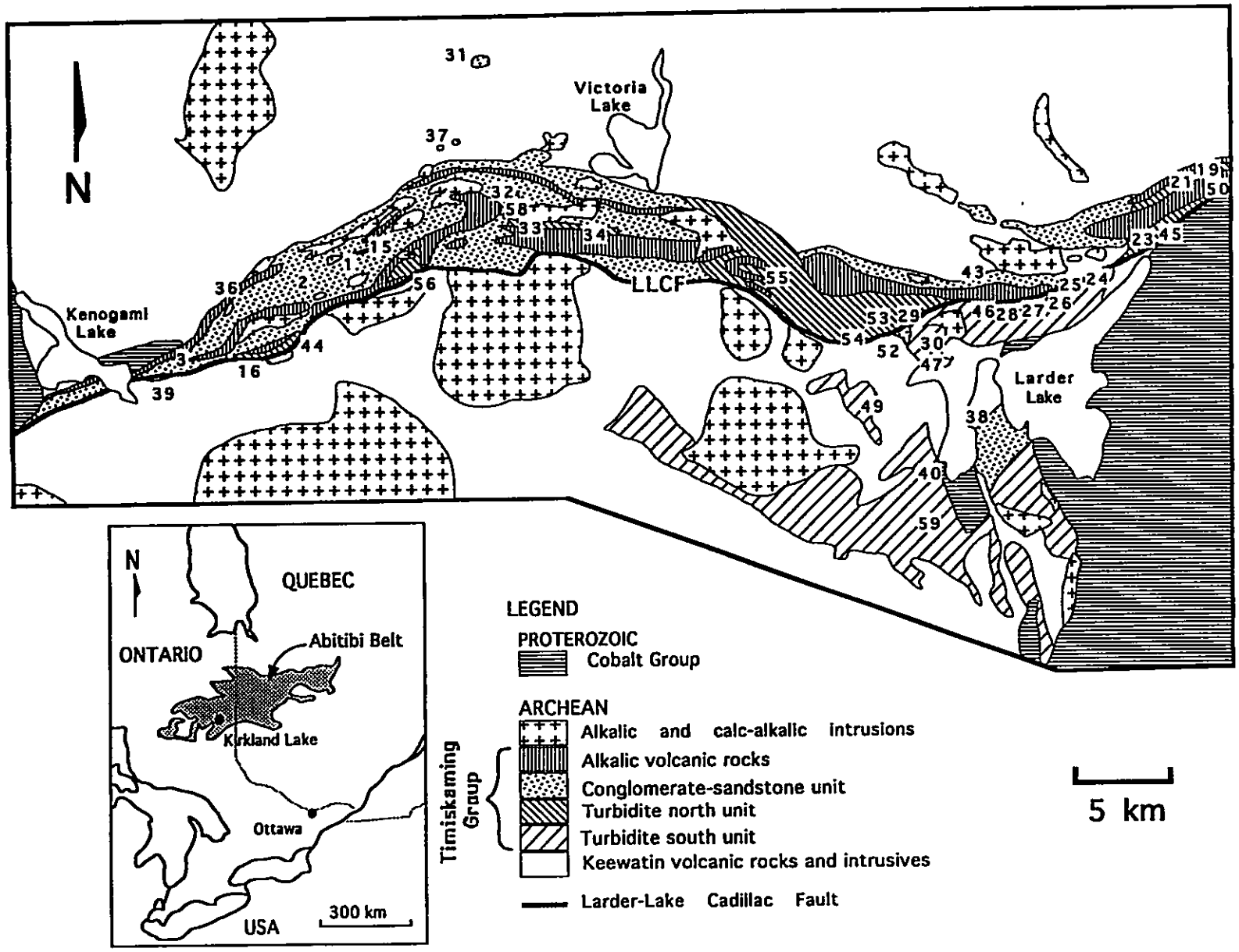
N
Victoria Lake
Kenogami Lake
LLCF
Larder Lake
N
QUEBEC
ONTARIO
Abitibi Belt
Kirkland Lake
Ottawa
USA
300 km
LEGEND
PROTEROZOIC
Cobalt Group
ARCHEAN
Alkalic and calc-alkalic intrusions
Alkalic volcanic rocks
Timiskaming Group
Conglomerate-sandstone unit
Turbidite north unit
Turbidite south unit
Keewatin volcanic rocks and intrusives
Larder-Lake Cadillac Fault
5 km

siltstones from the Timiskaming Group and discusses the relationship of the different units, and the provenance and geological setting of the Timiskaming Group.

ANALYTICAL METHODS

Over 50 outcrops of the sedimentary rocks in the area were examined in the summer of 1991 and 1992, in collaboration with Wulf Mueller of Université du Québec à Chicoutimi. Supplemental samples were collected at the Core Library of the Ministry of Northern Development of Mines in Swastika. Older sedimentary rocks intercalated with Keewatin volcanic rocks were also collected for comparison. Over 80 thin sections (22 CSU, 51 TU, 5 CSU clasts and 5 older sediments) of sandstones and matrix of conglomerates were examined, and 20 representative thin sections, covering most of the stratigraphic section of the Timiskaming Group, were selected for modal analysis, which involved mineral identification of > 1000 points in each thin section (Table 1). Grid size selected for point counting of these sections was at least twice the size of the average grain (~ 5 mm). Due to the low metamorphic grade of the Timiskaming Group (up to the lowermost greenschist; Jolly, 1980) minor amounts of fine-grained metamorphic chlorite, biotite, actinolite and epidote are easily distinguished from detrital minerals.

A portable γ-ray spectrometer, the GR256 model made by Exploranium Ltd., was used in the field for semiquantitative determination of K, U and Th concentrations for volumes of rock equal to a half sphere with a diameter of approximately 0.8 m (Table 2). Conglomerates contain clasts generally less than 10 cm and their measurements provide average radio-element concentrations of the clasts and matrix. Comparison of the results by γ-ray spectrometry and conventional analytical

Table 1. Modal compositions of sandstones, conglomerate matrices and sandstone clasts from CSU conglomerates.

Sample*1)	Type*2)	Unit*3)	Qtz	Pl*4)	Chl*5)	Bt*5)	Ep*5)	Zr	Ap	Op	LF*6)	Carb	Matrix	
													Sericite	Other
1x	SS	CSU	10.1	12.7	15.3	0.2	-	-	-	6.5	30.5	20.0	Tr	-
3y	SS	CSU	10.8	12.4	6.6	-	-	-	-	1.0	33.4	23.5	8.5	3.5
19a	CM	CSU	1.1	32.0	20.9	0.9	-	-	-	5.8	0.6	13.3	1.1	23.9
37a	CM	CSU	7.8	9.8	2.0	-	-	-	-	1.2	15.3	18.3	0.3	44.9
39l	SS	CSU	8.0	10.8	24.9	Tr	-	-	-	1.1	51.5	3.4	Tr	-
43b	CM	CSU	27.0	24.6	0.2	-	0.2	-	-	1.4	25.8	20.4	Tr	-
58a	SS	CSU	12.1	13.6	17.1	Tr	-	-	-	4.6	26.9	16.8	9.0	-
21a	SS	TNU	24.9	8.6	0.5	-	-	Tr	-	0.5	3.8	19.1	30.9	11.4
23b	SS	TNU	12.0	9.5	0.3	Tr	0.3	-	-	2.3	2.0	21.4	3.3	45.8
53c	SS	TNU	10.9	7.4	-	-	-	-	-	1.1	1.5	18.9	24.1	35.8
55b	SS	TNU	8.6	4.8	0.1	-	-	0.2	-	13.3	0.4	20.0	28.2	23.8
56b	SS	TNU	21.0	17.5	4.9	-	-	-	-	3.5	16.7	0.2	11.4	6.6
30c	SS	TSU	2.7	24.4	20.0	8.9	-	-	0.2	1.5	6.5	4.4	-	30.9
30g	SS	TSU	2.1	15.8	25.0	4.2	-	-	-	3.8	2.6	9.2	-	37.0
40a	SS	TSU	1.9	13.6	4.8	49.1	-	-	-	0.8	2.9	10.9	-	15.5
38b	SS	LLG	8.4	25.7	23.1	-	2.7			4.5	4.9	0.2	0.4	29.6
1f	CL	CSU	12.2	23.0	16.7	-	1.0	-	-	10.8	28.7	7.6	-	-
1q	CL	CSU	11.6	49.9	0.2	-	-	-	-	4.7	7.2	3.0	-	23.1
3j	CL	CSU	9.4	49.7	-	2.1	-	-	-	2.2	10.0	5.2	-	20.9
3p	CL	CSU	11.1	41.5	15.0	Tr	-	-	-	4.5	27.4	0.6	-	-
39d	CL	CSU	8.7	52.7	16.2	6.2	-	-	-	7.7	6.5	1.7	-	-

Qtz=quartz; Pl=plagioclase; Chl=chlorite; Bt=biotite; Ep=epidote; Zr=zircon; Ap=apatite; Op=opaque minerals (mostly hematite, magnetite and pyrite); LF=lithic fragments (mostly felsic and mafic volcanic rocks, chert, plagioclase-bearing porphyry and tonalite-trondhjemite); Carb= carbonate (mostly calcite); Matrix=sericite(mostly aggregates of very fine sericite of diagenetic or metamorphic origin) and other (mostly a mixture of fine quartz, plagioclase, chlorite and carbonate). (Tr) indicates < 0.1%; (-) indicates that grains were not observed.

*1) The numerical numbers correspond to the location numbers shown in Fig. 1.

*2) Rock type: CL=clasts of sandstone in conglomerate; CM=conglomerate matrix; SS=sandstone.

*3) Units: CSU=conglomerate-sandstone unit; TNU=turbidite north unit; TSU=turbidite south unit; LLG=Larder Lake Group.

*4) Staining tests show an essential absence of K-feldspar grains and feldspars are therefore classified as plagioclase.

*5) Coarse chlorite, biotite and epidote grains are considered to be epiclastic components derived from mafic volcanic rocks and porphyries. Fine metamorphic chlorite, actinolite and epidote are minor and do not figure in the modal analysis.

*6) Aggregates of fine-grained chlorite, albite, carbonate and quartz are considered to be altered lithic fragments or ferro-magnesian minerals and they are counted as lithic fragments.

Table 2. Average and standard deviation of radioelement contents determined by gamma-ray spectrometry.

		CSU			TNU			TSU		
		Avg.	St. Dev.	n	Avg.	St. Dev.	n	Avg.	St. Dev.	n
CG	K wt.%	0.9	0.5	9	-	-	-	0.6	0.4	4
	eU ppm	2.7	2.3	9	-	-	-	0.5	0.1	4
	eTh ppm	5.1	1.9	9	-	-	-	0.3	0.2	4
SS	K wt.%	1.5	0.6	12	1.8	0.3	6	1.3	0.1	2
	eU ppm	1.9	0.8	12	2.3	0.5	6	0.7	0.1	2
	eTh ppm	4.3	0.9	12	5.5	1.6	6	1.9	0.5	2
SH	K wt.%	1.4	0.5	3	2.3	0.3	11	1.5	0.6	5
	eU ppm	1.8	0.4	3	2.7	1.0	11	1.0	0.5	5
	eTh ppm	4.5	0.9	3	7.6	3.0	11	1.4	0.7	5

CG=conglomerate; SS=sandstone; SH=shale and argillite.
(n) refers to number of measurements for each rock-type of each unit.
Unit abbreviations as in Table 1.

techniques by Charbonneau et al. (1981) show that the results by the two methods are comparable. Values are expressed as K, eU and eTh, because measurements for U and Th are made on ^{214}Bi and ^{208}Tl respectively, and assume radioactive equilibrium. Measurements for K are made directly on ^{40}K. The detection limit for K is 0.1%; for eU and eTh it is 0.1 ppm. Analytical methods are described in Killeen (1979).

Medium-grained sandstones to fine-grained siltstones which do not show any apparent evidence of deformation or hydrothermal alteration were selected for chemical analyses. Major and minor elements were determined by X-ray fluorescence spectrometry (XRF) for 32 samples with precision of $\pm$ 1% for major elements and $\pm$ 10% for minor elements (Table 3). Rare-earth element (REE) concentrations of samples with an average grain size less than 0.06 mm were determined by instrumental neutron activation analysis (INAA) with precision of $\pm$ 5% (Table 4).

PETROGRAPHY

Sedimentary rocks in the area show two lithological units: a conglomerate-sandstone unit and a turbidite unit. The CSU represents non-graded clast-supported conglomerates, cross - bedded sandstones and argillites, which are interpreted as alluvial-fluvial sequences (Hyde, 1980; Mueller and Donaldson, 1992). This unit is intercalated with trachytic volcanic and volcaniclastic rocks. The TU includes interbedded sandstones and shales and graded conglomerates and are interpreted as resedimented turbidite sequences (Hyde, 1980). This unit is exposed mostly in the eastern part of the study area, both north and south of the LLCF (Fig. 1).

Table 3. Chemical compositions of medium-grained sandstones to fine-grained siltstones of the TSU, TNU, CSU and sandstone clasts from CSU conglomerates.

	40a	49b	40d	30c	46a	59b	48b	53b	21a	45a	56b	50b	55b	56a	25a	50a
Unit	TSU	TSU	TSU	TSU	TSU	TSU	TSU	TNU	TNU	TNU	TNU	TNU	TNU	TNU	TNU	TNU
SiO2 (wt.%)	53.1	48.8	49.7	56.7	56.7	56.6	54.7	59.5	64.4	61.7	65.8	60.5	58.8	64.8	62.7	59.2
Al2O3	12.2	14.0	11.9	14.6	17.2	16.7	15.7	16.3	11.1	19.0	13.6	10.8	14.0	14.3	14.1	21.5
Fe2O3 *	9.89	11.2	9.06	7.02	9.69	9.01	12.8	7.48	3.61	5.46	3.13	3.98	4.97	4.24	5.03	6.62
MgO	7.86	3.93	7.43	6.20	4.15	7.19	6.87	5.02	2.73	2.92	2.08	2.92	2.93	2.18	2.84	2.59
CaO	7.33	8.97	8.04	2.65	2.00	0.79	2.84	1.10	4.79	0.60	2.66	6.50	4.31	2.58	1.95	0.22
Na2O	3.69	3.69	2.81	4.76	2.55	2.20	2.30	6.04	2.23	3.64	3.24	4.87	3.76	2.69	3.19	2.70
K2O	1.22	0.02	1.19	1.39	1.96	2.33	0.73	0.63	2.63	3.15	2.82	0.65	2.48	2.91	2.45	3.64
TiO2	0.71	1.12	0.66	0.53	0.90	0.69	0.70	0.76	0.31	0.73	0.45	0.23	0.45	0.52	0.50	0.54
P2O5	0.14	0.09	0.14	0.14	0.13	0.11	0.16	0.27	0.08	0.24	0.13	0.08	0.18	0.14	0.17	0.12
S	0.10	0.88	0.13	0.09	0.33	0.10	0.27	0.09	0.09	0.06	0.11	0.29	0.12	0.12	0.17	0.09
MnO	0.15	0.27	0.14	0.11	0.08	0.10	0.15	0.09	0.11	0.01	0.05	0.13	0.07	0.05	0.06	0.01
Ba (ppm)	476	121	186	769	466	274	178	166	531	829	662	190	818	801	681	969
Cr	574	384	608	289	406	556	438	146	47	117	64	18	85	118	130	88
Zr	75	67	71	104	60	56	95	127	73	128	95	62	130	138	169	101
Sr	283	173	469	521	167	73	429	120	335	174	384	421	878	295	389	116
Rb	8	5	21	13	27	30	24	6	48	52	48	12	39	48	40	51
Y	6	14	6	< 5	7	5	12	10	6	12	< 5	< 5	6	7	5	9
Nb	< 5	7	< 5	< 5	< 5	< 5	10	6	< 5	< 5	< 5	< 5	< 5	6	< 5	< 5
Zn	51	143	82	388	46	47	87	44	< 5	6	< 5	14	60	39	70	67
Ni	246	224	306	187	216	238	218	109	22	109	6	< 5	75	69	49	47
Cu	< 5	15	50	10	< 5	< 5	< 5	< 5	< 5	< 5	< 5	< 5	< 5	< 5	< 5	< 5
Pb	< 5	< 5	7	222	< 5	< 5	< 5	< 5	< 5	< 5	< 5	< 5	< 5	6	< 5	< 5
V	n.d.	n.d.	n.d.	n.d.	n.d.	n.d.	n.d.	n.d.	n.d.	n.d.	n.d.	n.d.	n.d.	n.d.	n.d.	n.d.
LOI (%)	4.0	7.9	9.5	6.3	5.8	5.1	4.4	3.2	8.4	3.8	6.1	9.8	8.6	6.1	7.1	3.7
Sum (%)	100.56	100.63	100.84	100.81	101.49	101.06	101.6	100.58	100.52	101.41	100.22	100.67	100.79	100.67	100.35	101.11
Rock type	SS	SS	SS	SS	SH	SH	SH	SS	SS	SS	SS	SS	SS	SS	SS	SH

Sample numbers represent their locations in Fig. 1.
* Total Fe expressed as Fe2O3
(n.d.) not determined
Unit abbreviations as in Table 1
Rock types - Sandstone (SS); Siltstone and mudstone (SH); Sandstone clast (CL).

Table 3. Continued. Chemical compositions of medium-grained sandstones to fine-grained siltstones of the TSU, TNU, CSU and sandstone clasts from CSU conglomerates.

	29a	44b	44a	23a	33a	43d	1x	43c	58a	3y	1y	38b	1f	1q	3j	3p	39d
Unit	TNU	TNU	TNU	TNU	TNU	CSU	CSU	CSU	CSU	CSU	CSU	LLG	CSU	CSU	CSU	CSU	CSU
SiO2 (wt.%)	64.4	63.3	65.2	54.8	58.1	65.7	62.0	65.6	62.1	61.6	60.1	62.6	57.3	66.9	67.5	67.1	58.4
Al2O3	14.8	18.2	15.7	22.3	19.9	12.6	14.0	14.9	13.1	13.2	13.7	14.9	12.6	15.5	14.9	15.5	16.3
Fe2O3 *	4.49	6.19	5.50	5.06	6.39	6.13	6.36	7.19	5.56	6.35	5.40	7.19	5.53	2.49	2.21	2.75	6.40
MgO	2.54	2.88	2.33	3.03	2.70	2.25	4.30	2.29	4.07	3.18	3.03	4.69	3.01	0.96	0.93	1.23	5.90
CaO	2.39	0.35	1.81	0.69	0.54	3.23	3.07	1.31	3.55	3.25	3.31	1.52	7.40	2.09	2.49	1.68	1.63
Na2O	4.16	4.52	4.49	1.78	3.84	2.93	4.17	1.75	3.13	2.69	3.29	5.99	5.26	5.62	5.75	8.39	5.54
K2O	1.65	2.34	1.70	5.75	3.33	1.86	1.39	2.41	2.03	2.32	2.29	1.25	0.75	2.45	2.37	0.36	1.99
TiO2	0.47	0.68	0.53	0.62	0.70	0.55	0.53	0.51	0.50	0.55	0.43	0.63	0.49	0.29	0.24	0.24	0.63
P2O5	0.20	0.15	0.14	0.26	0.17	0.14	0.18	0.14	0.15	0.14	0.15	0.14	0.13	0.06	0.08	0.04	0.23
S	0.13	0.07	0.05	0.01	0.08	0.15	0.08	0.11	0.40	0.08	0.12	0.25	0.02	0.01	0.00	0.01	0.07
MnO	0.06	0.03	0.04	0.03	0.06	0.08	0.09	0.09	0.07	0.09	0.09	0.09	0.16	0.05	0.04	0.06	0.11
Ba (ppm)	470	532	466	1694	775	564	274	563	3797	664	732	369	485	885	686	182	1112
Cr	16	89	55	129	109	125	164	78	105	70	154	373	195	43	34	42	47
Zr	135	124	122	135	131	106	95	137	101	127	133	95	70	78	55	63	115
Sr	382	118	318	165	230	276	271	78	434	269	663	198	630	555	551	533	316
Rb	26	29	19	202	60	24	17	30	34	43	43	26	12	86	101	< 5	37
Y	< 5	7	6	15	7	8	7	7	6	8	6	11	16	< 5	< 5	< 5	21
Nb	< 5	< 5	< 5	< 5	7	< 5	< 5	< 5	< 5	< 5	< 5	<5	< 5	< 5	< 5	< 5	7
Zn	24	36	27	77	70	21	24	53	71	46	57	60	74	27	29	39	41
Ni	< 5	< 5	< 5	89	131	56	99	23	121	98	62	109	116	30	21	35	175
Cu	< 5	< 5	< 5	n.d.	< 5	< 5	< 5	< 5	< 5	< 5	< 5	<5	n.d.	n.d.	n.d.	n.d.	< 5
Pb	< 5	< 5	< 5	n.d.	< 5	< 5	< 5	< 5	< 5	< 5	< 5	49	n.d.	n.d.	n.d.	n.d.	< 5
V	n.d.	n.d.	n.d.	123	n.d.	n.d.	n.d.	n.d.	n.d.	n.d.	n.d.	n.d.	104	24	13	< 5	n.d.
LOI (%)	4.9	2.9	4.1	4.4	5.3	5.1	4.3	4.0	5.9	6.9	8.5	2.2	7.0	2.9	3.2	2.0	3.3
Sum (%)	100.33	101.79	101.65	98.96	101.36	100.78	100.55	100.31	100.92	100.47	100.57	101.35	99.80	99.50	99.92	99.50	100.61
Rock type	SH	SH	SS	SH	SH	SS	SS	SS	SS	SH	SH	SS	CL	CL	CL	CL	CL

Table 4. Trace and rare-earth element compositions of siltstones of the TNU, TSU and CSU.

	23a	34a	58b	50a	53a	44b	24a	40b	49c	48a	1y	43c	3y
Unit	TNU	TNU	TNU	TNU	TNU	TNU	TNU	TSU	TSU	TSU	CSU	CSU	CSU
La (ppm)	49.4	33.6	33.9	32.3	28.2	26.7	27.7	6.2	14.3	12.3	27.6	25.7	28.9
Ce	94.0	66.0	68.8	60.3	54.6	53.6	55.8	15.9	26.6	25.7	54.0	47.3	54.7
Nd	36.0	30.0	32.6	26.2	25.5	25.1	26.1	8.9	10.4	13.0	21.4	20.0	25.6
Sm	5.90	5.20	6.30	4.64	4.45	4.21	4.62	2.20	1.85	2.79	3.80	3.37	4.31
Eu	1.44	1.32	1.72	1.30	1.23	1.08	1.30	0.84	0.56	1.02	0.99	0.94	1.39
Tb	0.50	0.49	0.64	0.55	0.49	0.45	0.47	0.35	0.24	0.49	0.42	0.41	0.54
Dy	2.67	3.05	3.40	2.82	2.37	2.45	2.30	2.10	1.18	2.45	2.10	1.88	2.71
Ho	0.53	0.57	0.63	0.61	0.42	0.46	0.48	0.39	0.32	0.51	0.47	0.39	0.52
Yb	1.22	1.51	1.54	1.64	1.20	1.38	1.33	1.15	0.56	1.67	1.27	1.17	1.62
Lu	0.21	0.26	0.24	0.24	0.18	0.20	0.19	0.17	0.10	0.26	0.19	0.18	0.22
Sc	13.2	21.2	21.5	18.7	14.7	19.3	19.6	24.5	23.4	25.5	11.2	12.5	16.0
Cs	13.0	2.5	2.1	1.9	3.5	1.0	2.4	0.8	2.0	<0.3	4.5	1.3	1.9
Hf	4.5	3.2	-	2.8	3.3	3.3	3.3	-	3.4	2.6	-	3.6	3.2
Ta	0.88	0.69	0.37	0.54	0.81	0.49	0.38	0.43	2.28	0.72	0.75	0.80	0.96
Th	12.9	7.2	6.4	8.0	6.4	4.6	4.8	1.2	3.2	1.9	8.2	6.2	5.7
U	4.00	2.00	1.79	2.14	1.89	1.21	1.21	0.33	0.86	0.53	2.95	1.83	1.13

Conglomerate-sandstone unit (CSU)

The CSU is mostly confined north of the LLCF, but two occurrences have been observed south of the fault on the southwest shore of Larder Lake and east of Kenogami Lake by Hyde (1978; Fig. 1). A third occurrence (#52 in Fig. 1) was found during this study west of the town of Larder Lake.

The conglomerates are non-graded, clast-supported and are characterized by the common occurrences of red hematitic jasper and alkalic volcanic clasts. Point counting of clasts for 13 conglomerate beds (over 1800 points in total) indicates that there are 3 major clast types (Fig. 2A): alkalic volcanic rocks, mafic volcanic rocks and felsic porphyries. Minor clast types, generally less than 10% in a given outcrop, include tonalite-trondhjemite, spessartite lamprophyre, felsic volcanic rocks, chert (including hematitic jasper), vein quartz, epiclastic and volcaniclastic sedimentary rocks, ultramafic volcanic rocks, magnetite-rich banded iron formation and fuchsite-carbonate rocks. Diversity and proportion of clasts are in accord with the results of Hyde (1980) and Mueller and Donaldson (1992).

The sandstones are cross-bedded and are sometimes interbedded with lenses of argillite. They are medium- to coarse-grained, greenish gray litharenites following the classification of Pettijohn et al. (1973; Fig. 3B), and are similar in composition to the matrix of the conglomerates. Modal compositions of these rocks are highly variable, in part due to the grain size of the samples as pointed out by Hyde (1978); the coarser-grained arenites plot closer to the lithic fragment apex (Fig. 3B). However, samples show a constant ratio of quartz/plagioclase, 0.87 ± 0.12 (all uncertainties are 1 σ), except for #19a (0.03). This sample has low quartz content, 1.1 vol.%, and is associated with a clast-supported monomictic conglomerate in which almost all clasts are plagioclase-bearing volcanic rocks.

Figure 2. A) Average clast populations of 13 conglomerate beds of the CSU at locations 1, 2, 3, 15 and 39 in Figure 1. "Porphyry" includes felsic porphyry and spessartite lamprophyre; "Mafic Volc." include andesitic, tholeiitic and komatiitic volcanic rocks; "Alkalic volc." include alkalic volcanic and volcaniclastic rocks; "Sediment" include chert and epiclastic sedimentary rocks; "Tonalite" include tonalite and trondhjemite. B) Average clast populations of 5 representative conglomerate beds of the TSU at locations 30, 40 and 47 in Figure 1. "UM volc." include komatiitic volcanic rocks; "Mafic volc." include calc-alkaline andesites and basalts; "Felsic volc." include rhyolites and dacites.

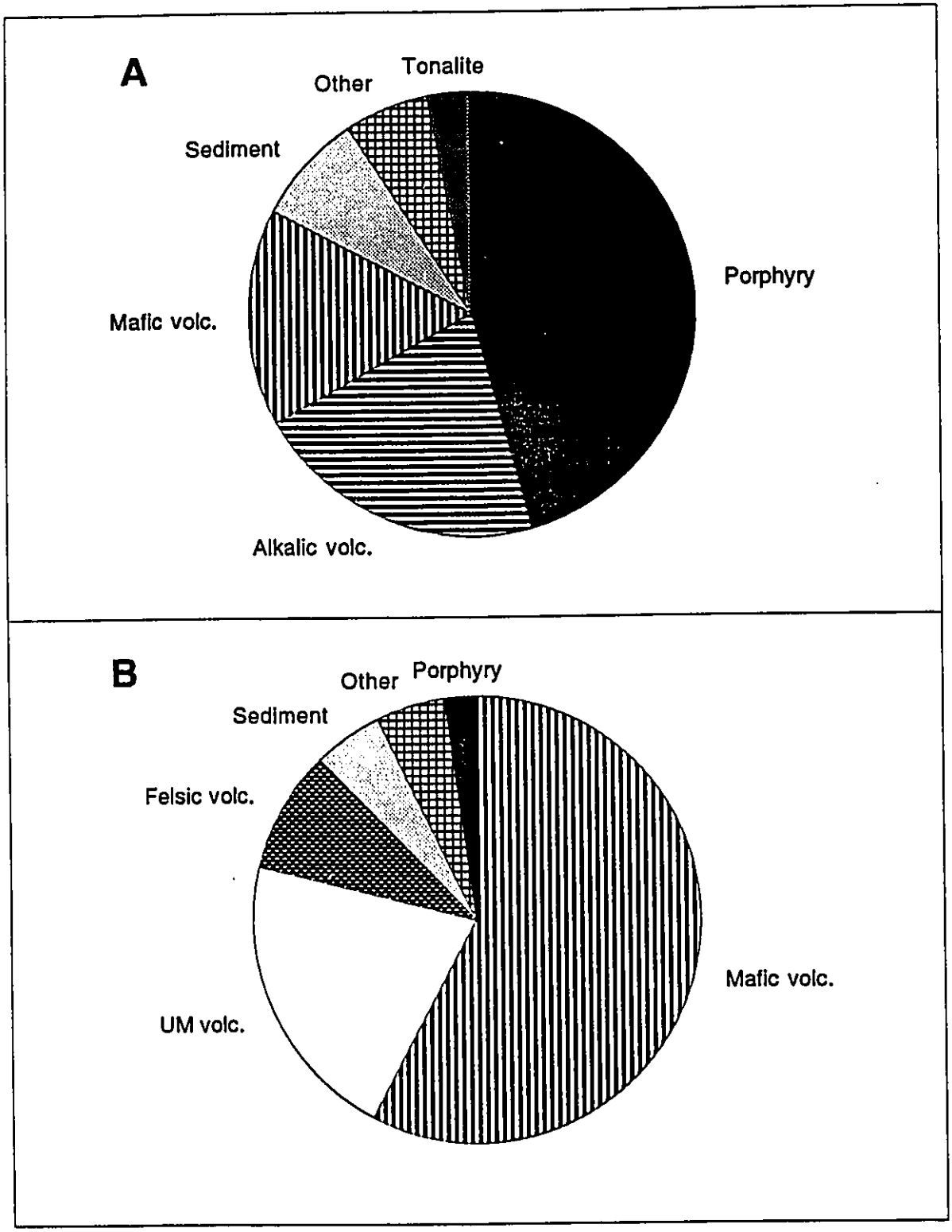
A
Other
Tonalite
Sediment
Porphyry
Mafic volc.
Alkalic volc.
B
Other
Porphyry
Sediment
Felsic volc.
Mafic volc.
UM volc.

Figure 3. Classification of sandstones following Pettijohn et al. (1973). A) Wackes (matrix between 15% and 75%) from the turbidite unit are classified into two sub-units: TNU and TSU. B) Arenites (matrix < 15%) from the conglomerate-sandstone unit. Sandstone clasts range from arenites to wackes. Lithic fragments include coarse chlorite and biotite grains as they were derived from mafic volcanic rocks and porphyries.

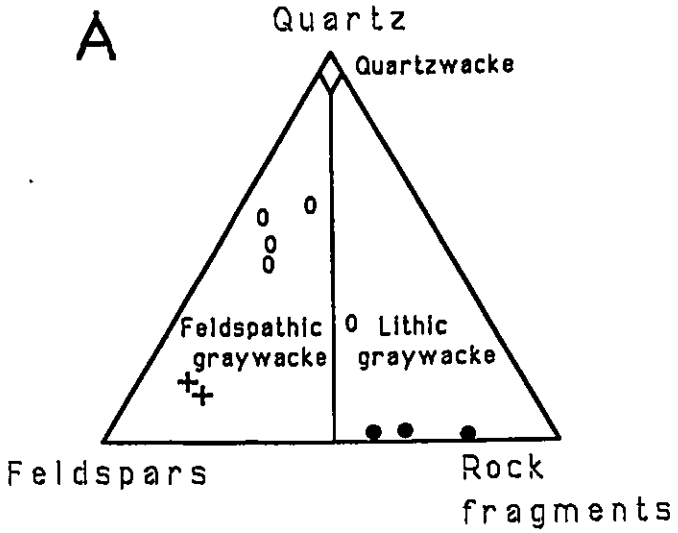

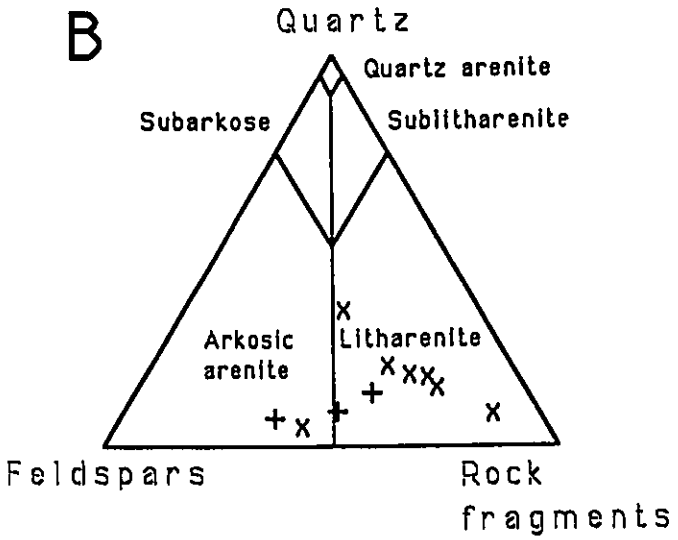

● TSU o TNU x CSU + Clasts

Sandstone clasts from conglomerates of the CSU have variable mineralogy and texture. In general, they are mostly quartz-rich and range from arkosic to litharenites and feldspathic graywackes following the classification of Pettijohn et al. (1973; Fig. 3A and B). The arenite clasts are mineralogically similar to plagioclase-rich arenites of the CSU (i.e., #19a; Table 1). Both have low ratios of quartz/plagioclase and high amounts of detrital chlorite (15 to 21 vol.%). Graywacke clasts contain abundant plagioclase (~ 50 vol.%) and quartz (~ 10 vol.%) and minor carbonates (~ 4 vol.%; Table 1). Chlorite and biotite grains are rare. These clasts are not similar to any other rocks examined in thin section in this study.

Turbiditic unit (TU)

Interbedded sandstones and shales north of the LLCF are light brown and quartz-rich, whereas similar rocks south of the fault are greenish gray and quartz-poor. The alternating sandstone and shale beds are commonly arranged in Bouma sequences, considered to represent proximal turbidites (Hyde, 1980).

Conglomerates in the TU south of the LLCF are monomictic to polymictic, and they are mostly graded, matrix-supported and are characterized by the presence of spinifex-textured ultramafic clasts. Clast types are highly variable from one conglomerate bed to another, but detailed examination of 5 conglomerate beds indicates that the predominant clasts are felsic volcanic rocks, mafic volcanic rocks and ultramafic volcanic rocks (Fig. 2B). Minor clasts include quartz porphyry, gabbro, gray chert, quartz-magnetite banded iron formation, spessartite lamprophyre, feldspar porphyry and epiclastic sedimentary rocks. Conglomerates are rare in the turbidites north of the LLCF and they are very different from conglomerates in the turbidites south of the LLCF. Instead they are similar

to those of the CSU.

Significant differences are noted between turbidites north and south of the LLCF. Turbidites north of the LLCF (TNU) contain quartz-rich feldspathic graywackes, whereas turbidites south of the LLCF (TSU) contain quartz-poor lithic graywackes (Fig. 3A). The latter has low quartz (< 3 vol.%) and carbonate (< 11 vol.%), and high chlorite (> 5 vol.%) and biotite (> 4 vol.%; Table 1). Furthermore, the TSU graywackes do not contain any sericite in their matrix, but it constitutes up to 75% of the matrix in the TNU. Sedimentary rocks intercalated with komatiites and tholeiitic basalts south of the LLCF are also different from the TSU. These rocks commonly contain higher quartz (~10 vol.%) and epidote (~3 vol.%) and essentially no carbonate or biotite (Table 1).

In general, the TNU graywackes are similar to the CSU arenites, including high ratios of quartz/plagioclase (1.20 to 2.90) and high carbonate contents (16.5 $\pm$ 6.1 vol.% for CSU, 19.5 $\pm$ 1.2 vol.% for TNU). Most of the carbonate grains appear to be the product of alteration processes, such as preferential replacement of plagioclase and hydrothermal alteration of volcanic source rocks, but some grains appear to have been derived from quartz-carbonate veins (fragments of these have been observed in thin sections). The main difference between these two units is the amount of lithic fragments: the TNU contains lesser amounts of lithic fragments (6.0 $\pm$ 7.9 vol.%) than the CSU (38.9 $\pm$ 18.5 vol.%).

GEOCHEMISTRY

Major and trace element chemistry also show a distinction between the TSU and the other two units, TNU and CSU. Graywackes and shales from the latter units are similar and they contain

lower $MgO+Fe_2O_{3tot}$, Cr, Ti/Zr, and Ni and higher SiO_2, large ion lithophile elements (LILE) and REE than those of the TSU (Fig 4, 5, 6 and 7). The differences of major elements reflect different amounts of quartz, chlorite and biotite grains in the sandstones. All three units, however, show a negative correlation between SiO_2 and $MgO+Fe_2O_{3tot}$ with a correlation coefficient of -0.76 (Fig. 5).

The CSU rocks have low Cr (70 to 186 ppm) and low Ti/Zr ratios (32 to 66), whereas the TSU rocks have high Cr (289 to 608 ppm) and elevated Ti/Zr ratios (51 to 167; Fig. 6) due to high TiO_2 and low Zr (Table 3). The data for all three units show a positive trend with a correlation coefficient of 0.59. Nickel is correlated with Cr and is high in the TSU rocks (187 to 306 ppm) and low in the CSU and TNU rocks (< 131 ppm). The contents of LILE of CSU and TNU are higher than those from the TSU (Table 2). The conglomerates of CSU have elevated eU (2.6 ± 2.2 ppm) and eTh (4.9 ± 1.9 ppm; Fig. 4A). Sandstones and siltstones from the CSU also have high concentrations of eU (~ 1.9 ppm) and eTh (~ 4.3 ppm; Fig. 4B and C). The TSU conglomerates show generally low values of eU (0.5 ± 0.1 ppm) and eTh (0.3 ± 0.2 ppm; Fig. 4A). Graywackes and shales of turbiditic sequences, however, display a wide range of eU and eTh. The TSU is characterized by generally low eU (~ 0.8 ppm) and eTh (~ 1.6 ppm) whereas the TNU rocks have relatively high eU (~ 2.5 ppm), eTh (~ 6.5 ppm; Fig. 4B and C) and K (~ 2.0 %). Higher K contents of the TNU are attributed to the large amounts of sericite (Table 2).

Abundances of REE also confirm the similarity between CSU and TNU and dissimilarity between the TSU and the former two units (Fig. 7). Shales from the TNU show highly fractionated REE patterns with high La/Yb_N ratios (13.6 to 27.9), a slight negative Eu anomaly ($Eu/Eu^* = 0.82$ to 0.92; $Eu^* = 2/3\ Sm + 1/3\ Tb$), and high total REE contents (112.72 to 188.67 ppm; Table 4). The REE patterns for the CSU are fractionated with elevated La/Yb_N ratios (12.3 to 15.1), variable

Figure 4. Uranium and Th concentrations of CSU, TNU and TSU conglomerates (a), sandstones (b) and siltstones (c) obtained by in-situ γ-ray spectrometry measurements.

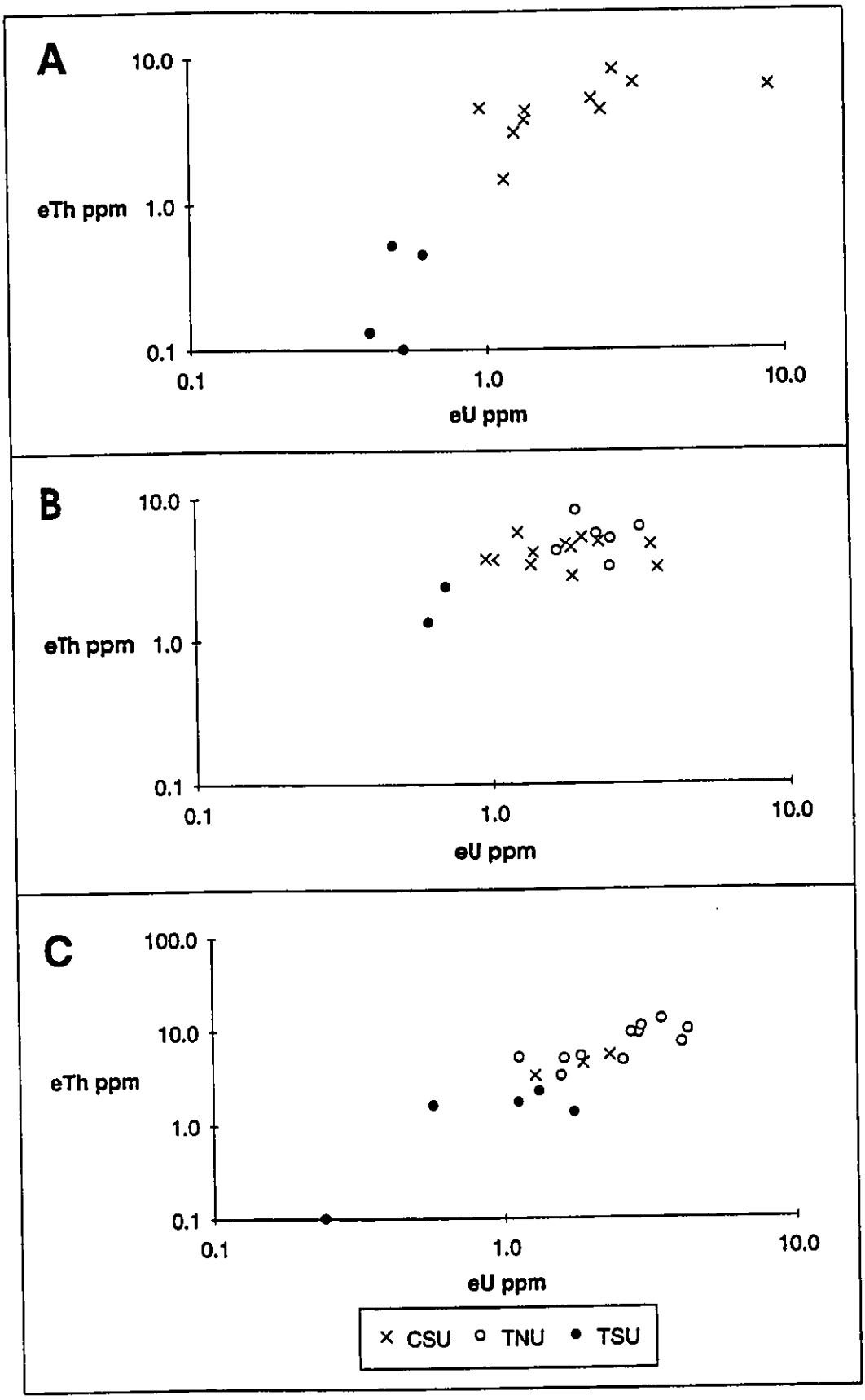
A
10.0
eTh ppm 1.0
0.1
0.1
1.0
10.0
eU ppm
B
10.0
eTh ppm 1.0
0.1
0.1
1.0
10.0
eU ppm
C
100.0
10.0
eTh ppm
1.0
0.1
0.1
1.0
10.0
eU ppm
× CSU ○ TNU • TSU

Figure 5. SiO_2 versus ($MgO+Fe_2O_3$) diagram. Note that the TSU rocks are distinct from the TNU, and that TSU has high ($MgO+Fe_2O_3$) and low SiO_2.

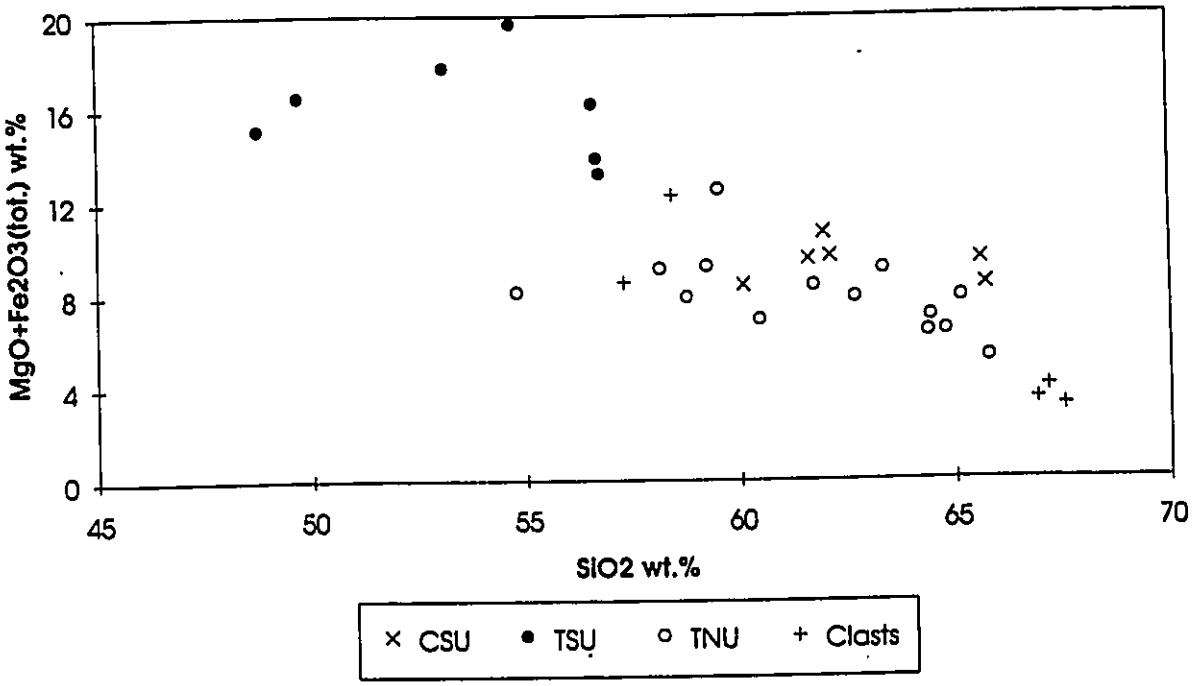
20
16
12
8
4
0
MgO+Fe2O3(tot.) wt.%
45
50
55
60
65
70
SiO2 wt.%
× CSU
• TSU
o TNU
+ Clasts

Figure 6. Chromium versus Ti/Zr ratios. Note that the TSU is characterized by high Cr and Ti/Zr ratios.

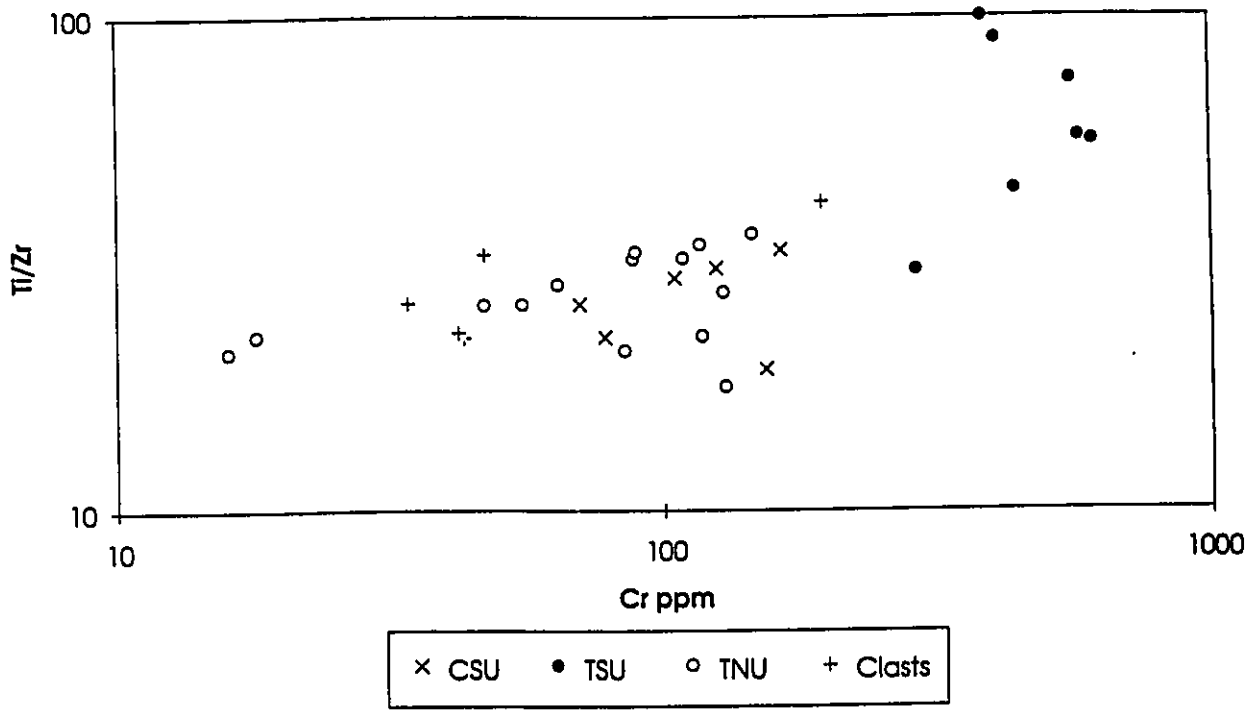
100
10
Ti/Zr
10
100
1000
Cr ppm
× CSU
• TSU
o TNU
+ Clasts

Figure 7. Chondrite-normalized REE patterns for siltstones of the TNU (A), CSU (B) and TSU (C). Values of C1 chondrite from Anders and Grevesse (1989).

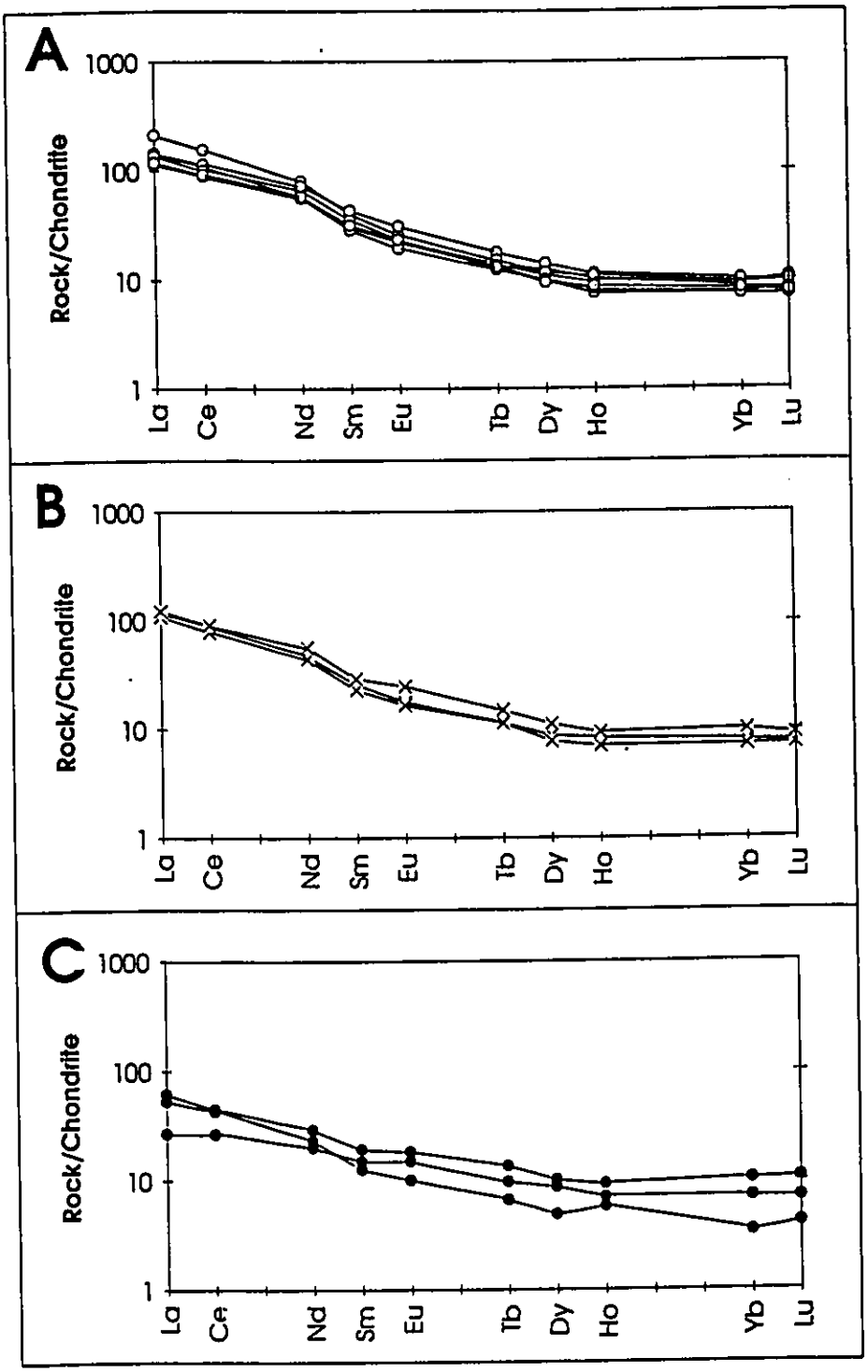
A
B
C
Rock/Chondrite
1000
100
10
1
La
Ce
Nd
Sm
Eu
Tb
Dy
Ho
Yb
Lu

Eu anomalies (Eu/Eu^* = 0.84 to 1.01) and high total REE contents (99.07 to 117.28 ppm). The REE patterns for the TSU shales are quite different from the patterns observed for the CSU and TNU. They are less fractionated (La/Yb_N = 3.8 to 17.6), and show variable Eu anomalies (Eu/Eu^* = 0.94 to 1.14) and low total REE contents (35.71 to 57.23 ppm). Our results are similar to the values of siltstones at outcrop #1 and shales at outcrop #59 in Fig. 1 reported by Feng and Kerrich (1990).

Sandstone clasts within the CSU have high SiO_2 (> 57 wt.%) reflecting their high quartz contents and variable MgO +$Fe_2O_{3(tot.)}$(3.14 to 8.54 wt.%) which are lower than sandstones of the CSU at comparable SiO_2 (Fig. 5). They also show variable Ti/Zr (37 to 70) and Cr (34 to 195 ppm; Fig. 6).

Sandstone within the Larder Lake Group has Cr and Ni contents similar to those of the TSU (Table 3), but higher SiO_2 and Zr, and lower Ti/Zr ratio (40) than those for the TSU.

DISCUSSION

The chemical composition of clastic sedimentary rocks is controlled by source rock compositions, weathering, sedimentary sorting, and post-depositional alteration. The following paragraphs examine the effects of post-depositional alteration and weathering on compositions of the studied Timiskaming samples.

Most of the sedimentary rocks of the Timiskaming Group exhibit greenschist facies metamorphism (Jolly, 1980). Rocks adjacent to intrusions may grade up to amphibolite facies whereas the central part of the Timiskaming Group (between Victoria Lake and LLCF; Fig. 1) only

exhibits sub prehnite-pumpellyite facies (Jolly, 1980; this study). Some major elements, especially LILE, are mobile during low-grade metamorphism (e.g., Merriman et al., 1986), but REE and high field strength elements (HFSE) are generally least susceptible to remobilization (e.g., Cullers et al., 1974; Condie and Martell, 1983) and therefore their concentrations should reflect those of their source rocks.

Submarine hydrothermal alteration of sediments may increase Na_2O and MgO contents by forming albite and chlorite (e.g., Nesbitt and Young, 1989). Na/K and Mg/K ratios are mostly low (< 10) and do not show any evidence of submarine alteration, such as low contents of mobile trace elements (i.e., Rb and Ba). High Na/K (177) and Mg/K (307) ratios of one sample, 49b, are attributed to low K_2O (0.02 %), and not due to an increase in Na_2O (3.69 %) and MgO (3.93 %). It is, therefore, concluded that none of the samples have undergone pervasive seawater alteration.

Alteration of feldspars to clay minerals is the dominant process during weathering. The Chemical Index of Alteration, (CIA; $(Al_2O_3/Al_2O_3+CaO+Na_2O+K_2O)x100$), was introduced by Nesbitt and Young (1982) as a measure of the degree of weathering of the source rocks. Only CIA values for samples with low carbonate contents were calculated, because CaO in the CIA is the amount of CaO incorporated in the silicate fraction of the rock. The CIA values of shale samples from the TNU and TSU vary from 68 to 77, which fall within typical shales (70 to 75; Nesbitt and Young, 1982). The high CIA values are consistent with common occurrences of sericite (CIA = 75) and chlorite (CIA = 100) in the shales. Similar values between fine-grained sedimentary rocks of the CSU (68 ± 5; n = 2), the TNU (72 ± 3; n = 6) and the TSU (75 ± 2; n = 2) indicate that these units were formed from moderately to highly weathered rocks and that they were deposited in similar climatic environments.

Comparison of compositions of rocks of similar grain sizes indicates that the different compositions are not due to sorting. Sedimentary rocks of the TNU and TSU form similar trends lying between the weathering trends of granitic (A) and basaltic (B) sources; the TSU appearing to have a more mafic source (Fig. 8). Shales of the TU are depleted in alkalies (i.e., Na_2O, K_2O) suggesting moderate to high chemical weathering while sandstones indicate lower degrees of weathering (more plagioclase). Diagenesis does not appear to have been accompanied by significant changes in the composition of the sedimentary rocks since samples within each unit do not exhibit chloritization or sericitization trends (Fig. 8). We conclude therefore that the compositions of the studied rocks, except for mobile elements, should reflect those of their sources.

Provenance

High LILE are expected for the CSU sedimentary rocks as they contain clasts of alkalic volcanic rocks which have elevated LILE (U = 3.9 $\pm$ 2.6 ppm; Th= 22.5 $\pm$ 7.0 ppm; Ujike, 1985). High LILE along with similar mineralogy and chemical compositions of the TNU and CSU indicate that the two units had alkaline volcanic rocks as a source. The overall low U and Th concentrations of the TSU precludes the possibility that the unit formed from a similar source as the CSU and the TNU.

Source-rock types for the units are evaluated by examining clast types of associated conglomerates. Clasts from the CSU conglomerates are mostly mafic and alkalic volcanic rocks, and felsic porphyries (Fig. 2). The TSU conglomerates have contrasting major clast types: ultramafic, mafic and felsic volcanic rocks (Fig. 2).

Source rocks may be further estimated from chemical compositions of shales. Although

Figure 8. Ternary diagram Al_2O_3-($CaO+Na_2O+K_2O$)-($FeO_{tot}+MgO$) showing weathering trends of granitic source (arrow with A) and basaltic source (arrow with B) according to Nesbitt and Young (1989). Ka = kaolinite; Ill = illite; Chl = chlorite; Bt = biotite; Kfs = feldspar; Hb = hornblende; Ms = muscovite; Sm = smectite. Shale samples are circled with stippled line.

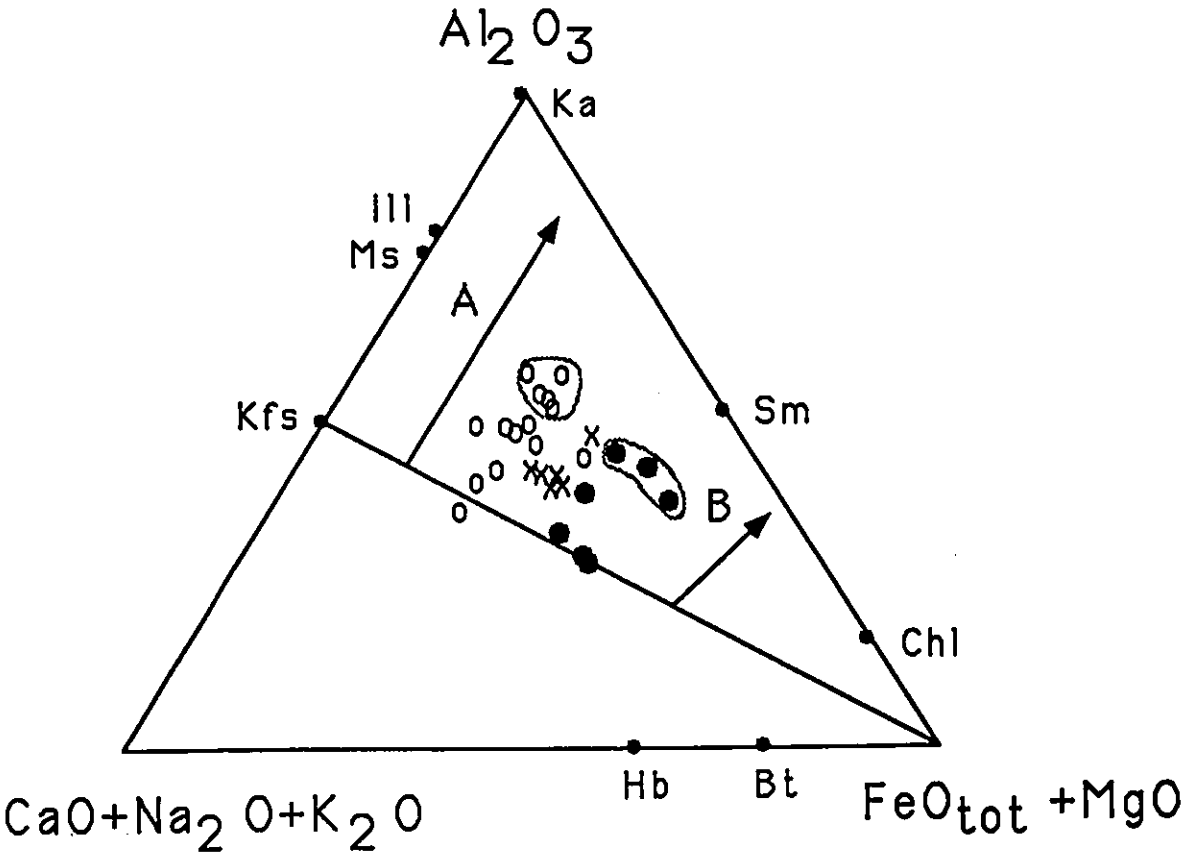

x CSU o TNU • TSU

chemical compositions of sandstones and shales are similar, shales are more suitable for the provenance studies because of their chemical homogeneity and post-depositional impermeability. High Cr, Ni and MgO of TSU shales suggest a large influx of ultramafic rocks as suggested by Feng and Kerrich (1990). The occurrence of spinifex-textured ultramafic volcanic rocks as clasts in the conglomerates of TSU support this view. The Cr/Th ratios (120 to 460) of TSU are significantly higher than TNU (12 to 18) and CSU (10 to 31) and are similar to those of late Archaean basalts (400; Condie, 1993), which again confirms a large contribution of mafic volcanic rocks to the TSU. The elevated $Fe_2O_{3(tot.)}$ content (> 10 wt.%) of some TSU rocks may also suggest the influx of banded-iron formation which has also been observed in clasts.

Five relatively immobile trace elements (Cr, Ni, Th, Ti, and Zr) are selected for the calculation of sources. Three rock types, abundant as clasts in associated conglomerates, are assumed to be the sources for turbidites: trachyte, Mg-rich tholeiitic basalt and calc-alkaline quartz monzodiorite for the TNU and komatiite, andesite and rhyolite for the TSU (Table 5 and 6). Compositions of sources (except for komatiite and rhyolite) are taken from chemical analysis of conglomerate clasts of the CSU and TSU. Trace element compositions are taken from published data from the southern Abitibi greenstone belt that have major element compositions similar to the analyzed clasts. Komatiite and rhyolite compositions were taken from Condie (1981) and Jensen and Langford (1985) for komatiite, and Goodwin (1979) and Taylor and McLennan (1985) for rhyolite, as chemically representative of these two rock types. Contributions of each source to the TNU and TSU shales were then calculated using mass balance equations and assuming no losses of elements during weathering/transportation. There is no known mecanisms to remove these elements during sedimentary processes and therefore this assumption is reasonable.

Results of model calculations suggest that the TNU was derived from 20% trachytic volcanic rocks, 20% tholeiitic basalts and 60% calc-alkaline quartz monzodiorites (Table 5). Discrepancies of trace element contents between calculated and observed values are less than 10%. Source rocks for the TSU are estimated at 12% rhyolites, 18% komatiites and 70% calc-alkaline andesites (Table 6). The difference between calculated and observed trace element concentrations is less than 15%. The higher discrepancy for the latter is probably due to the poor constraints of compositions of the source rhyolites and komatiites. The results are in general agreement with observed clast populations of TSU conglomerates (67% mafic volcanic, 23% ultramafic volcanic and 10% felsic volcanic; Fig. 2b) and CSU conglomerates (55% felsic porphyry, 26% alkalic volcanic and 19% mafic volcanic; Fig. 2a). The results are also in accord with the two-component mixing model of Feng and Kerrich (1990).

Calculated source-rock proportions for the TNU and TSU are also consistent with trace and REE data. The La-Th-Sc and Th-Sc-Zr/10 diagrams in Fig. 9 display the compositional trends of the different units and indicate that the end-member sources could have produced the observed compositions of TNU and TSU shales. Flat chondrite-normalized REE patterns for TSU shales are similar to the patterns of mafic-ultramafic volcanic rocks, and support that these were the major sources (Fig. 7). The highly fractionated REE patterns of the TNU shales are similar to those of calc-alkaline and alkaline rocks of the area, and support the interpretation that these were major source components (Fig. 7). Relatively elevated HREE values may indicate the presence of heavy minerals in the shales. REE contents calculated from the modeled sources give patterns that are similar to those of the shales from the turbidite units (Fig. 10). The agreement between the calculated and observed values further confirm the proposed sources for the sedimentary rocks.

Table 5. Modelling results for TNU shales.

	End-members				
	Trachyte	Porphyry	Basalt	Model	Observed#
Cr (ppm)	39	97	261	118	110
Ni	18	70	175	81	76
Th	23	6.0	0.5	8.3	7.6
Ti	4500	1920	7440	3540	3420
Zr	246	101	88	127	132
Contributions	0.20	0.60	0.20	1.00	
Ref.	a, b	b	b, c		

#-average of 7 samples
References: a-Ujike, 1985; b-Legault and Hattori, in prep.;
c-Goodwin, 1979.

Table 6. Modelling results for TSU shales.

	End-members				
	Komatiite	Andesite	Rhyolite	Model	Observed#
Cr (ppm)	2000	136	13	457	521
Ni	1000	81	12	238	232
Th	0.09	0.7	6.8	1.32	1.41
Ti	2700	5580	1680	4594	4980
Zr	35	72	210	82	73
Contributions	0.18	0.70	0.12	1.00	
Ref.	a, b	c, d	e, f		

#-average of 3 samples

References: a-Condie, 1981; b-Jensen and Langford, 1985; c-Ujike and Goodwin, 1987; d-Legault and Hattori, in prep.; e-Goodwin, 1979; f-Taylor and McLennan, 1985.

Figure 9. Trace element composition of the CSU, TSU and TNU on tectonic discrimination diagrams. Fields are from Bhatia and Crook (1986). A - Oceanic island arc; B - Continental island arc; C - Active continental margins; D - Passive margins. Solid lines link TNU and CSU mixing end-members (Tr-trachyte; Cap-calc-alkaline porphyry; Tb-tholeiitic basalt) while dashed lines link TSU mixing end-members (Kom-komatiite; And-andesite; Rhy-rhyolite). Compositions of end-members are from references in Table 5 and 6.

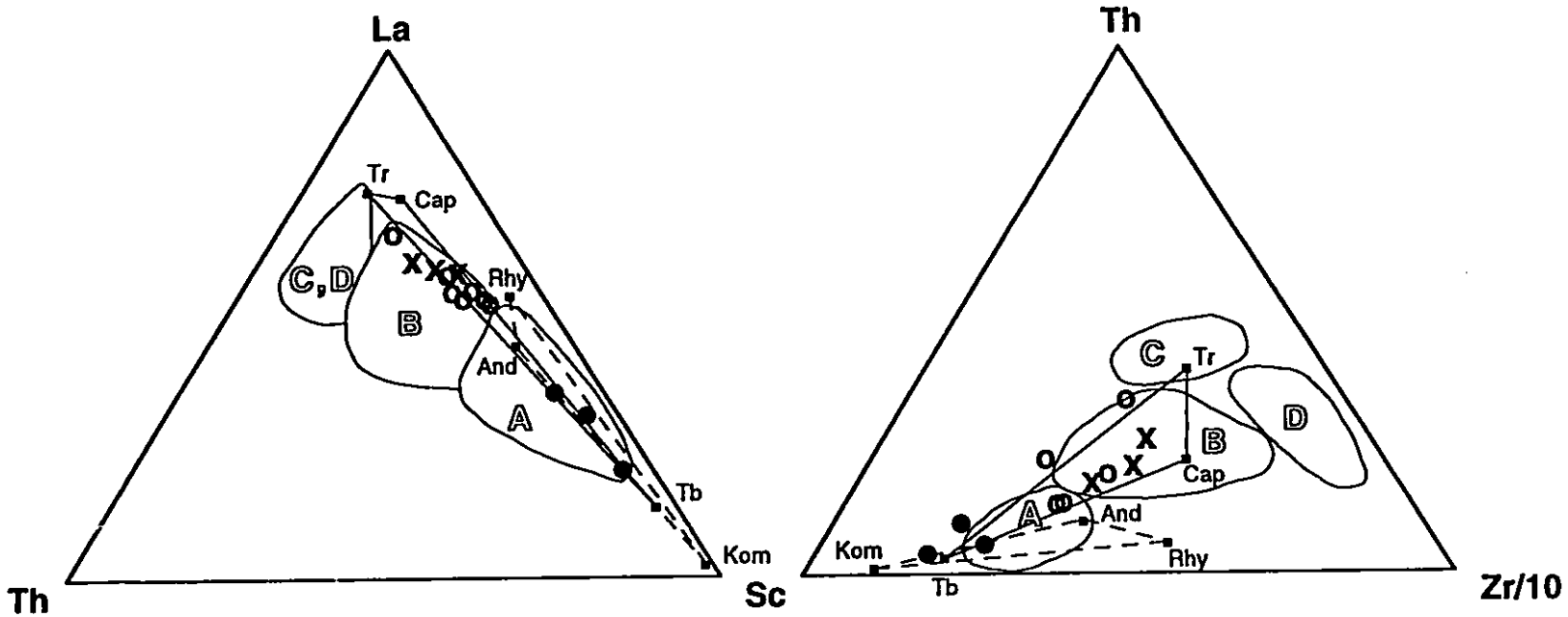

X CSU o TNU ● TSU

Figure 10. Chondrite-normalized REE patterns for modelled concentrations of TSU (A) and TNU (B) shales. C1 Chondrite values from Anders and Grevesse (1989). Observed patterns are stippled.

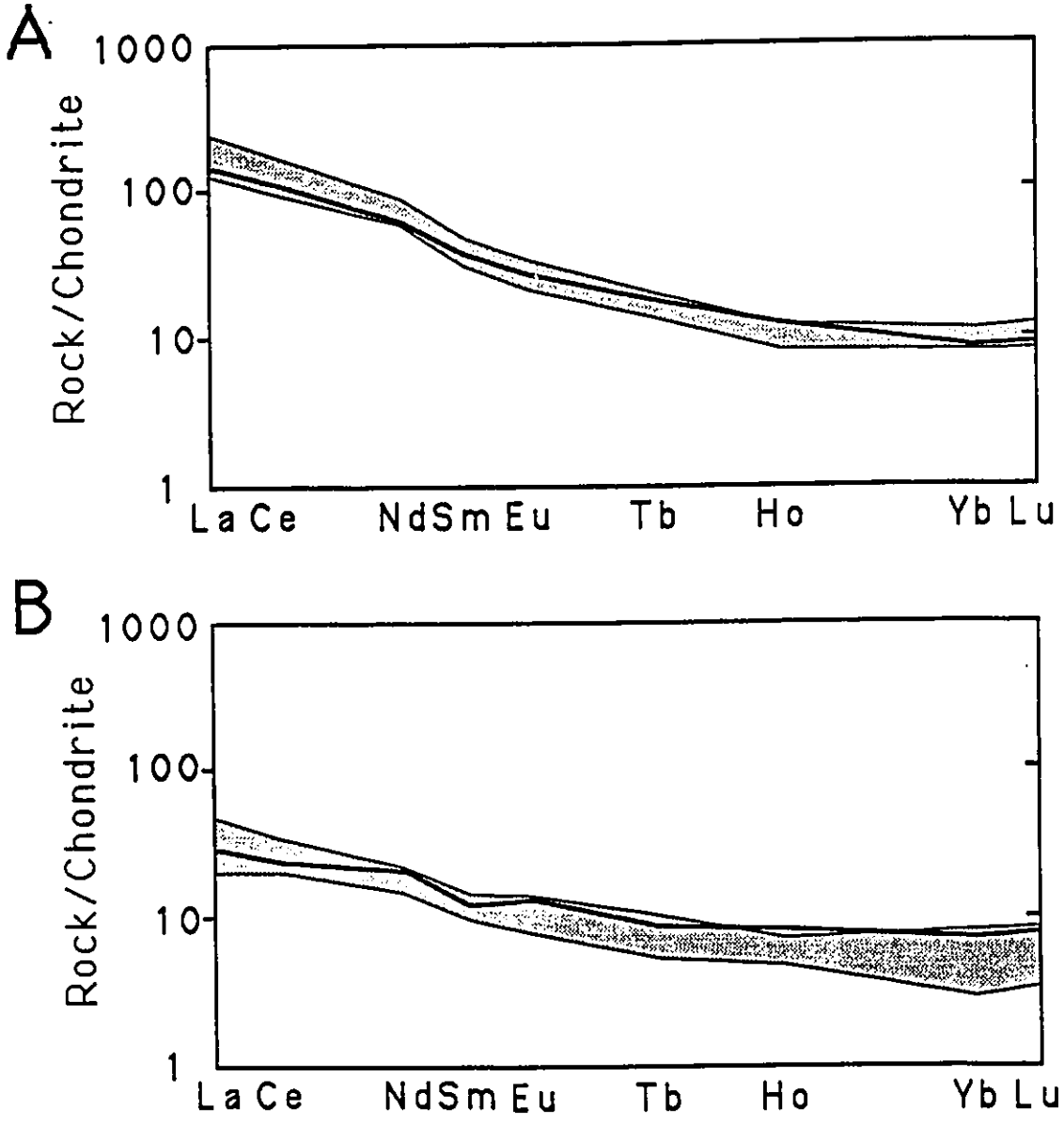
A
1000
100
10
1
Rock/Chondrite
La Ce
Nd Sm Eu
Tb
Ho
Yb Lu
B
1000
100
10
1
Rock/Chondrite
La Ce
Nd Sm Eu
Tb
Ho
Yb Lu

Redefinition of turbidite south of Larder Lake - Cadillac Fault

The TSU has generally been considered to be identical to the TNU(Hewitt, 1963; Hyde, 1980), but it is evident that the TSU is significantly different from the TNU and CSU. Such different sources for the two turbidite units may suggest that the TSU does not belong to the Timiskaming Group. Jensen (1985a, 1985b) proposed that the TSU is part of the Keewatin volcanic sequence, Larder Lake Group. We discount his proposal. First, the TSU overlies already deformed Larder Lake Group (Hewitt, 1949; this study). Second, the main source for the TSU is andesitic volcanic rocks whereas the Larder Lake Group is predominantly komatiitic volcanic rocks. Third, intercalated sedimentary rocks of the Larder Lake Group are petrographically and chemically dissimilar to the TSU (Table 1 and 3).

Spatial proximity of the TSU to the Pontiac Subprovince and similar sedimentary facies and mafic volcanic rock association has lead to the proposal that the TSU may be equivalent to the turbidites of the Pontiac Subprovince (Dimroth et al., 1982). The Pontiac turbidites, which occur ~15 km to the east, are highly deformed and metamorphosed to upper amphibolite grade (Dimroth et al., 1983). Sedimentary rocks are mature, high in quartz (> 90 vol.%), SiO_2 (~ 64 wt.%) and Zr (~ 150 ppm) and low in lithic fragments (mostly chert and quartzite), MgO (~ 3.5 wt.%) and Cr (~ 225 ppm)(Lajoie and Ludden, 1984: Camiré et al., 1993). The compositions and mineralogy are very different from the TSU and they were not derived from a similar source. We conclude therefore that the TSU is part of the Timiskaming Group and the tectonic setting for the sedimentation of the TSU was different from that for the CSU and TNU.

Geological setting

The LLCF deformation zone formed during a north-south compressional regime due to oblique accretion in the late Archaean (e.g., Card, 1990). The LLCF may be a zone dividing two tectonic blocks: northern Blake River block and southern Round Lake block (Ludden et al., 1986; Kerrich and Feng, 1992). It is generally accepted that the Timiskaming Group sedimentary rocks formed during this accretion process, but no consensus has been reached on the depositional setting. Proposed models include volcaniclastic sedimentation associated with uplift of calc-alkalic volcanic rocks along the LLCF before accretion (e.g., Dimroth et al., 1983), fault scarp sedimentation during accretion (e.g., Hodgson and Hamilton, 1989) or a pull-apart basin after accretion (e.g., Card, 1990).

The occurrences of abundant andesitic volcanic fragments, inclusion-free monocrystalline quartz grains and subhedral to euhedral, albite-twinned plagioclase grains suggest that graywackes from the TSU had an undissected arc provenance. Inclusion-free monocrystalline quartz is likely to represent phenocrysts of intermediate to felsic volcanic rocks. Sub to euhedral, albite-twinned plagioclase also suggests volcanic sources. Andesite clasts show "arc signatures" (e.g., Arculus and Powell, 1986) with low HFSE (TiO_2 = 0.7 to 0.9 wt.%, Zr = 99 to 134 ppm, Nb < 10 ppm). The inferred source-rock compositions and the lower abundances of quartz in the TSU rocks indicate a larger contribution from mafic-ultramafic volcanic rocks than the TNU and CSU.

The calc-alkaline and alkaline volcanic and subvolcanic rocks as sources for arenites of the CSU suggest they were also formed in arc setting. Quartz to plagioclase ratios of the arenites near 1 are similar to those in modern basins along the Circum-Pacific belt, such as western U.S.A., south-western Japan, Alaska and New Zealand (Dickinson, 1982). An arc setting is also in accord with the presence of intercalated shoshonitic volcanic rocks which are commonly found in mature arcs in

Phanerozoic terranes (Morrison, 1980).

Graywackes of TNU have similar compositions to the arenites of the CSU which suggest similar geological settings for the two. The mineralogical immaturity of the two, low quartz and high plagioclase, may reflect rapid erosion and short transportation for the sedimentary rocks. If the sources are similar, slightly higher ratios of quartz to plagioclase for the TNU than those of CSU may indicate that it was deposited further away from the source than the CSU.

Although it is recognized that the overall Archaean plate tectonic mechanism was different from that of today (e.g., Nisbet, 1984), late Archaean features may be satisfactorily explained by a variant of modern plate tectonics (Capdevila et al., 1982). The tectonic discrimination diagrams empirically developed from post-Archaean sedimentary rocks, such as those proposed by Dickinson and Suczek (1979), Dickinson et al. (1983), Bhatia (1983) and Bhatia and Crook (1986), may assist in differentiating various Archaean sedimentary rocks and provide an insight of the source rock types and depositional environments.

Tectonic settings inferred from petrographic and chemical data of the TSU, TNU and CSU are consistent with the interpretations described above. The graywackes of the TSU plot in the undissected arc sub-field, suggesting derivation from near-surface arc volcanic rocks (Dickinson et al., 1983; Fig. 11). Chemically the TSU is similar to sedimentary rocks deposited in an island arc setting (Fig. 9).

Sandstones of the CSU and TNU show chemical compositions similar to sediments deposited in a continental arc setting (Fig. 9) which is consistent with the inference of a thicker crust during alkaline volcanism of the Timiskaming Group (Capdevila et al., 1982). Petrographic data of the CSU indicates that this unit formed in a transitional volcanic arc terrane where subvolcanic intrusions

Figure 11. Abundances of framework minerals of sandstones from Kirkland Lake area; Qm = monocrystalline quartz grains; F = feldspar grains; Lt = lithic fragments. Fields are from Dickinson and Suczek (1979); MA = Magmatic Arc provenance; CB = Continental Block provenance; RO = Recycled Orogen provenance.

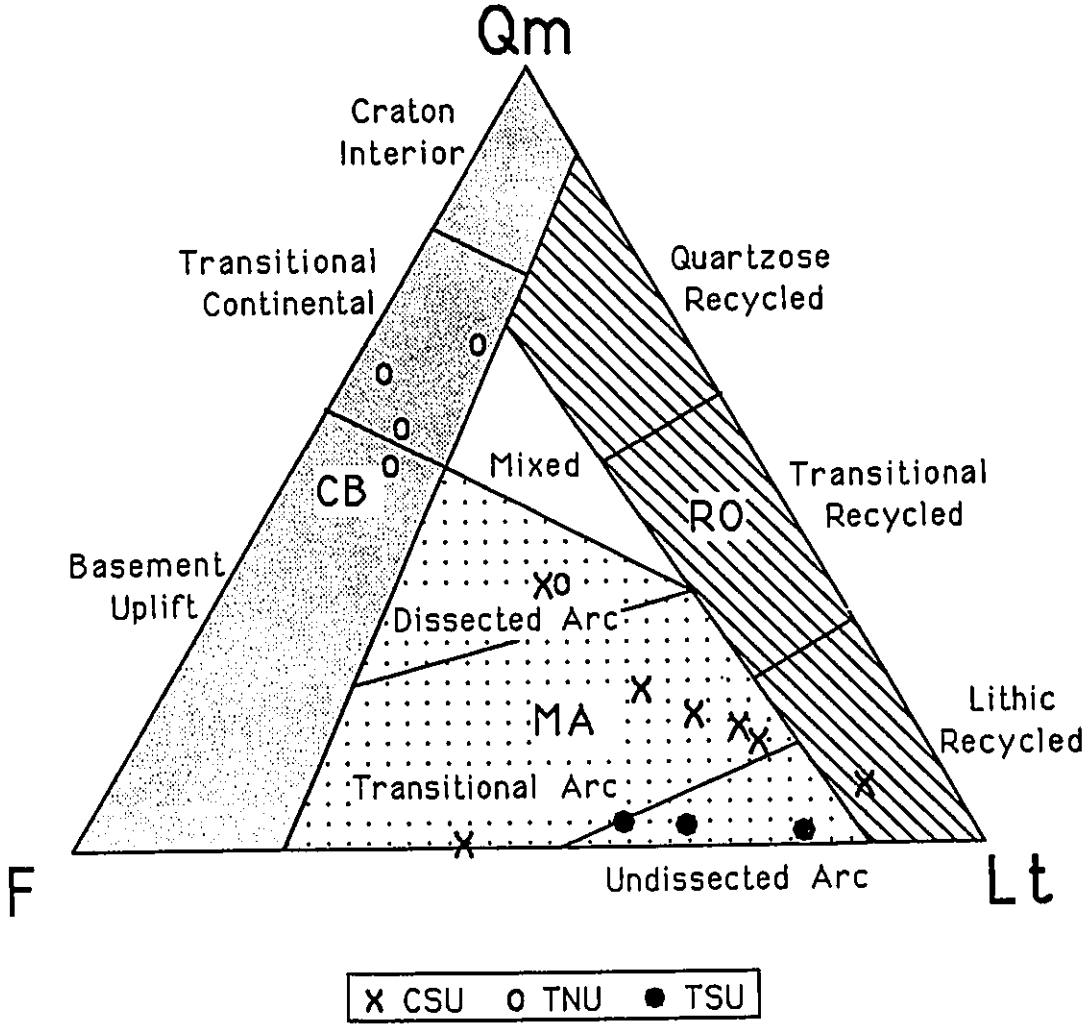
Qm
Craton
Interior
Transitional
Continental
Quartzose
Recycled
Mixed
Transitional
Recycled
CB
RO
Basement
Uplift
Dissected Arc
MA
Lithic
Recycled
Transitional Arc
Undissected Arc
F
Lt
X CSU
O TNU
● TSU

were exposed (Fig. 11).

The graywackes of the TNU plot mostly within the transitional sub-field of the petrographic discrimination diagram (Fig. 11), indicative of sediments derived from dissected source rocks in an unstable terrane (Dickinson et al., 1983).

Phanerozoic sedimentary rocks from a given tectonic setting commonly show a wide range of compositional variations and the range of compositions from one tectonic setting overlap with those of different tectonic settings (e.g., Dickinson et al., 1983; Bhatia and Crook, 1986). It is apparent, however, that the tectonic settings for the TSU and the CSU/TNU are different. Additional constraints are required to differentiate whether they formed in continental or oceanic arc settings.

Timing

Since alkalic volcanic rocks and coeval intrusions represent the youngest magmatism in the southern Abitibi belt (Corfu et al., 1991), the lack of an alkalic rock component in the TSU indicates its deposition before initiation of alkaline volcanism. It suggests that the TSU is the oldest unit of the Timiskaming Group. A maximum age is provided by the age of Keewatin volcanic rocks in the area (2700 Ma; Corfu et al, 1989) since the TSU overlies previously deformed ultramafic volcanic rocks (Hewitt, 1949). The minimum age is the maximum age of the CSU which is believed to have formed 2688 to 2677 Ma (Corfu et al, 1991).

The age of TSU corresponds to the cycle 3 (2700 - 2687 Ma) of the four basin-forming events within the Abitibi greenstone belt proposed by Mueller and Donaldson (1992), but the TSU is not mineralogically and chemically similar to other sedimentary rocks of this cycle as described by

Feng and Kerrich (1990). It would appear that this is due to the large influx of ultramafic volcanic rocks into the TSU. The contribution of ultramafic rocks is minor in other cycle 3 sedimentary rocks except for parts of the Dome Formation in Timmins (Feng and Kerrich, 1990).

The CSU was deposited after unroofing of calc-alkaline porphyries and during alkaline volcanism. Volcanic agglomerate of the Timiskaming Group, about 3 km north of Larder Lake, has been dated at 2677 $\pm$ 2 Ma (Corfu et al., 1991). The absence of K-rich holocrystalline clasts in the CSU conglomerates indicate that sedimentation ceased before unroofing of syenitic intrusions, which were co-magmatic with Timiskaming volcanic rocks and dated at ~2680 Ma (Corfu et al., 1989). An age of 2677 to 2688 Ma for the deposition of the CSU (Corfu et al., 1991) is consistent with the above observations.

Similar sources inferred for the TNU and CSU suggest that the two are contemporaneous. Slightly higher quartz/plagioclase ratios of the TNU graywackes than the CSU arenites suggest a distal source for the former, and a proximal source for the latter. Elevated abundances of lithic fragments in the rocks of the CSU are also consistent with a proximal source. If the two units were formed in the same basin, they were later structurally juxtaposed as suggested by Hamilton and Hodgson (1984). Alternatively, the TNU may have been deposited shortly after the formation of the CSU from similar sources. This is consistent with the observation that the TNU generally occurs south of the CSU, which youngs to the south. Also Thomson (1941) and Hewitt (1963) reported that the turbidite unit north of Larder Lake appears to conformably overlie the volcanic agglomerate of 2677 Ma (Corfu et al, 1991), which implies that the TNU may be younger than 2677 Ma.

To examine whether the TSU was a minor source for the CSU, sandstone clasts from CSU conglomerates were examined in detail. The clasts, however, are not similar to the graywackes of the

TSU. Sandstone clasts from the CSU are plagioclase- and quartz-rich arenites and graywackes, compared to lithic graywackes of the TSU. Chemical compositions of the clasts also differ from the TSU. Arenite clasts, however, are similar both chemically and mineralogically to plagioclase-rich arenites of the CSU. Graywacke clasts do not show any resemblance to exposed sedimentary rocks of the area. Their ratio of quartz to feldspar is much lower than that of the sandstones of the TNU and CSU. The results suggest that arenite clasts may be intrabasinal while the graywacke clasts may have come from sedimentary rocks that are now eroded or alternatively, they may have been derived from minor volcaniclastic sedimentary rocks that are present in the greenstone volcanic rocks of the area.

Geological development of the area

The results of the present study indicate that the TSU formed as a result of erosion of an undissected volcanic arc terrane, because most clasts are of volcanic origin with little contribution of subvolcanic component. Chemical compositions of the abundant calc-alkaline volcanic clasts suggest that they were derived from an uplifted arc. The presence of an ultramafic component was attributed to sedimentation in proximity to an active rift by Feng and Kerrich (1990). This interpretation is however not consistent with the abundance of calc-alkalic clasts. We propose that the high ultramafic component is due to obduction of oceanic crust before or during sedimentation, probably by a mechanism similar to the ophiolitic suites along modern convergent plate margins (Moores, 1982). The most likely depositional site for the TSU is inferred to be a fore-land basin during oblique accretion and uplift of calc-alkaline volcanic rocks. The temporal relationship of sedimentation of the TSU with arc accretion is consistent with the interpretation that cycle 3 basins

connected arc terranes (Mueller and Donaldson, 1992).

The CSU has carbonatized ultramafic clasts, carbonatized porphyry clasts and detrital carbonate grains, which were in part derived from carbonate veins. This evidence may indicate that the activity of LLCF was initiated before sedimentation of the CSU, providing the conduit for CO_2-rich hydrothermal fluids.

The CSU may have formed during arc volcanism before accretion (Dimroth et al., 1983), in a pull-apart basin along the LLCF (e.g., Thurston and Chivers, 1990; Card, 1990) or as a fault-scarp deposit that accumulated during oblique thrusting along the LLCF (e.g., Hodgson and Hamilton, 1989). The presence of CSU occurrences north and south of the LLCF indicates that sedimentation of this unit appears to have taken place after juxtaposition and is therefore not consistent with the model proposed by Dimroth et al. (1983). The findings of this study are consistent with the latter two interpretations. Contemporaneous alkaline volcanism may favour a pull-apart basin since it can provide a crustal-scale dilation zone for magma to ascend.

The lack of clasts similar to the TSU in the CSU indicates that the TSU was not eroded during sedimentation of the CSU. The CSU may therefore have been deposited directly on the TSU. Subsequent vertical movement along the LLCF (south-side up; Hodgson and Hamilton, 1989; Jackson and Sutcliffe, 1990) may have caused preferential erosion of the rocks south of the fault, so that only occurrences of TSU and CSU in fault-bounded blocks are preserved south of the LLCF (Corfu et al., 1991). Contacts between the CSU and TSU are faulted, which prevents examination of their original relationship. Alternatively, the TSU may not have been present in the area during CSU sedimentation, but was later juxtaposed due to strike slip movement along the LLCF. The occurrence of the CSU north and south of the LLCF only in the area appears to discount the latter

interpretation.

Late Archaean upper crust

This study indicates that calc-alkaline volcanic rocks and associated subvolcanic intrusions were the major sources for the sedimentary rocks of the Timiskaming Group and were prominently exposed rock-types in the area. The erosion of these rocks has led to the exposure of tholeiitic basalts and intrusions which are presently exposed.

Andesite is estimated to represent 16% of presently exposed late Archaean volcanic rocks and 5% of the upper continental crust in late Archaean time (Condie, 1993). Low abundances of andesite are consistent with other estimates on the aerial exposure of Archaean rock-types (e.g., Taylor and McClennan, 1985; Ayres and Thurston, 1985). Although erosion was considered for the calculations of the upper continental crust (Condie, 1993), the proportion of volcanic rock-types exposed at present were assumed to be identical in the eroded volcanic rocks. This study suggests that the proportion of currently exposed rocks is biased towards basalts because they were below the erosional level and therefore the inferred composition of late Archaean upper continental crust appears to underestimate the amount of andesite.

SUMMARY

Two distinct turbidite units are recognized in the Kirkland Lake area. The TSU consists of quartz-poor lithic graywackes and shales with minor conglomerates which were derived from a source of rhyolite (12%), komatiite (18%) and andesite (70%). The TNU is composed of interbedded

quartz-rich feldspathic graywackes and shales, with rare occurrences of conglomerates, and was derived from trachyte (20%), tholeiitic basalt (20%) and calc-alkaline quartz monzodiorite (60%). The rocks in the latter unit are similar to arenites and siltstones of the CSU. The TNU and CSU were derived from similar sources.

The TSU, the oldest unit of the Timiskaming Group sedimentary succession, was likely deposited in a fore-land basin during uplift of calc-alkaline volcanic rocks and obduction of ultramafic rocks associated with accretion. Deposition of this unit took place prior to the juxtaposition of tectonic blocks along the LLCF. The CSU was deposited during alkaline volcanism and after the unroofing of calc-alkaline porphyry intrusions. It was likely deposited after juxtaposition of the two tectonic blocks along the LLCF. The TNU is inferred to have formed at the same time as the CSU, or shortly thereafter. Deposition of the two, however, terminated before the unroofing of K-rich intrusive rocks, which are now predominant in the area. Andesitic volcanic rocks indicated as a major source for the TSU suggest that these rocks were more extensively exposed but removed by erosion.

ACKNOWLEDGEMENTS

We thank Wulf Mueller and Josée Desgagné of Université du Québec à Chicoutimi for collaboration, and advice in the field, Brian Charbonneau of the Geological Survey of Canada for permission to use the γ-ray spectrometer, Ron Hartree of the University of Ottawa and Richard Rousseau of the Geological Survey of Canada for XRF analyses, Greg Kennedy of Université de Montréal (INAA) for REE determinations and Zoran Mador at the Drill Core Library of the

Ministry of Northern Development and Mines at Swastika for supplemental samples. The manuscript benefited from comments by J. Allan Donaldson, K.C. Condie and anonymous journal reviewers. The project was funded by a Natural Sciences and Engineering Research Council of Canada grant to K.H..

REFERENCES

Anders, E. and Grevesse, N., 1989. Abundances of the elements: Meteoric and solar. Geochim. Cosmochim. Acta, 53: 197-214.

Arculus, R.J. and Powell, R., 1986. Source component mixing in the regions of arc magma generation. J. Geophys. Res., 91: B5913-B5926.

Ayres, L.D. and Thurston, P.C., 1985. Archean supracrustal sequences in the Canadian Shield: a review. In: L.D. Ayres, P.C. Thurston, K.D. Card and W. Weber (Editors), Evolution of Archean Supracrustal Sequences, Geol. Assoc. Can. Spec. Pap., 28: 343-380.

Bhatia, M.R., 1983. Plate tectonics and geochemical compositions of sandstones. J. Geol., 91: 611-627.

Bhatia, M.R. and Crook, K.A.W., 1986. Trace element characteristics of greywackes and tectonic setting discrimination of sedimentary basins. Contrib. Miner. Petrol., 92: 181-193.

Camiré, G.E., Laflèche, M.R. and Ludden, J.N., 1993. Archaean metasedimentary rocks from the northwestern Pontiac Subprovince of the Canadian Shield: Chemical characterization, weathering and modelling of the source areas. Precambrian Res., 62:285-305.

Capdevila, R., Goodwin, A.M., Ujike, O. and Gorton, M.P., 1982. Trace element geochemistry of Archean volcanic rocks and crustal growth in SW Abitibi belt, Canada. Geology, 10: 418-422.

Card, K.D., 1990. A review of the Superior Province of the Canadian Shield, a product of Archean accretion. Precambrian Res., 48: 99-156.

Charbonneau, B.W., Ford, K.L. and Cameron, G.W., 1981. Equilibrium between U and eU (214Bi)

in surface rocks of Canada. Geol. Surv. Can. Pap., 81-1C: 45-50.

Condie, K.C., 1981. Archean Greenstone Belts. Elsevier, Amsterdam, 434pp.

Condie, K.C., 1993. Chemical composition and evolution of the upper continental crust: Contrasting results from surface samples and shales. Chem. Geol., 104, 1-37.

Condie, K.C. and Martell, C., 1983. Early Proterozoic metasediments from north-central Colorado: Metamorphism, provenance, and tectonic setting. Geol. Soc. Am. Bull., 94: 1215-1224.

Corfu, F., Krogh, T.E., Kwok, Y.Y and Jensen, L.S., 1989. U-Pb zircon geochronology in the southwestern Abitibi greenstone belt, Superior Province. Can. J. Earth Sci., 26: 1747-1763.

Corfu, F., Jackson, S.L. and Sutcliffe, R.H., 1991. U-Pb ages and tectonic significance of late Archean alkalic magmatism and nonmarine sedimentation: Timiskaming Group, southern Abitibi belt, Ontario. Can. J. Earth Sci., 28: 489-503.

Cullers, R.L., Yeh, L. and Chaudhuri, S., 1974. Rare earth elements in Silurian pelitic schists from NW Maine. Geochim. Cosmochim. Acta, 38: 389-400.

David, J. and Lajoie, J., 1989. Sedimentology of an Archean submarine channel-fill deposit in the Abitibi greenstone belt of Canada. Can. J. Earth Sci., 26: 1453-1462.

Dickinson, W.R., 1982. Compositions of sandstones in circum-Pacific subduction complexes and fore-arc basins. Am. Assoc. Petroleum Geol. Bull., 66: 121-137.

Dickinson, W.R. and Suczek, C.A., 1979. Plate tectonics and sandstone compositions. Am. Assoc. Petroleum Geol. Bull., 63: 2164-2182.

Dickinson, W.R., Beard, L.S., Brakenridge, G.R., Erjavec, J.L., Ferguson, R.C., Inman, K.F., Knepp, R.A., Lindberg, F.A. and Ryberg, P.T., 1983. Provenance of North American Phanerozoic sandstones in relation to tectonic setting. Geol. Soc. Am. Bull., 94: 222-235.

Dimroth, E., Imreh, L., Rocheleau, M. and Goulet, N., 1982. Evolution of the south-central part of the Archean Abitibi Belt, Quebec. Part I: Stratigraphy and paleogeographic model. Can. J. Earth Sci., 19: 1729-1758.

Dimroth, E., Imreh, L., Goulet, N. and Rocheleau, M., 1983. Evolution of the south-central segment of the Archean Abitibi belt, Quebec. Part III: Plutonic and metamorphic evolution and geotectonic model. Can. J. Earth Sci., 20: 1374-1388.

Feng, R. and Kerrich, R., 1990. Geochemistry of fine-grained clastic sediments in the Archean Abitibi greenstone belt, Canada: Implications for provenance and tectonic setting. Geochim. Cosmochim. Acta, 54: 1061-1081.

Goodwin, A.M., 1979. Archean volcanic studies in the Timmins Kirkland Lake Noranda region of Ontario and Quebec. Geol. Surv. Can. Bull., 278.

Hamilton, J.V. and Hodgson, C.J., 1984. Structural geology and gold mineralization in Kirkland-Larder Lake Deformation Zone. Ont. Geol. Surv. Misc. Paper, 119: 220-225.

Hewitt, D.F., 1949. Geology of Skead Township, Larder Lake area. Ont. Dept. Mines, Annu. Rep., 58: 1-43.

Hewitt, D.F., 1963. The Timiskaming Series of the Kirkland Lake area. Can. Mineral., 7: 497-522.

Hodgson, C.J. and Hamilton, J.V., 1989. Gold mineralization in the Abitibi Greenstone Belt: End-stage result of Archean collisional tectonics?. Econ. Geol. Monograph, 6: 86-100.

Hyde, R.S., 1978. Sedimentology, volcanology, stratigraphy, and tectonic setting of the Archean Timiskaming Group, Abitibi greenstone belt, northeastern Ontario, Canada. Ph.D. thesis, McMaster University, Hamilton (unpubl.), 422pp.

Hyde, R.S., 1980. Sedimentary facies in the Archean Timiskaming Group and their tectonic

implications, Abitibi greenstone belt, northeastern Ontario, Canada. Precambrian Res., 12: 161-195.

Jackson, S.L. and Fyon, J.A., 1991. The Western Abitibi Subprovince. In: P.C. Thurston, H.R. Williams, R.H. Sutcliffe and G.M. Stott (Editors), Geology of Ontario, Ont. Geol. Surv. Spec. Vol., 4: 405-482.

Jackson, S.L. and Sutcliffe, R.H., 1990. Central Superior Province geology: evidence for an allochthonous, ensimatic, southern Abitibi greenstone belt. Can. J. Earth Sci., 27: 582-589.

Jensen, L.S., 1985a. Stratigraphy and petrogenesis of Archean metavolcanic sequences, southwestern Abitibi Subprovince, Ontario. In: L.D. Ayres, P.C. Thurston, K.D. Card and W. Weber (Editors), Evolution of Archean supracrustal sequences, Geol. Assoc. Can. Spec. Pap., 28: 65-87.

Jensen, L.S., 1985b. Synoptic mapping of the Kirkland Lake -Larder Lake areas, District of Timiskaming. Ont. Geol. Surv. Misc. Pap., 126: 112-120.

Jensen, L.S. and Langford, F.F., 1985. Geology and petrogenesis of the Archean Abitibi Belt in the Kirkland Lake area, Ontario. Ont. Geol. Surv. Misc. Pap., 123: 130 pp.

Jolly, W.T., 1980. Development and degradation of Archean lavas, Abitibi area, Canada, in light of major element geochemistry. J. Petrol., 21: 323-363.

Kerrich, R. and Feng, R., 1992. Archean geodynamics and the Abitibi-Pontiac collision: Implications for advection of fluids at transpressive collisional boundaries and the origin of giant quartz vein systems. Earth Sci. Rev., 32: 33-60.

Killeen, P.G., 1979. Gamma-ray spectrometric methods in uranium exploration - application and interpretation. In: P.J. Hood (Editor), Geophysics and Geochemistry in the Search for

Metallic Ores, Geol. Surv. Can., Econ. Geol. Rep., 31: 163- 229.

Lajoie, J. and Ludden, J., 1984. Petrology of the Archean Pontiac and Kewagama sediments and implications for the stratigraphy of the southern Abitibi belt. Can. J. Earth Sci., 21: 1305-1314.

Ludden, J., Hubert, C. and Gariépy, C., 1986. The tectonic evolution of the Abitibi greenstone belt of Canada. Geol. Mag., 123: 153-166.

Merriman, R.J., Bevins, R.E. and Ball, T.K., 1986. Petrological and mineralogical variations within the Tal y Fan intrusion: A study of element mobility during low-grade metamorphism with implications for petrotectonic modelling. J. Sediment. Petrol., 27: 1409-1436.

Moores, E.M., 1982. Origin and emplacement of ophiolites. Reviews of Geophysics and Space Physics, 20: 735-760.

Morrison, G.W., 1980. Characteristics and tectonic setting of the shoshonite rock association. Lithos, 13: 97-108.

Mueller, W., Donaldson, J.A., Dufresne, D. and Rocheleau, M., 1991. The Duparquet Formation: sedimentation in a late Archean successor basin, Abitibi greenstone belt, Quebec, Canada. Can. J. Earth Sci., 28: 1394-1406.

Mueller, W. and Donaldson, J.A., 1992. Development of sedimentary basins in the Archean Abitibi belt, Canada: an overview. Can. J. Earth Sci., 29: 2249-2265.

Nesbitt, H.W. and Young, G.M., 1982. Early Proterozoic climates and plate motions inferred from major element chemistry of lutites. Nature, 299: 715-717.

Nesbitt, H.W. and Young, G.M., 1989. Formation and diagenesis of weathering profiles. J. Geol., 97: 129-147.

Nisbet, E.G., 1984. The continental and oceanic crust and lithosphere in the Archaean: isostatic, thermal, and tectonic models. Can. J. Earth Sci., 21: 1426-1441.

Pettijohn, F.J., Potter, P.E. and Siever, R., 1973. Sand and sandstone. Springer-Verlag, Berlin, 628 pp.

Shegelski, R.J., 1980. Archean cratonization, emergence and red bed development, Lake Shebandowan area, Canada. Precambrian Res., 12: 331-347.

Taylor, S.R. and McLennan, S.M., 1985. The continental crust, its composition and evolution. Blackwell, Oxford, 312 pp.

Thomson, J.E., 1941. Geology of McGarry and McVittie townships. Ont. Dept. Mines, Annu. Rep., 50, part 7: 99 pp.

Thurston, P.C. and Chivers, K.M., 1990. Secular variation in greenstone sequence development emphasizing Superior Province, Canada. Precambrian Res., 46: 21-58.

Ujike, O., 1985. Geochemistry of Archean alkalic volcanic rocks from the Crystal Lake area, east of Kirkland Lake, Ontario, Canada. Earth Planet. Sci. Lett., 73: 333-344.

Ujike, O. and Goodwin, A.M., 1987. Geochemistry and origin of Archean felsic metavolcanic rocks, Central Noranda area, Quebec, Canada. Can. J. Earth Sci., 24: 2551-2567.

PROVENANCE OF IGNEOUS CLASTS IN CONGLOMERATES OF THE ARCHAEAN TIMISKAMING GROUP, KIRKLAND LAKE AREA, ABITIBI GREENSTONE BELT, CANADA

Marc I. Legault and Keiko Hattori

Ottawa-Carleton Geoscience Centre and Department of Geology, University of Ottawa, Ottawa, Ontario, Canada, K1N 6N5

To be submitted to

Canadian Journal of Earth Sciences

November, 1993

ABSTRACT

The alluvial-fluvial assemblage of the Timiskaming Group was examined north and south of the Larder Lake-Cadillac Fault (LLCF). The clasts within conglomerates are mostly of igneous origin with a small proportion of sedimentary origin. Four main types of igneous clasts were recognized: calc-alkaline porphyry, alkaline volcanic rocks, trondhjemite and tholeiitic volcanic rocks. Calc-alkaline porphyry clasts were not comagmatic with the late porphyry intrusions presently exposed in the area. They are comagmatic with early diorite intrusions north of the LLCF and genetically related to the underlying calc-alkalic volcanic rocks of the Blake River Group. Alkaline volcanic and associated sub-volcanic clasts were derived from Timiskaming Group alkalic rocks. Trondhjemite clasts appear to have been derived from the marginal phases of the Round Lake batholith whereas the tholeiitic volcanic rocks are from the underlying greenstone belt volcanic rocks.

Initial sedimentation of the alluvial-fluvial assemblage postdated unroofing of calc-alkaline porphyries (2685 Ma) and predated unroofing of exposed syenites and feldspar porphyries (2677 Ma). The distribution of alkaline clasts only in proximity to the LLCF suggest that alkaline magmatism was confined along the fault. This is consistent with the hypothesis that dilation associated with strike-slip movement along the LLCF provided a conduit for alkaline magmatism. The calc-alkaline porphyry clasts are chemically and mineralogically similar to intrusions of Phanerozoic arcs. Their genetic relationship with the Blake River Group, which is considered to be the product of island-arc volcanism, suggests the main source was an island-arc terrane. Abundance of andesitic clasts decreases and clasts of porphyry and tholeiitic basalt increase up the stratigraphic section. This suggests progressive dissection of an arc terrane. Presence of the

alluvial-fluvial assemblage on both sides of the LLCF indicates that the Round Lake and Blake River tectonic blocks were juxtaposed before sedimentation. Proximal sources of clasts on both sides of the LLCF appears to favor a pull-apart basin for deposition of the alluvial-fluvial assemblage, with a small amount of strike-slip movement during and after sedimentation.

INTRODUCTION

Late Archaean orogenic sedimentary successions in the Superior Province of the Canadian Shield lie unconformably over greenstone-belt metavolcanic rocks and are referred to as Timiskaming-type rocks (e.g., Shegelski, 1980; Mueller et al., 1991; Rice and Donaldson, 1992). The type locality of the Timiskaming Group is in the Kirkland Lake area (Hewitt, 1963; Fig. 1) where it consists of an alluvial-fluvial assemblage intercalated with trachytic volcanic rocks, and a turbidite assemblage.

Various tectono-sedimentary settings have been proposed for the Timiskaming Group, including volcaniclastic sedimentation related to the final stages of island arc volcanism before accretion (e.g., Hyde, 1980; Dimroth et al., 1983), a fault-scarp deposit along an oblique thrust of the Larder Lake-Cadillac Fault (LLCF; e.g., Hodgson and Hamilton, 1989) and a pull-apart basin along the LLCF after juxtaposition of arc terranes (e.g., Thurston and Chivers, 1990; Card, 1990). Previous work on the sedimentary rocks include stratigraphic (Hewitt, 1963), sedimentological (Hyde, 1980; Mueller et al., 1992) and geochemical (Feng and Kerrich, 1990a) studies. No detailed petrological or geochemical work has been carried out on the clasts.

Conglomerate clasts reflect rocks exposed during sedimentation, and provide relevant

Figure 1. Geology map of the Kirkland Lake area modified from Hyde (1980). Inset: location of Kirkland Lake within the Abitibi Greenstone belt. A - Komatiitic volcanic rocks; B - Tholeiitic volcanic rocks; C - Calc-alkalic volcanic rocks; GP - Goodfish quartz porphyry; BP - Bidgood quartz porphyry; OS - Otto stock. Numbers represent outcrop locations of conglomerate sampling and point counting; solid circles indicate other examined conglomerates.

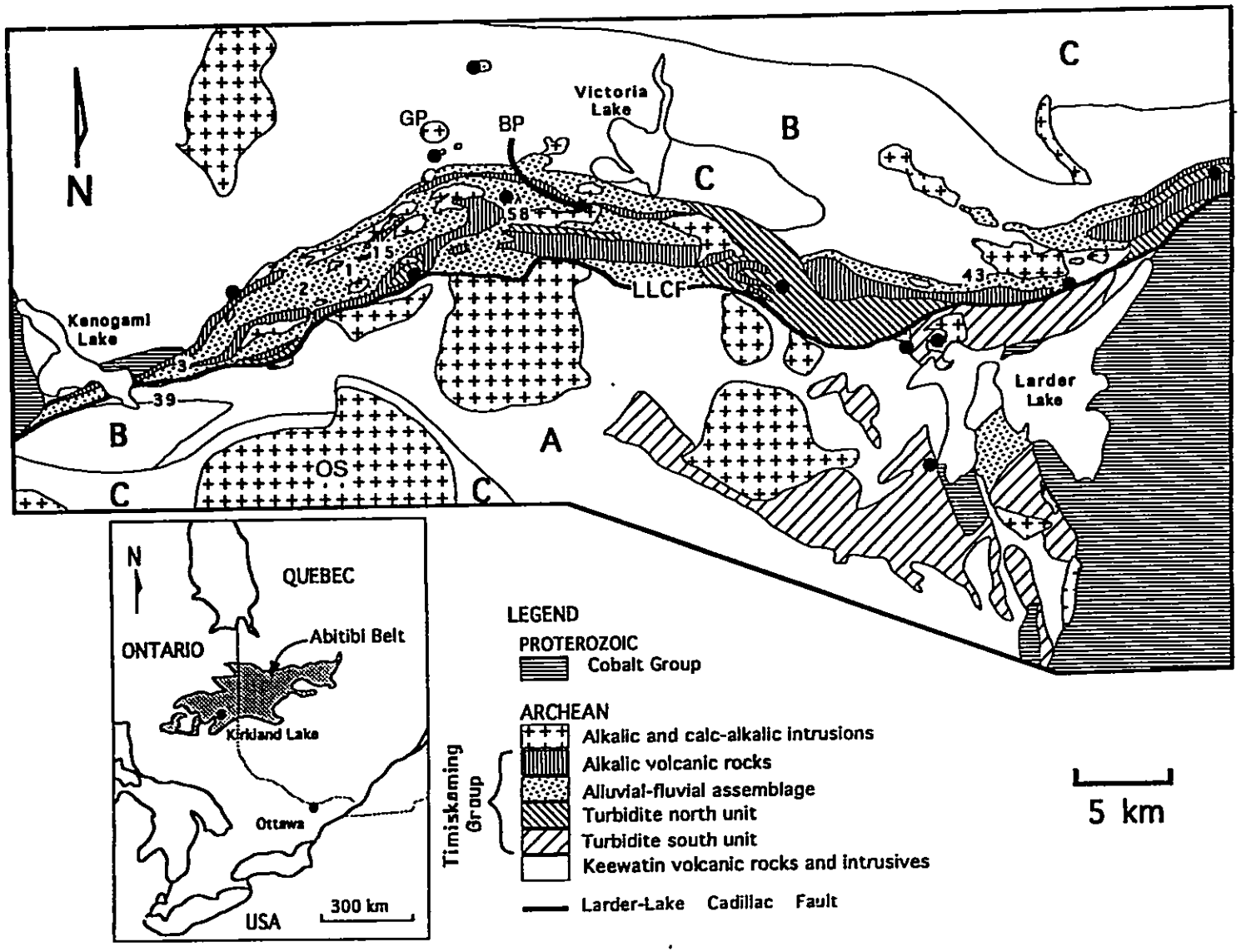
N
GP
BP
Victoria Lake
C
B
C
S8
1
2
15
LLCF
43
Kenogami Lake
3
39
B
A
OS
C
C
Larder Lake
N
QUEBEC
ONTARIO
Abitibi Belt
Kirkland Lake
Ottawa
USA
300 km
LEGEND
PROTEROZOIC
Cobalt Group
ARCHEAN
Alkalic and calc-alkalic intrusions
Timiskaming Group
Alkalic volcanic rocks
Alluvial-fluvial assemblage
Turbidite north unit
Turbidite south unit
Keewatin volcanic rocks and intrusives
Larder-Lake Cadillac Fault
5 km

information on the tectonic evolution of Phanerozoic and Proterozoic terranes (e.g., Seiders and Blome, 1988; Girard, 1992). With emphasis on provenance, this paper presents data on the petrology and geochemistry of igneous clasts from conglomerates of the Timiskaming Group in the Kirkland Lake area, and discusses the tectonic setting of the Timiskaming Group and the evolution of the southern Abitibi greenstone belt in the late Archaean.

GENERAL GEOLOGY

The general geology of the Kirkland Lake area has been described by Jensen and Langford (1985), Jackson and Fyon (1991). Greenstone-belts consist of volcanic rocks and associated intrusions ranging from komatiitic (Larder Lake Group) and tholeiitic (Kinojevis Group) to calc-alkalic (Blake River and Skead Groups; Fig. 1) and minor sedimentary rocks, including chert, banded iron formation and volcaniclastic rocks. Similar ages for the Larder Lake (2705 +3/-2 Ma), Blake River (2701 ± 2 Ma) and Skead Groups (2701 +3/-2 Ma) indicate that these greenstone belt volcanic rocks are broadly coeval (Corfu et al., 1989). The bulk of deformation and metamorphism of these rocks appears to have spanned 2680 to 2700 Ma, and was possibly due to north-south compression during oblique terrane accretion (e.g., Card, 1990).

The Timiskaming Group is composed of alluvial-fluvial and turbidite assemblages. The former is an east-trending, moderately south-dipping (30 to 60°) sequence, mostly north of the Larder Lake-Cadillac Fault (LLCF), but with a few occurrences south of the fault. The alluvial-fluvial assemblage is in angular unconformity with underlying greenstone belt volcanic rocks (Thomson, 1946). The assemblage consists mainly of clast-supported conglomerates interbedded

with cross-bedded sandstones and lenses of argillite. Conglomerates of this assemblage are the focus of this study.

Alkalic volcanic rocks intercalated with the sedimentary rocks consist mostly of trachyte (felsic, mafic and leucitic), and are inferred to represent the final stages of arc magmatism (Cooke and Moorhouse, 1969; Ujike, 1985). These rocks are associated with comagmatic syenite intrusions (2680 Ma; Corfu et al., 1989). They were later intruded by feldspar ± quartz porphyries (2677 Ma; Corfu et al., 1991) and lamprophyre dykes (2674 Ma; Wyman and Kerrich, 1989).

The metamorphic grade of the greenstone volcanic rocks in the area ranges from prehnite-pumpellyite to greenschist facies, except for rocks adjacent to intrusions (Jolly, 1980). Most Timiskaming Group rocks have undergone lower greenschist metamorphism, although some areas are at only sub prehnite-pumpellyite metamorphic grade (Jolly, 1980).

ANALYTICAL METHODS

Field investigations were carried out during the summers of 1991 and 1992. Deformation of conglomerate beds is intense only in the vicinity of the LLCF and other splay structures. In general, the conglomerates show no evidence of alteration, except in areas adjacent to gold deposits. Sixteen conglomerate outcrops were examined, of which 13 undeformed beds were point-counted with a 1 m^2 square grid divided into 10 cm x 10 cm squares in order to provide volumetric abundances of clast types (Table 1). A grid size equal to about twice the size of the average clast was chosen in order to eliminate counting of a same clast twice. Care was

Table 1. Abundances of clasts for conglomerate beds in percent. Location numbers refer to outcrops on Fig. 1. Roman numerals indicate the relative stratigraphic position of the beds within a location; i being the lowest.

Locations	1i	1ii	1iii	1iv	1v	1vi	2	3i	3iii	3iv	15	39i	39ii
Number of clast counted	148	128	157	137	75	50	133	95	110	132	308	144	99
Volcanic rocks	**47**	**30**	**19**	**18**	**25**	**24**	**14**	**69**	**39**	**38**	**33**	**75**	**56**
Felsic volcanic	-	2	-	9	9	3	-	-	-	-	-	2	2
Mafic volcanic	30	14	10	3	9	21	4	8	21	18	9	22	26
Ultra-mafic volcanic	4	Tr	2	-	-	-	-	-	-	5	Tr	-	1
Trachytic	4	11	4	-	4	-	-	61	12	12	12	32	18
Tuffaceous	9	3	3	6	3	-	10	-	1	3	12	18	9
Porphyritic rocks	**38**	**42**	**60**	**66**	**35**	**45**	**70**	**26**	**44**	**43**	**51**	**15**	**34**
Quartz-feldspar	5	7	18	12	14	12	10	3	15	10	11	6	10
Hornblende-feldspar	29	31	37	54	21	33	55	23	25	33	31	8	21
Feldspar	4	2	5	-	-	-	-	-	-	-	9	-	2
Lamprophyre	-	2	-	-	-	-	5	-	4	-	Tr	1	1
Coarse-grained holocrystalline rocks	**5**	**12**	**10**	**9**	**16**	**9**	**10**	**Tr**	**4**	**6**	**7**	**1**	**2**
Sedimentary rocks	**11**	**15**	**9**	**3**	**23**	**24**	**3**	**5**	**13**	**12**	**9**	**5**	**3**
Sandstone	-	-	7	3	18	21	-	3	6	3	4	3	-
Chert	11	15	2	Tr	5	3	3	2	7	9	5	2	3
Monomineralic rocks	**Tr**	**2**	**-**	**3**	**2**	**-**	**2**	**-**	**-**	**1**	**Tr**	**3**	**4**
Vein quartz	Tr	2	-	-	Tr	-	-	-	-	1	Tr	2	2
Magnetitite	Tr	-	-	3	2	-	2	-	-	-	-	1	2

taken to point count areas devoid of large clasts (> 10 cm). Standard deviation of results is estimated as $S_A = [P_A(1-P_A)/n]^{1/2}$, where P_A is the fraction of points falling on clast A and n is the total number of points in the analysis. Point-counting locations were selected as being representative of conglomerates of the alluvial-fluvial assemblage and they were chosen to cover most of the stratigraphic section. Approximately 90 clasts were sampled for further petrographic examination. These samples were selected to cover a wide range of clast mineralogy, texture and color within the different types of igneous clasts.

Loss on ignition (LOI) was determined by heating ~ 1g of sample at 1050°C for one hour. Major and minor elements were analyzed by X-ray fluorescence spectrometer (XRF) for 54 igneous clasts with precision of ± 1% for major elements and ± 10% for minor elements (Table 2). Rare-earth elements (REE) of selected clasts were determined by inductively coupled plasma atomic emission spectrometry (ICP-AES) and by instrumental neutron activation analysis (INAA) with precision of ± 5%.

Mineral compositions were determined using a Cambridge Microscan 5 electron microprobe (Table 3). The operating conditions were 20 keV accelerating potential, 9.0 nA specimen current and 100 s live counting time. Standards for amphiboles are tephroite (Mn), tugtupipe (Cl) and Kakanui hornblende (Si, Al, Ti, Fe, Mg, K, Ca and Na) and those for plagioclases are albite (Si, Al, Na), anorthite (Ca) and Kakanui hornblende (K, Fe). Raw X-ray spectra were converted to wt.% using the computer program EDDI of Pringle (1989). An average of 3 crystals were probed on each section and up to 3 measurements were made on each crystal.

Table 2. Major and trace element concentration of various clasts. Sample number refers to location of samples on Fig. 1.

Sample #	39j	39e	15d	39c	1s	2h	1b	2f	3r	1l	1r	3g	2e	3z	3q	3o	3t	43a	39k	58f	43e	37b	2d
SiO2 (wt.%)	67.7	61.5	63.0	60.1	64.8	60.5	56.5	54.5	65.6	65.6	68.5	57.1	59.2	71.3	72.7	65.2	71.3	66.3	67.4	67.5	67.0	66.4	60.4
Al2O3	15.8	14.1	15.8	14.2	16.0	15.8	16.3	14.4	14.7	15.6	15.5	13.6	14.5	14.9	13.2	15.8	14.4	17.1	14.7	13.6	14.7	14.4	14.1
Fe2O3(tot)	1.66	2.43	3.17	4.85	2.46	7.01	5.20	7.70	3.67	4.44	3.44	4.88	6.21	2.20	1.86	2.74	3.98	2.93	0.67	1.46	1.64	1.27	6.22
MgO	1.36	1.53	1.59	4.53	1.25	4.49	2.34	5.48	1.56	1.55	1.69	2.36	4.44	0.75	0.38	1.18	1.48	1.39	0.40	1.46	0.69	0.94	4.79
CaO	1.98	6.45	3.19	4.89	2.95	1.75	5.24	7.07	2.54	2.19	0.83	7.29	4.67	1.25	0.90	2.63	1.33	3.24	4.48	1.88	3.80	5.13	4.94
Na2O	5.71	6.15	6.67	4.72	6.79	4.96	7.85	5.94	6.90	6.88	7.23	5.75	6.55	6.47	6.44	6.77	5.64	6.41	6.76	6.24	8.30	5.77	5.21
K2O	3.61	2.71	2.48	2.63	1.54	1.59	0.65	0.58	0.66	0.79	1.02	0.83	0.67	1.37	2.07	1.37	1.32	0.61	2.50	2.05	0.18	1.48	1.59
TiO2	0.26	0.30	0.35	0.48	0.33	0.73	0.42	0.67	0.33	0.40	0.34	0.32	0.53	0.31	0.11	0.28	0.39	0.40	0.11	0.19	0.16	0.21	0.58
P2O5	0.09	0.17	0.15	0.17	0.18	0.16	0.31	0.20	0.13	0.24	0.14	0.18	0.17	0.08	0.04	0.11	0.12	0.10	0.05	0.12	0.07	0.12	0.25
MnO	0.05	0.11	0.07	0.10	0.06	0.15	0.13	0.15	0.07	0.06	0.05	0.14	0.11	0.03	0.04	0.05	0.05	0.04	0.04	0.03	0.07	0.07	0.10
S	0.07	0.26	0.00	0.05	0.01	0.01	0.01	0.01	0.01	0.01	0.01	0.01	0.01	0.06	0.01	0.00	0.06	0.04	0.12	0.08	0.08	0.14	0.01
Ba (ppm)	1374	860	886	1265	930	424	764	277	602	596	372	406	366	453	983	459	383	305	889	4283	117	1147	640
Cr	<10	15	32	72	25	183	114	209	48	33	50	90	140	<10	32	38	12	<10	<10	<10	<10	<10	204
Zr	108	98	84	116	90	137	163	89	78	116	86	86	85	135	65	50	154	84	67	87	75	87	105
Sr	795	657	1035	647	951	407	906	746	681	883	606	1107	681	377	161	922	278	431	689	640	448	433	917
Rb	81	49	65	56	24	52	11	<10	22	25	27	29	<10	58	55	57	47	16	49	33	11	41	31
Y	<10	<10	<10	<10	<10	19	19	18	<10	11	<10	12	13	<10	<10	<10	<10	<10	<10	<10	<10	<10	17
Nb	<10	<10	<10	<10	<10	<10	<10	<10	<10	<10	<10	<10	<10	<10	<10	<10	13	<10	<10	<10	<10	<10	<10
Zn	15	<10	43	29	38	93	62	78	54	57	47	71	88	<10	42	47	33	<10	<10	<10	<10	<10	71
Ni	<10	<10	35	76	26	118	77	116	40	38	39	78	102	<10	24	26	17	<10	<10	<10	<10	<10	148
Cu	<10	<10	n.d.	<10	n.d.	n.d.	n.d.	n.d.	n.d.	n.d.	n.d.	n.d.	n.d.	<10	n.d.	n.d.	<10	<10	<10	<10	<10	<10	n.d.
Pb	<10	<10	n.d.	<10	n.d.	n.d.	n.d.	n.d.	n.d.	n.d.	n.d.	n.d.	n.d.	<10	n.d.	n.d.	<10	21	<10	<10	<10	<10	n.d.
V	n.d.	n.d.	12	n.d.	<10	132	109	177	38	43	40	29	115	n.d.	<10	36	n.d.	n.d.	n.d.	n.d.	n.d.	n.d.	84
LOI (%)	2.30	4.90	3.24	3.50	2.79	3.02	4.89	3.79	2.93	2.26	1.84	7.26	1.95	1.80	1.69	3.06	1.70	2.00	3.90	3.40	3.80	5.40	1.71
Total (%)	100.86	100.60	99.95	100.45	99.44	100.37	100.13	100.65	99.29	100.21	100.71	100.02	99.23	100.62	99.55	99.38	101.81	100.65	101.22	98.53	100.53	101.36	100.12
	HPP	HPP	HPP	HPP	HPP	HPP	HPP	HPP	HPP	HPP	HPP	HPP	HPP	QPP1	QPP1	QPP1	QPP1	QPP2	QPP2	QPP2	QPP2	QPP2	S

HPP - Hornblende-plagioclase porphyry; QPP1 - Quartz-plagioclase porphyry 1; QPP2 - Quartz-plagioclase porphyry 2;
S - Spessartite; KP - Potash feldspar porphyry; H - Holocrystalline; MV - Mafic volcanic; T - Trachyte
n.d. - not determined
Total iron expressed as Fe2O3(tot)

Table 2. Continued. Major and trace element concentration of various clasts. Sample number refers to location of samples on Fig. 1.

Sample #	2l	1c	15l	1o	1m	1p	1t	2g	3k	39f	1e	3x	15g	39h	15j	1w	43b	1n	39g	3d	1u	1h	15h
SiO2 (wt.%)	52.0	54.1	55.3	67.1	69.4	68.6	69.2	71.7	68.5	50.3	61.5	55.3	61.7	45.3	57.5	50.4	45.9	20.1	51.4	57.2	58.5	49.0	47.5
Al2O3	16.4	16.7	17.1	14.7	15.1	15.5	15.8	15.8	15.8	13.6	15.7	15.6	16.0	13.0	14.9	14.6	16.5	14.4	11.1	15.3	16.8	17.1	14.9
Fe2O3(tot)	6.35	6.31	4.86	2.18	1.74	0.98	2.31	1.23	1.06	7.67	6.12	5.05	4.51	6.97	8.60	13.7	6.49	21.7	12.0	5.42	5.99	6.35	7.47
MgO	2.50	1.90	2.59	0.85	0.54	0.38	0.72	0.37	0.43	6.98	2.83	2.26	1.87	5.62	5.38	8.53	2.96	11.4	11.3	2.28	4.47	3.57	3.58
CaO	7.88	4.49	3.35	3.52	2.07	2.78	1.77	0.77	2.68	6.22	2.58	6.49	2.83	10.2	1.32	3.69	11.1	13.5	3.71	4.32	2.91	6.47	7.43
Na2O	5.65	2.76	3.26	5.62	7.84	7.44	6.32	6.74	6.68	2.62	2.69	1.88	4.57	0.54	3.08	1.75	6.25	0.00	0.65	4.21	7.41	3.15	1.21
K2O	2.72	8.14	7.94	2.22	0.77	1.03	2.14	1.43	1.36	3.51	3.58	4.05	3.63	6.78	2.33	0.11	0.40	0.01	0.54	3.05	1.63	6.35	7.37
TiO2	0.85	0.59	0.60	0.22	0.17	0.09	0.28	0.12	0.11	0.65	0.50	0.69	0.50	0.62	0.88	1.15	0.89	0.67	0.50	0.72	0.66	0.50	0.48
P2O5	0.33	0.25	0.47	0.07	0.08	0.02	0.08	0.04	0.05	0.40	0.12	0.12	0.11	0.44	0.05	0.10	0.25	0.02	0.03	0.42	0.36	0.31	0.32
MnO	0.12	0.10	0.10	0.00	0.01	0.01	0.01	0.00	0.00	0.16	0.01	0.01	0.00	0.19	0.05	0.00	0.16	0.12	0.08	0.09	0.08	0.00	0.00
S	0.00	0.03	0.01	0.05	0.04	0.03	0.03	0.03	0.04	0.38	0.08	0.14	0.08	0.19	0.13	0.28	0.15	0.37	0.20	0.15	0.09	0.17	0.19
Ba (ppm)	998	6309	3748	861	334	558	682	393	330	1656	690	543	886	2894	10413	1193	166	60	237	1083	379	4272	4358
Cr	130	<10	14	39	40	18	28	36	25	454	34	84	94	127	100	163	171	5043	2889	73	95	13	55
Zr	130	178	542	66	47	31	71	49	30	139	91	110	96	182	10	24	99	32	25	207	201	313	232
Sr	1087	2956	1024	731	822	1028	764	562	774	673	259	246	409	981	1219	1366	217	484	203	721	388	1552	1552
Rb	74	114	166	36	14	30	44	34	32	69	167	144	216	115	146	<10	18	<10	15	144	33	103	149
Y	24	37	50	<10	<10	<10	<10	<10	<10	23	11	15	13	27	18	17	13	16	<10	23	17	29	24
Nb	<10	<10	23	<10	<10	<10	<10	<10	<10	<10	<10	<10	<10	<10	<10	<10	<10	<10	<10	<10	12	10	<10
Zn	57	49	68	36	27	29	40	27	73	71	65	50	45	19	109	167	11	607	124	88	68	85	86
Ni	77	23	38	27	30	24	23	17	23	275	43	67	71	162	102	118	<10	1348	916	79	31	55	81
Cu	n.d.	n.d.	n.d.	n.d.	n.d.	n.d.	n.d.	n.d.	n.d.	<10	n.d.	n.d.	n.d.	<10	n.d.	n.d.	<10	<10	<10	114	<10	n.d.	n.d.
Pb	n.d.	n.d.	n.d.	n.d.	n.d.	n.d.	n.d.	n.d.	n.d.	<10	n.d.	n.d.	n.d.	<10	n.d.	n.d.	<10	<10	<10	<10	<10	n.d.	n.d.
V	138	184	175	<10	<10	<10	11	<10	<10	n.d.	109	186	89	n.d.	460	371	n.d.	n.d.	n.d.	n.d.	n.d.	174	142
LOI (%)	6.03	3.75	3.68	2.82	2.01	2.22	1.18	1.63	2.76	7.20	4.03	7.80	4.35	4.90	5.00	6.14	9.80	17.10	8.50	7.20	1.80	6.59	7.49
Total (%)	101.15	100.17	99.97	99.58	99.92	99.33	100.05	100.04	99.60	99.84	99.93	99.55	100.32	100.44	100.37	100.81	100.79	100.52	100.57	100.61	100.84	100.41	98.72
	S	KP	KP	H	H	H	H	H	H	Tuff	Tuff	Tuff	Tuff	Tuff	MV	MV	MV	MV	MV	T	T	T	T

Table 3. Average microprobe analyses of amphiboles of igneous clasts. Sample number refers to outcrop location on Fig. 1. (n) refers to the number of measurements on each thin section. Formula was calculated on the basis of 24 O following the recommended procedure of Leake (1978). Ferric and ferrous iron were calculated by stoichiometry.

Sample #	39c	39e	39j	2e	2f	2g	2d	2l
n	9	9	8	9	9	9	9	9
Clast type	HPP hK	HPP hK	HPP hK	HPP lK	HPP lK	H	S	S
SiO2	44.52	43.46	41.40	44.64	44.01	49.88	44.13	42.56
TiO2	1.86	0.93	1.11	1.39	1.84	1.21	1.44	2.20
Al2O3	9.46	10.16	13.77	10.84	10.15	5.27	10.84	11.47
Cr2O3	0.02	0.04	0.00	0.00	0.00	0.00	0.00	0.00
FeO*	13.69	17.92	17.76	12.77	13.76	8.91	11.15	12.25
MnO	0.18	0.18	0.05	0.10	0.16	0.18	0.12	0.07
MgO	13.73	10.98	9.39	14.41	13.48	17.79	15.94	14.55
CaO	10.94	10.64	10.82	11.14	11.19	11.29	11.02	10.94
Na2O	1.95	2.69	2.42	2.20	2.26	1.61	2.00	2.19
K2O	0.37	1.17	1.23	0.70	0.78	0.61	0.65	0.82
H2O	2.00	2.00	1.99	2.05	2.02	2.06	2.05	2.02
Cl	0.05	0.00	0.00	0.00	0.00	0.06	0.00	0.00
Total	98.76	100.23	99.94	100.24	99.65	98.85	99.34	99.07
Si(IV)	6.63	6.55	6.25	6.53	6.52	7.21	6.47	6.31
Al(IV)	1.37	1.45	1.75	1.47	1.48	0.79	1.53	1.69
T site	8.00	8.00	8.00	8.00	8.00	8.00	8.00	8.00
Al(VI)	0.29	0.35	0.70	0.40	0.30	0.11	0.34	0.32
Ti	0.21	0.11	0.13	0.15	0.21	0.13	0.16	0.25
Cr	0.00	0.00	0.00	0.00	0.00	0.00	0.00	0.00
Mg	3.05	2.47	2.11	3.14	2.98	3.83	3.48	3.22
Fe +2	1.46	2.06	2.07	1.31	1.52	0.92	1.02	1.22
M1,2,3	5.00	5.00	5.00	5.00	5.00	5.00	5.00	5.00
Fe +2	0.25	0.19	0.17	0.25	0.19	0.15	0.35	0.30
Mn	0.02	0.02	0.01	0.01	0.02	0.02	0.01	0.01
Ca	1.73	1.72	1.75	1.74	1.78	1.75	1.64	1.69
Na	0.00	0.07	0.07	0.00	0.01	0.07	0.00	0.00
M4 site	2.00	2.00	2.00	2.00	2.00	2.00	2.00	2.00
Ca	0.02	0.00	0.00	0.01	0.00	0.00	0.09	0.05
Na	0.56	0.72	0.64	0.62	0.63	0.38	0.57	0.63
K	0.07	0.22	0.24	0.13	0.15	0.11	0.12	0.16
A site	0.65	0.94	0.88	0.76	0.78	0.49	0.78	0.83

HPP hK - Hornblende-plagioclase porphyry with K2O > 2 wt.%; HPP lk - Hornblende-plagioclase porphyry with K2O < 2 wt.%; H - Coarse-grained holocrystalline; S - Spessartite.
* - Total iron expressed as FeO

CONGLOMERATES

Conglomerate units vary in thickness from one pebble layer to 15 m. They are massive, non-graded, and clast-supported, with sub-rounded to rounded clasts averaging 5 cm in size. Volcanic rocks and felsic porphyries dominate the clasts. Volcanic clasts generally decrease while porphyry clasts increase up the stratigraphic section (Table 1). The matrix of the conglomerate is composed mainly of quartz, plagioclase, carbonates, Fe-oxides, and chlorite, which gives it a greenish tinge.

Conglomerates and sandstones north and south of the LLCF are comparable. Conglomerates south of the LLCF only show basal sections near the unconformity. Trachyte clasts are present (> 18 %; Table 1) in these sections but are absent in basal sections north of the LLCF. Sandstones and matrices of conglomerates south of the LLCF are similar to those north of the fault (Legault and Hattori, in press), although the former contain higher amounts of lithic fragments and lower carbonate contents.

Clasts are classified into five groups: volcanic rocks (trachytic, felsic, mafic, and ultramafic volcanic rocks, and tuff), porphyritic rocks (hornblende-feldspar porphyry, quartz-feldspar porphyry, feldspar porphyry, spessartite lamprophyre), coarse-grained holocrystalline rocks, sedimentary rocks (sandstone, chert), and monominerallic rocks (vein quartz ± minor carbonate, magnetitite). The proportion of clast types varies greatly depending on the location (Table 1) and the underlying rocks (Fig. 2).

Figure 2. Schematic cross-section of outcrop 3 east of Kenogami Lake (Fig. 1). Note the decrease of alkalic volcanic clasts up the stratigraphic section.

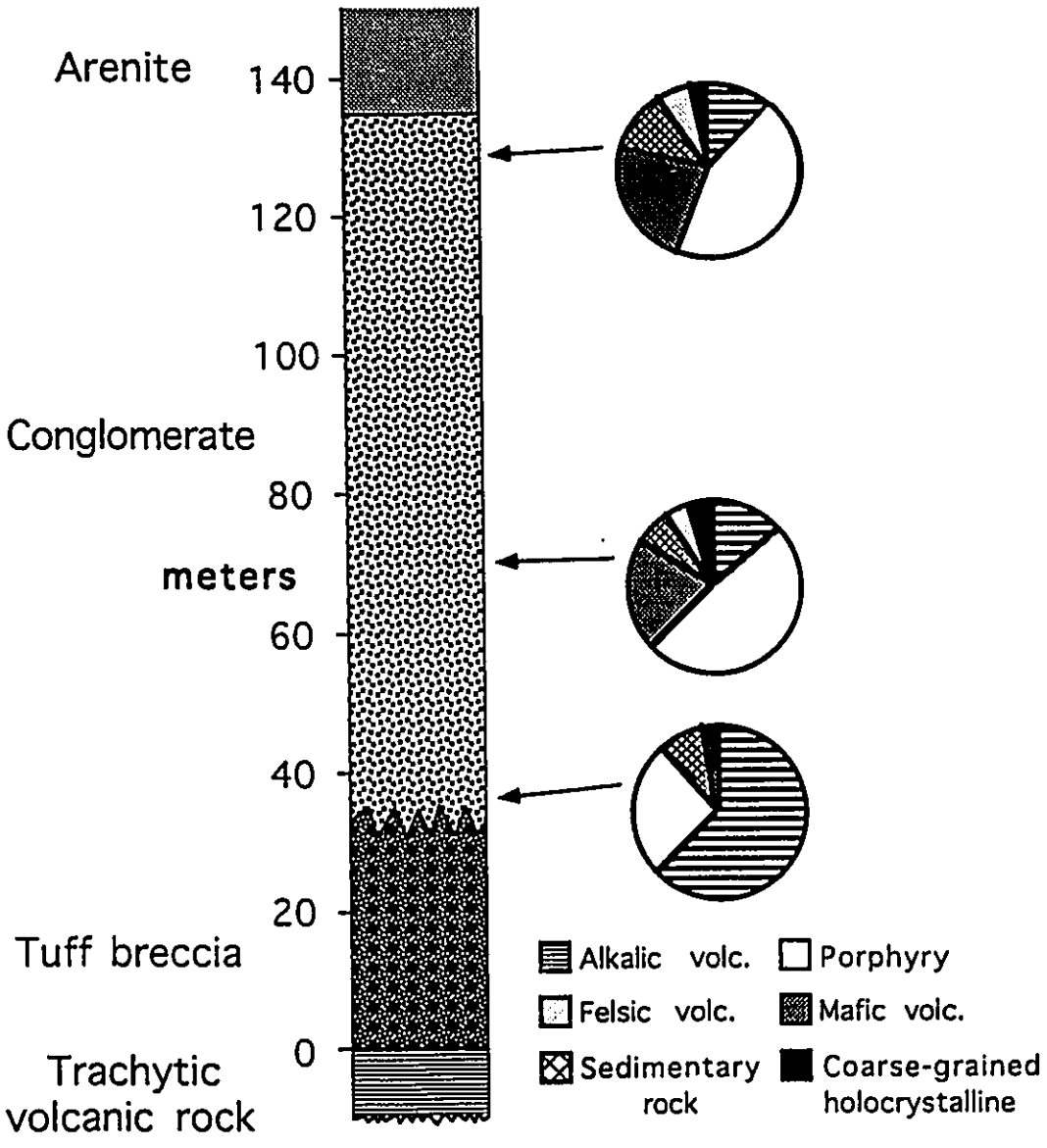
Arenite
140
120
100
Conglomerate
80
meters
60
40
20
Tuff breccia
0
Trachytic volcanic rock
Alkalic volc.
Porphyry
Felsic volc.
Mafic volc.
Sedimentary rock
Coarse-grained holocrystalline

IGNEOUS CLASTS

Porphyry clasts

Two types of porphyries are recognized: calc-alkaline and alkaline (Fig. 3). Calc-alkaline porphyries are hornblende-plagioclase porphyry and quartz-plagioclase porphyry. Spessartite lamprophyre and calc-alkaline porphyry clasts display linear compositional trends on Larsen diagrams, suggesting that they are comagmatic. Pervasively carbonatized porphyry clasts are common, containing veinlets (up to 0.5 cm) of quartz-carbonate and epidote-quartz-carbonate, which do not extend beyond the rims of the clasts, indicating that the veins were emplaced in the source rocks.

Hornblende-plagioclase porphyry (HPP):

Clasts of this composition range from light to dark reddish brown. Phenocrysts are subhedral plagioclase (0.5 to 3.0 mm) and euhedral hornblende (0.5 to 1.5 mm), with minor apatite, zircon, and quartz. Plagioclase is lightly to moderately saussuritized, and some grains exhibit zoning. Hornblende is edenitic hornblende to ferroan pargasite (Fig. 4) and is mostly pseudomorphed by a mixture of chlorite, hematite, magnetite, quartz, and calcite.

Chemical compositions of these porphyry clasts plot mostly in the monzonite - quartz monzonite field (Fig. 5). The chemical analyses show a wide range of SiO_2 (56 - 68 wt.%), high Na_2O/K_2O (1.58 to 12.1 in wt. ratio; Table 2) and fractionated REE (La/Yb_N = 18.5 to 35.8) with total REE less than 250 ppm.

Figure 3. Total alkali versus SiO2 plot delineating alkaline and sub-alkaline fields by Irvine and Baragar (1971). Fields for syenite and porphyry series of exposed intrusions are also shown (Kerrich and Watson, 1984; Hicks and Hattori, 1988; Ontario Geological Survey, 1986; our unpubl. data).

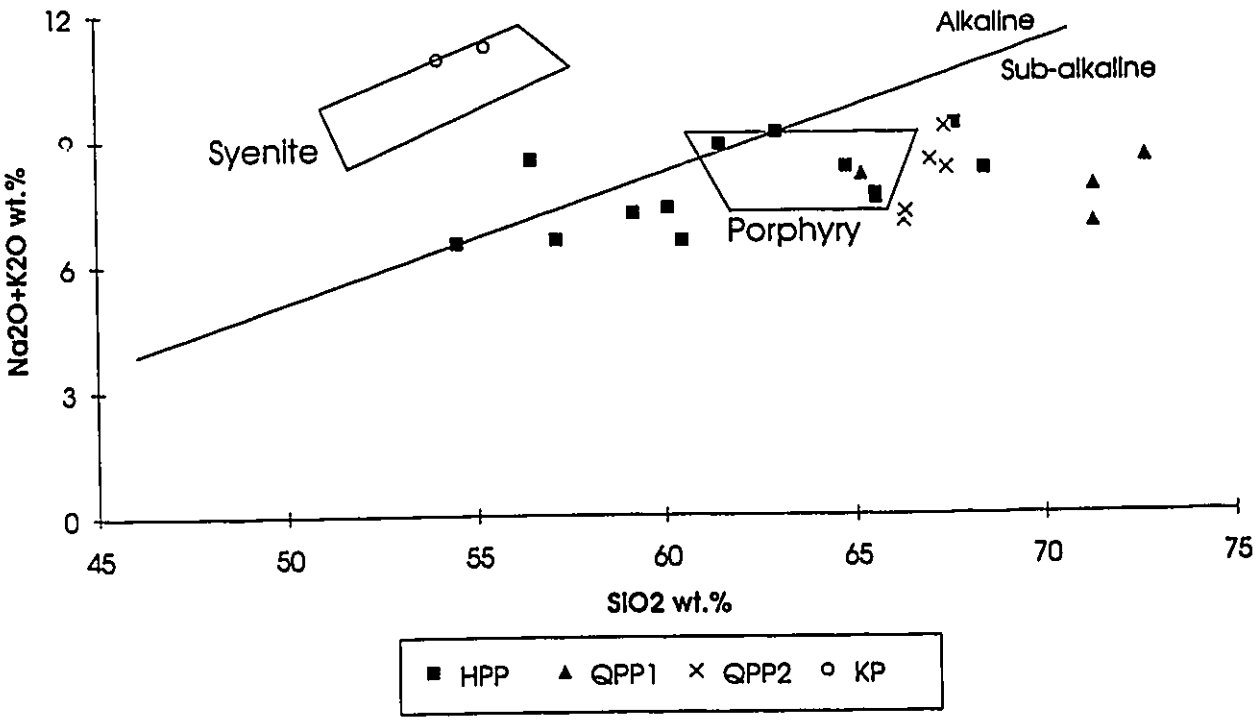
12
9
6
3
0
Na2O+K2O wt.%
45
50
55
60
65
70
75
SIO2 wt.%
Alkaline
Sub-alkaline
Syenite
Porphyry
HPP
QPP1
QPP2
KP

Figure 4. Classification of calcic amphiboles (Leake, 1978). E - edenite; EH - edenitic hornblende; PH - pargasitic hornblende; FPH - ferroan pargasitic hornblende; FP - ferroan pargasite; P - pargasite. Stippled area shows compositional range of amphiboles from intrusions of the porphyry series (n = 40; G. Levesque, written comm., 1993).

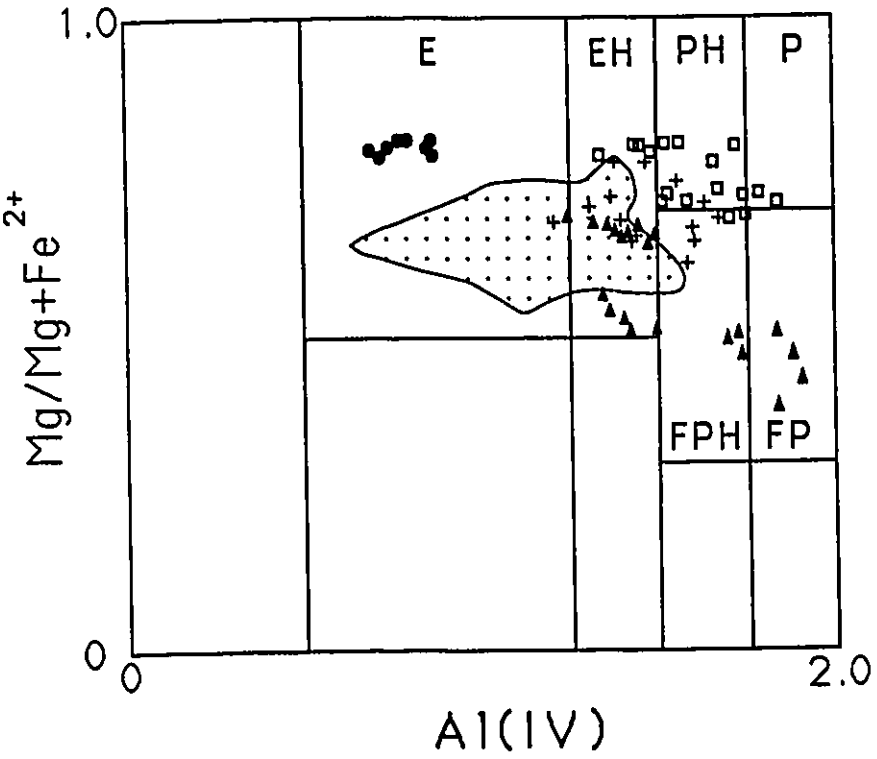

▫ Hornblende-plagioclase porphyry (K_2O < 2.0 wt.%; n = 18)

▲ Hornblende-plagioclase porphyry (K_2O > 2.0 wt.%; n = 26)

\+ Spessartite (n = 16)

● Coarse-grained holocrystalline (n = 9)

Quartz-plagioclase porphyry (QPP):

This porphyry is further classified into two types: reddish type (QPP1) and white leucocratic type (QPP2). Both have anhedral to subhedral, moderately saussuritized plagioclase phenocrysts, similar mafic assemblages (including chlorite, magnetite, hematite) and compositions (SiO_2 > 65 wt.%; Na_2O/K_2O > 2.29 in wt. ratio; La/Yb_N > 10.0; Table 2). However, QPP2 clasts contain coarse (up to 7 mm), embayed, rounded quartz phenocrysts, higher CaO and lower $Fe_2O_{3(tot.)}$, MgO, Cr and Ni. Chemical compositions plot in the granite - quartz monzonite - tonalite field (Fig. 5).

Lamprophyre

These clasts are light to dark brown, and are a minor constituent. They contain abundant euhedral crystals (~0.75 mm) of hornblende (edenitic to pargasitic; Fig. 4) in a matrix of plagioclase, hematite, chlorite, quartz, and apatite. The clasts are spessartite, following the classification of Rock (1987). These are different from exposed lamprophyre dykes in the area which are mostly biotite-rich minettes and clinopyroxene-rich vogesites (Levesque et al., 1991).

Analyses of the spessartites show SiO_2 varying from 52 to 60 wt.%, fractionated REE (La/Yb_N = 17.5 to 29.6) and a high Na_2O/K_2O (2.08 to 3.93 in wt. ratio; Table 2). They plot in the calc-alkaline lamprophyre field of Rock (1987).

K-feldspar porphyry (KP):

These clasts are mostly dark reddish-brown and contain subhedral to euhedral, zoned K-feldspar (< 3.0 cm). The K-feldspar contains numerous inclusions (hematite, quartz, chlorite,

Figure 5. Classification of porphyry clasts using R_1R_2-diagram by De La Roche et al. (1980).

MG - monzogabbro; M - monzonite; QM - quartz monzonite.

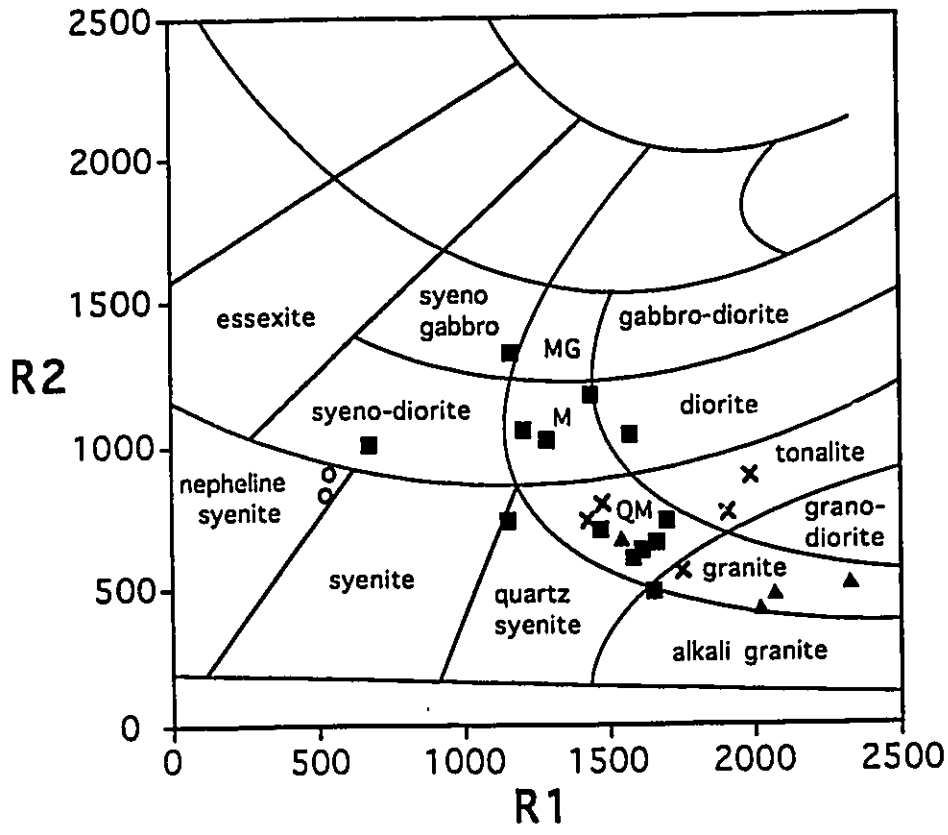

■ - HPP ▲ - QPP1 × - QPP2 o - KP

calcite) which gives it a light pink color. Ferromagnesian minerals are replaced by a mixture of chlorite, magnetite, hematite, calcite, and quartz. These clasts show highly fractionated REE (La/Yb_N = 24.4 to 35.7) with elevated total REE (> 350 ppm) and low Na_2O/K_2O (0.34 to 0.41 in wt. ratio; Table 2). They plot in the nepheline syenite field (Fig. 5).

Coarse-grained holocrystalline clasts

These clasts are massive to foliated and are well rounded. They are mostly trondhjemite and probably represent the "granite clasts" referred to by earlier workers (Wilson 1956, Hewitt, 1963). Plagioclase and quartz are predominant, with accessory hornblende, chlorite, hematite, magnetite, epidote, apatite, and zircon. Relic hornblende (edenite; Fig. 4), was observed in one sample, and it is usually pseudomorphed by a mixture of chlorite, hematite, magnetite, calcite and epidote. Foliated clasts are devoid of hornblende and foliation is mostly defined by chlorite. Plagioclase (An_{13-27}; 1.0 - 3.0 mm) is anhedral, and moderately saussuritized. Quartz (0.30 - 0.75 mm) is anhedral, monocrystalline to polycrystalline, and has straight to undulose extinction. Foliated and massive trondhjemite clasts are chemically similar and are characterized by low Zr (30 to 71 ppm) and Rb (14 to 44 ppm), low total REE (13 to 83 ppm) and high SiO_2 (67 to 72 wt.%; Table 2).

Volcanic clasts

Dark green tholeiitic basalt is the most abundant volcanic clast (La/Yb_N = 3.1 - 5.9). Light green andesite clasts occur mostly in the basal section north of the LLCF, and their composition and texture are similar to andesite clasts found in conglomerates associated with

turbidites south of the LLCF (La/Yb_N = 10.3 - 16.5). Felsic and ultramafic volcanic clasts are minor. Some of the latter show spinifex texture, and some are highly altered to fuchsite-carbonate rocks, suggesting that carbonate alteration took place in the source rocks. Trachyte clasts are the predominant clasts in conglomerates in erosional contact with trachyte volcanic rocks (Fig. 2). Trachyte clasts are absent in basal conglomerates north of the LLCF, but they are present in basal conglomerates south of the fault. Two occurrences were examined within 500 m south of the LLCF and four basal conglomerates more than 1.5 km north of the LLCF were also studied (Fig. 1). The presence of trachyte clasts in basal conglomerates appears to be related to the proximity of these sections to the LLCF.

DISCUSSION

Weathering does not appear to have altered the composition of the igneous clasts. Only thin (< 5 mm) weathering rims, consisting mostly of sericite, quartz and chlorite, were observed on clasts, and they were removed prior to chemical analysis.

Values of LOI are generally less than 5 %, except for the volcanic clasts. Trachytic clasts have compositions comparable to intercalated trachytic rocks. Some trachyte clasts have lower LOI values than exposed trachytic volcanic rocks, suggesting that the clasts are less altered than presently exposed source rocks, as previously pointed out by Cooke and Moorhouse (1969).

SOURCE ROCKS

Classification of clasts

The clasts are grouped into 2 types: greenstone-derived and others. Greenstone-derived clasts are holocrystalline trondhjemitic rocks, felsic, mafic and ultramafic volcanic rocks, chert, magnetitite and banded iron-formation (magnetite + chert). These are common in underlying greenstone-belt rocks. Clasts classified as "others" include porphyritic, tuffaceous, and trachytic clasts. Some of these were apparently derived from other units of the Timiskaming Group. Trachyte clasts at outcrop 3 in Fig. 1 are identical in appearance and composition to the underlying trachytic volcanic rocks, confirming their derivation from the volcanic rocks of the Timiskaming Group (Table 2). Chemical compositions of the tuff clasts are similar to the trachyte, suggesting derivation from the Timiskaming Group (Table 2).

Calc-alkaline porphyry clast source

Porphyry intrusions abundantly exposed in the area were believed to be the source of the porphyry clasts, based on their texture (e.g., Hewitt, 1963; Hodgson, 1986). Sedimentological work inferring a proximal source (Hyde, 1980; Mueller and Donaldson, 1992), is in agreement with this interpretation. The mineralogy and compositions are, however, different between porphyry clasts and porphyry intrusions exposed in the area, as described below.

Thomson (1948) recognized five types of intrusions that post-dated deformation of the greenstone belt. They include early diorite/quartz diorite and granodiorite porphyry (referred to as quartz porphyry by Thomson (1948)), and late lamprophyre, syenite and feldspar/quartz-

feldspar porphyry. Dioritic intrusions are intruded by feldspar porphyries (Thomson, 1948) and U-Pb ages of granodiorite porphyries (2685 ± 3 Ma) and feldspar porphyries (2677 +3/-2 Ma; Corfu et al., 1991) support this interpretation.

Cooke and Moorhouse (1969) classified the late intrusions and volcanic rocks into two series: syenite and porphyry series. Trachytic volcanic rocks and syenitic intrusions form the syenite series whereas quartz-feldspar porphyry and feldspar porphyry form the porphyry series. Larsen diagrams show that the first two types of igneous rocks, granodiorite porphyries and diorites/quartz diorites north of the LLCF, are comagmatic (Fig. 6), and that they are not related to feldspar porphyries.

The calc-alkaline porphyry clasts are not comagmatic with the exposed intrusions of the porphyry series. First, the two porphyries have different mineralogy. The only primary ferromagnesian phenocryst in the clasts is hornblende, whereas exposed intrusions, along with hornblende, also contain biotite. Porphyry intrusions without biotite phenocrysts are very rare (Levesque et al., 1991).

Second, intrusions of the porphyry series are commonly high in large ion lithophile elements (LILE; K_2O = 3.46 ± 0.86 wt.%, Ba = 2240 ± 776 ppm, Rb = 99 ± 31 ppm; n=92; all uncertainties are 1 σ)(Kerrich and Watson, 1984; Hicks and Hattori, 1988; Ontario Geological Survey, 1986; our unpubl. data). However, clasts contain lower LILE (K_2O = 1.45 ± 0.78 wt.%, Ba = 713 ± 459 ppm and Rb = 39 ± 22 ppm; n=24; Fig. 7). Major element concentrations and their trends are also different between the two as illustrated on Larsen diagrams (Fig. 8). REE of calc-alkaline porphyry clasts (La/Yb_N = 18.0 to 35.8) are generally more fractionated than those for porphyry intrusions of the area (La/Yb_N ~ 15; Kerrich and Watson, 1984; G. Levesque, written

Figure 6. Selected Larsen diagrams showing the similar trends for quartz porphyries (+), diorite/quartz diorite intrusions (closed squares) and calc-alkaline porphyry clasts (open squares). Data of quartz porphyries and diorites/quartz diorites from Jensen and Langford (1985), Ontario Geological Survey (1986) and our unpubl. data. Values correspond to the correlation coefficient of regression lines for the combined data of diorites/quartz diorites and calc-alkaline porphyry clasts.

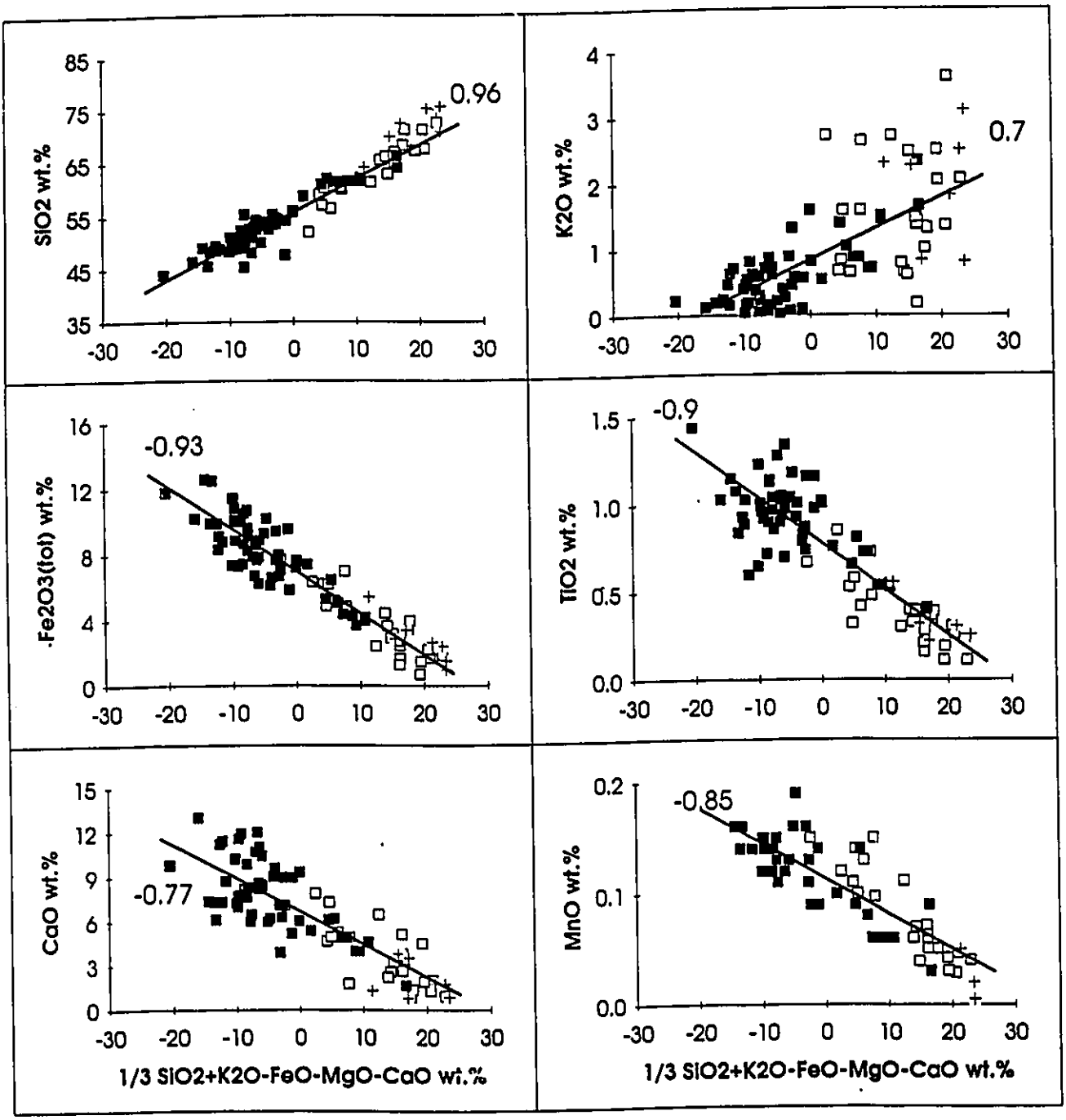
SiO2 wt.%
0.96
K2O wt.%
0.7
Fe2O3(tot) wt.%
-0.93
TiO2 wt.%
-0.9
CaO wt.%
-0.77
MnO wt.%
-0.85
1/3 SiO2+K2O-FeO-MgO-CaO wt.%
1/3 SiO2+K2O-FeO-MgO-CaO wt.%

Figure 7. Primitive mantle normalized spidergram for average calc-alkaline porphyry clasts. Normalizing values from Sun and McDonough (1989). Averages for porphyry intrusions (n=5; solid line) and syenite intrusions (n=3; stippled line) are also shown (our unpubl. data).

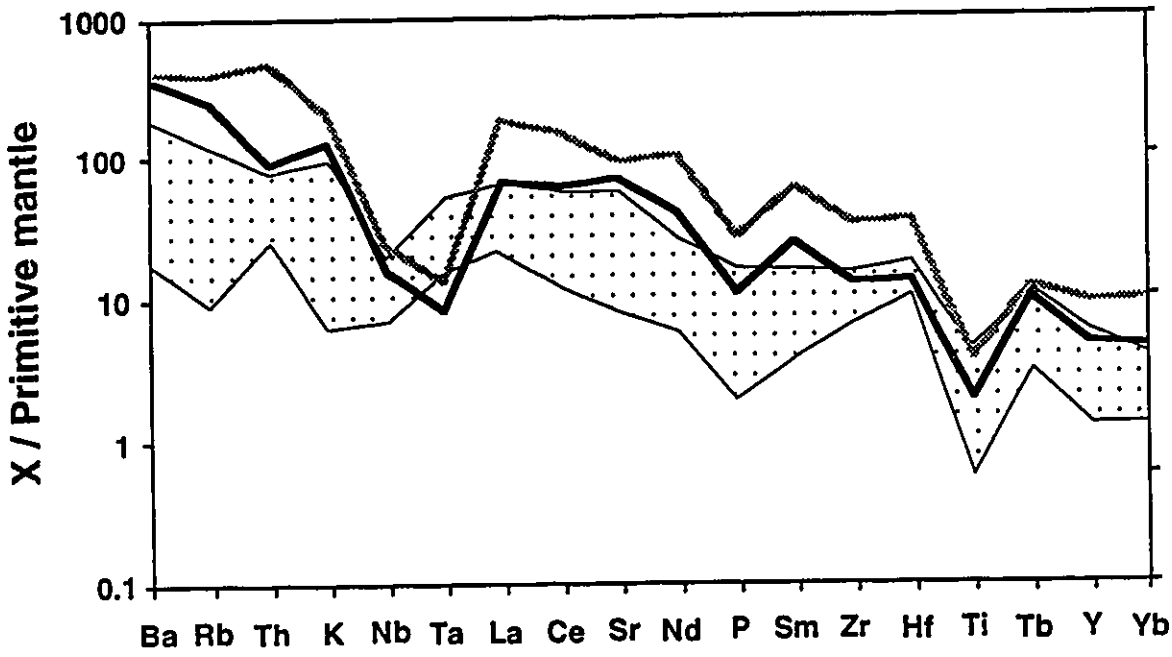
1000
100
10
1
0.1
X / Primitive mantle
Ba Rb Th K Nb Ta La Ce Sr Nd P Sm Zr Hf Ti Tb Y Yb

Figure 8. Selected Larsen diagrams showing the different trends for calc-alkaline porphyry clasts (solid squares) and intrusions of the porphyry series (open squares). Data for intrusions are from Kerrich and Watson (1984), Hicks and Hattori (1988), Ontario Geological Survey (1986) and our unpublished data. Values correspond to the correlation coefficient of regression lines for each data set.comm., 1993).

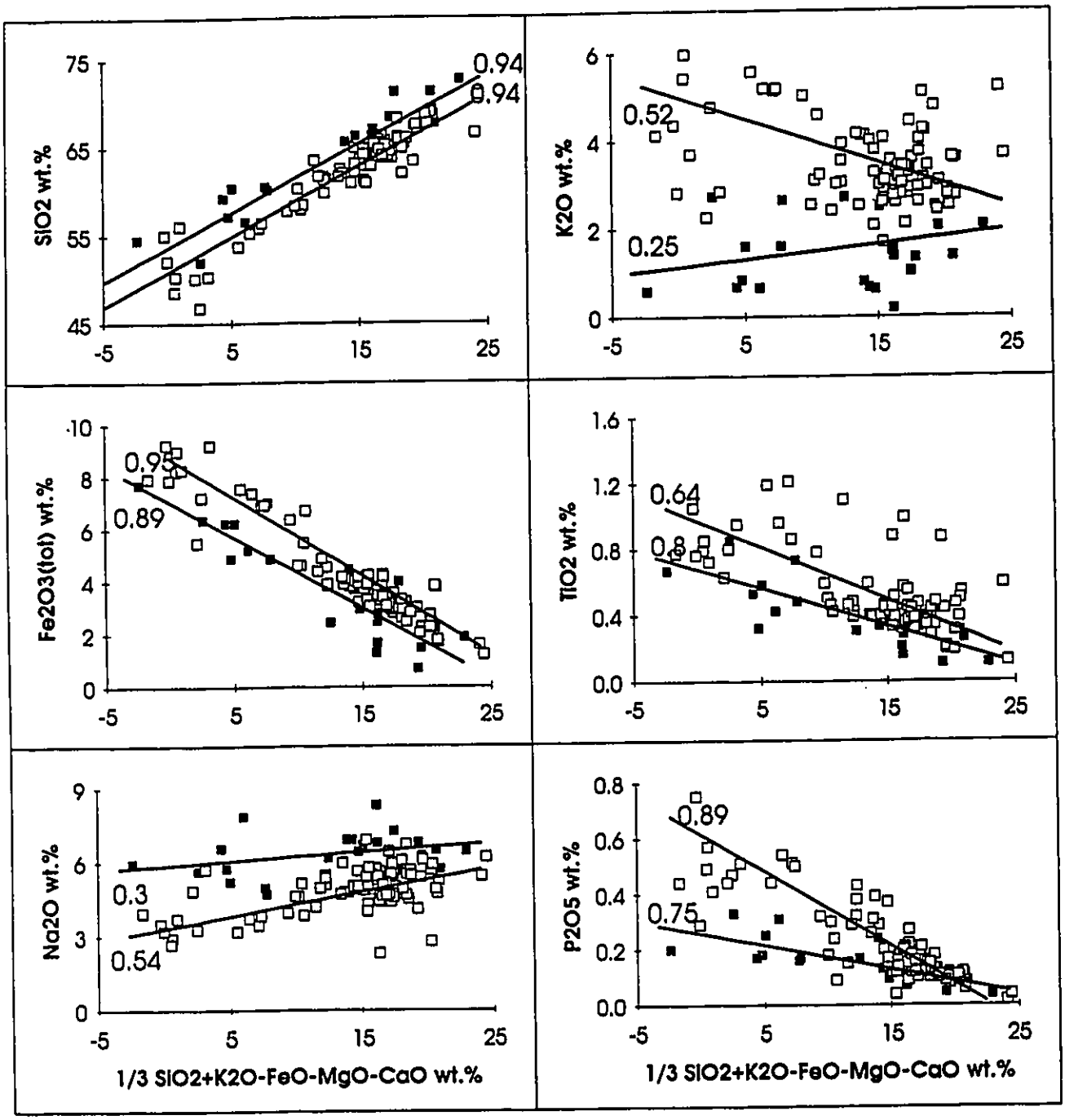
SiO2 wt.%
75
65
55
45
-5
5
15
25
0.94
0.94
K2O wt.%
6
4
2
0
0.52
0.25
Fe2O3(tot) wt.%
10
8
6
4
2
0
0.95
0.89
TiO2 wt.%
1.6
1.2
0.8
0.4
0.0
0.64
0.8
Na2O wt.%
9
6
3
0
0.3
0.54
P2O5 wt.%
0.8
0.6
0.4
0.2
0.0
0.89
0.75
1/3 SiO2+K2O-FeO-MgO-CaO wt.%
1/3 SiO2+K2O-FeO-MgO-CaO wt.%

Third, amphiboles from the clasts are more Al-rich (Al^{iv} = 1.53 ± 0.17; Al^{vi} = 0.37 ± 0.16; n=44) than those of the intrusions (Al^{iv} = 1.23 ± 0.27; Al^{vi} = 0.33 ± 0.13; n=40; G. Levesque, written comm., 1993), although both are calcic, varying from edenite to pargasite with similar Fe and Mg contents (Fig. 4). Pressure has been proposed as being the dominant factor in accounting for the observed differences in Al contents of calcic amphiboles in calc-alkalic plutonic rocks (i.e., Hammarstrom and Zen, 1986). However, porphyry clasts appear to have been derived from sub-volcanic intrusions, and since the late feldspar porphyries are also sub-volcanic intrusions, the difference in Al contents of the respective amphiboles does not appear to be related to the depth of emplacement. Amphiboles crystallizing from more siliceous melts contain higher SiO_2 (lower Al^{iv})(Cawthorne, 1976). Melts for the porphyry intrusions therefore contained higher SiO_2 at given Fe and Mg activities.

Fourth, the porphyry intrusions (2677 Ma; Corfu et al., 1991) are younger that the syenite intrusions (2680 ± 1 Ma; Corfu et al., 1989), and no coarse-grained holocrystalline syenite clasts were observed. The lack of such clasts suggest that these intrusions were not exposed during sedimentation.

Possible source of the clasts

The QPP2 clasts are mineralogically and chemically similar to white leucocratic granodiorite porphyry intrusions such as the Goodfish and Bidgood quartz porphyries (Fig. 1). A predominance of angular QPP2 clasts in basal conglomerates of an outcrop located just south of the Goodfish granodiorite porphyry is consistent with their derivation from the intrusion. Other similar leucocratic granodiorite porphyries that intrude greenstone belt calc-alkalic volcanic rocks

north and south of the LLCF have also been noted (Jensen and Langford, 1985).

Source rocks that are texturally and mineralogically similar to the HPP, QPP1 and spessartite clasts have not been observed in exposed rocks of the area. However these clasts may be related to the diorite/quartz diorite intrusions. The diorites and quartz diorites are composed of equigranular plagioclase, hornblende ± quartz and have only been observed north of the LLCF. The diorites/quartz diorites and the calc-alkaline porphyry clasts show linear trends that are parallel for most major and trace elements on Larsen diagrams (Fig. 6). Regression lines for combined data of the two are significant at a confidence level of 99.9%, suggesting that the two sets of data are from the same population. The clasts appear to represent a hypabyssal component of the dioritic intrusions that has been removed by erosion and preserved only as clasts.

Diorite/quartz diorite and granodiorite porphyry intrusions are widespread north of the LLCF whereas south of the LLCF, diorite/quartz diorite intrusions are absent and granodiorite porphyries are scarce. This suggests that most of the porphyry clasts were derived from the north. Alternatively, diorites/quartz diorites may have been present south of the LLCF, but were removed by erosion. However, this seems unlikely because granodiorite porphyries of similar age are still exposed south of the LLCF and coarse-grained holocrystalline clasts of diorite were not observed.

Alkaline porphyry clast source

The clasts are chemically similar to syenite intrusions of the area, which are coarse-grained holocrystalline and mostly equigranular. The clasts have elevated K_2O (7.94 to 8.14 wt.%), Ba

(3 748 to 6 309 ppm) and Y (37 to 50 ppm) and low Na_2O (2.76 to 3.26 wt.%) and Cr (< 14 ppm; Table 2). Similar to the syenitic intrusions, these clasts show highly fractionated (La/Yb_N = 24.4 to 35.7) and elevated REE (397 to 648 ppm). It appears that the clasts represent the erosion of high level syenitic intrusions.

Coarse-grained holocrystalline clast source

The holocrystalline clasts have low Zr, Rb and Yb (Table 2). Such values are atypical of most Archaean trondhjemite-tonalite intrusions (Fig. 9) although trondhjemite-tonalite intrusions are abundant within greenstone belts. In the southern Abitibi greenstone belt, syn-volcanic tonalite intrusions (e.g., Flavrian and Bourlamaque plutons) have much higher Zr and Yb at a given SiO_2 than the clasts (Fig. 9) and therefore do not appear to have been the source.

Two batholiths close to the Kirkland Lake area are the Lac Abitibi (~ 60 km) and Round Lake batholiths (~ 15 km). They have foliated trondhjemite-tonalite phases near their border (Lafleur, 1986; Smith and Sutcliffe, 1988). Foliated phases of the Lac Abitibi batholith have hornblende as the dominant mafic mineral. This is in contrast with foliated clasts which have no hornblende or relic hornblende. The foliation in the clasts is mostly defined by chlorite, and the texture and mineral assemblages associated with chlorite grains indicate that they did not form as an alteration product of hornblende after erosion. The trondhjemite-tonalite phases of the Lac Abitibi batholith are generally higher in Zr, Rb and Yb than the clasts (Fig. 9), and therefore it is unlikely to be the source for the clasts.

Trondhjemite-tonalite phases of the Round Lake batholith (2697-2698 Ma; Mortensen, 1993) are texturally and mineralogically similar to the holocrystalline clasts. Although the clasts

Figure 9. Compositions of local and well-known tonalite-trondhjemite intrusions. Solid circles = coarse-grained holocrystalline clasts.

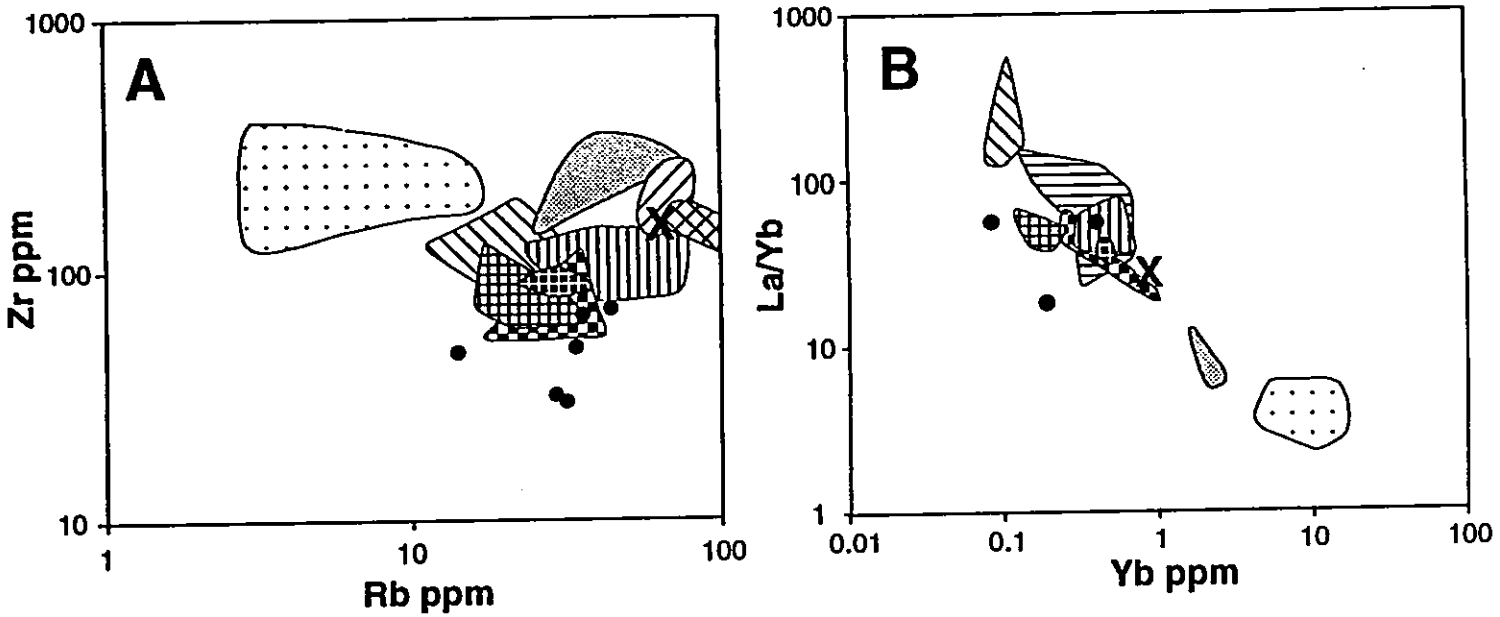

Border phase of Round Lake batholith (n = 6; Feng and Kerrich, 1992)

Central phase of Round Lake batholith (n = 5; feng and Kerrich, 1992)

Tonalite phase of Lac Abitibi batholith (n = 10; Sutcliffe et al., 1990; Feng and Kerrich, 1992)

Bourlamaque pluton (n = 5; Taner and Trudel, 1989; Feng and Kerrich, 1992)

Flavrian pluton (n = 16; Paradis et al., 1988)

Trondhjemite gneisses of eastern Finland (n = 10; Martin, 1987)

Transvaal tonalites (n = 8; Condie and Hunter, 1976; Glikson, 1979)

Lewisian trondhjemite (n = 4; Tarney et al., 1979)

Western Superior Province trondhjemite (average +/- 1 standard deviation; Ermanovics et al., 1979)

Mount Edgar batholith (n = 2; Glikson, 1979)

X Average composition of Archean tonalite-trondhjemite-granodiorite (Condie, 1993)

tend to be lower in Zr compared to the border phases of the Round Lake batholith, there is some overlap, and Rb and Yb values are similar (Fig. 9). Other trace element compositions (Cr < 40 ppm; Ni < 30 ppm; V < 30 ppm) are also similar and plots of the data from the intrusion and the clasts on Larsen diagrams indicate that they are comagmatic (Fig. 10). The source for the holocrystalline clasts is, therefore, most likely the marginal phase of the Round Lake batholith. The presence of clasts derived from the Round Lake batholith indicates that the intrusion was uplifted and eroded before or during sedimentation of the alluvial-fluvial assemblage.

Mafic and intermediate volcanic rock clast source

Mafic and intermediate volcanic rock clasts constitute about 20% of the conglomerate clasts (Table 1). Mafic volcanic clasts are mostly tholeiitic basalts while intermediate clasts are calc-alkaline andesites (Table 2). These volcanic clasts show high LILE and low high field strength elements (HFSE), suggesting that they were derived from an arc (e.g., Arculus and Powell, 1986). Rocks with similar compositions occur in greenstone belts, both north and south of the LLCF.

IMPLICATIONS FOR LATE ARCHAEAN DEVELOPMENT

The type of source rocks identified for the alluvial-fluvial assemblage of the Timiskaming Group in the Kirkland Lake area suggests that the sources were mostly contained in an arc terrain which was uplifted and dissected. Calc-alkaline porphyry clasts of the alluvial-fluvial assemblage show arc signatures in their compositions (high LILE/HFSE; Fig. 7)(Pearce et al., 1984). The

Figure 10. Selected Larsen diagrams showing the different trends for holocrystalline clasts (solid squares), border phase of the Round Lake batholith (open squares) and central phases of the Round Lake batholith (open triangles). Data for Round Lake batholith from Feng and Kerrich (1992). Values correspond to the correlation coefficient of regression lines for combined data.

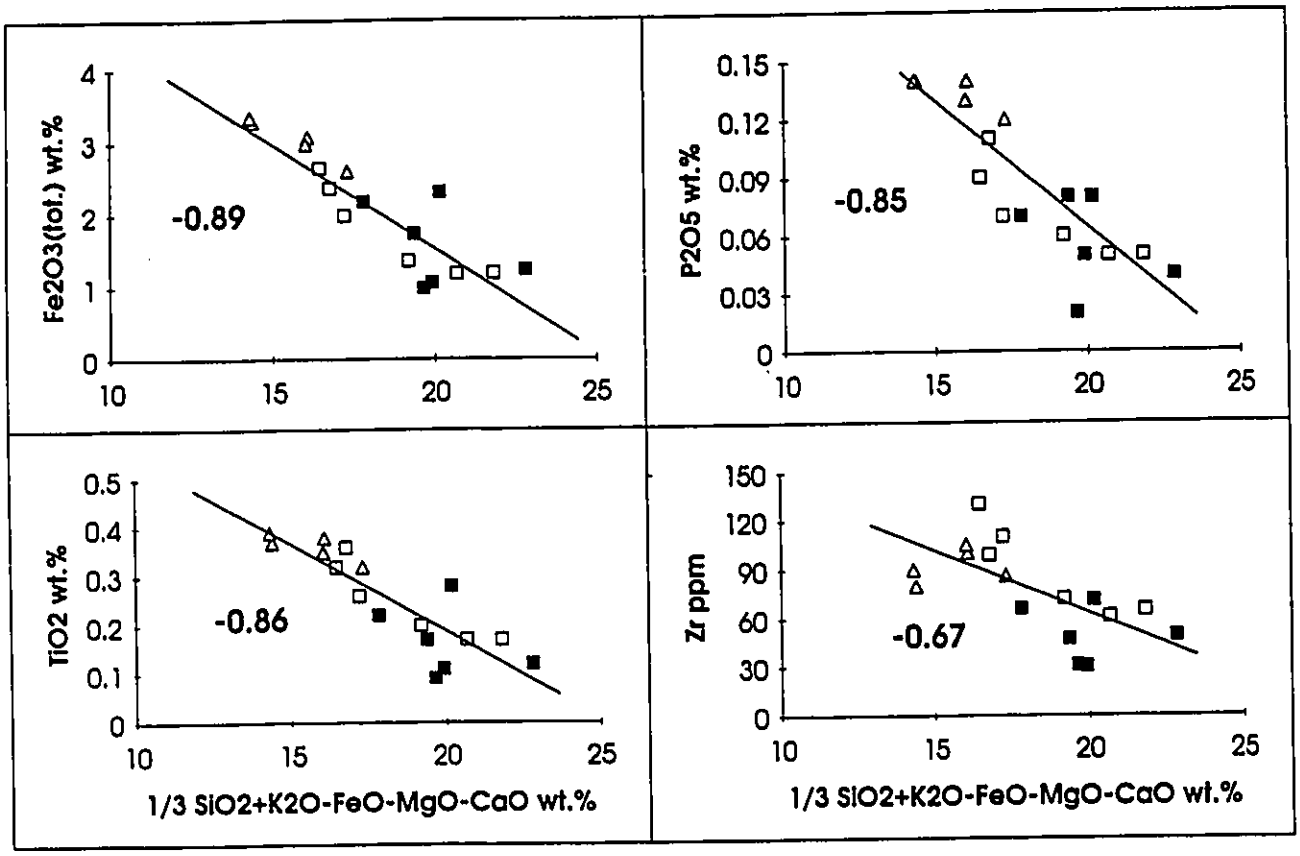
Fe2O3(tot.) wt.%
-0.89
P2O5 wt.%
-0.85
TiO2 wt.%
-0.86
Zr ppm
-0.67
1/3 SiO2+K2O-FeO-MgO-CaO wt.%
1/3 SiO2+K2O-FeO-MgO-CaO wt.%

compositional trend of the calc-alkaline porphyry clasts (monzonite to granite; Fig. 5) are commonly observed in Phanerozoic arc terranes such as in western North and South America (Lameyre and Bowden, 1982). Spessartite lamprophyre dykes also occur in arc environments (e.g., Suzuki and Shiraki, 1980; Rock et al., 1988).

Calc-alkaline porphyry clasts are comagmatic with granodiorite porphyry and diorite/quartz diorite intrusions, but they also have similar trends on Larsen diagrams with calc-alkalic volcanic rocks of the area (i.e., Blake River Group). Although intrusive contacts have been reported for the granodiorite porphyry and diorites/quartz diorites into the Blake River Group (i.e., Jensen and Langford, 1985), these intrusions may be cogenetic with the calc-alkaline volcanic rocks. However these rocks are not associated with the younger alkalic intrusive and volcanic rocks.

Amphibole compositions of the calc-alkaline porphyry clasts (Al^{iv} = 1.53), however, are typical of Phanerozoic island-arc rocks such as those in circum-Pacific areas (Jakes and White, 1972), whereas amphiboles of the syenite and porphyry series (Al^{iv} = 1.23; G. Levesque, pers. comm., 1993) are similar to those of rocks from continental arcs (e.g., Dodge et al., 1968; Reid and Hamilton, 1987). This is consistent with the Blake River Group having formed in an island-arc setting (Fowler and Jensen, 1989) whereas volcanic rocks of the Timiskaming Group formed in a thickenned crust (Capdevila et al., 1982). It appears therefore that the magma for the calc-alkaline porphyry clasts intruded in an island-arc. The difference between early and late porphyry intrusions may be viewed as a change from island-arc magmatism to "continental-arc". This change may be related to an increase in crust thickness, due to accretion.

Alkaline clasts were not observed in basal conglomerates of the alluvial-fluvial assemblage

north of the LLCF, suggesting either alkaline magmatism was not widespread but rather confined along the LLCF or alkaline magmatism started after the onset of sedimentation. The current distribution of trachytic volcanic rocks and the presence of trachyte clasts in basal conglomerates close to and south of the LLCF indicates a spatial relationship between alkaline magmatism and the LLCF. No coarse-grained holocrystalline alkalic clasts are observed throughout the stratigraphic section therefore syenitic intrusions (~2680 Ma) were not exposed during sedimentation. The presence of alkalic porphyry clasts with similar compositions to the syenite intrusions and volcanic rocks, however, indicates that subvolcanic intrusions (possibly feeders for the volcanic rocks) were exposed in the area.

The presence of andesite clasts at the base of the alluvial-fluvial assemblage and in the older turbidite assemblage south of the LLCF indicates that erosion of andesitic volcanic rocks took place during Timiskaming time. An increase in tholeiitic volcanic clasts combined with the decrease in andesite clasts throughout the alluvial-fluvial assemblage indicate a change in the lithology of the exposed rocks. The change is attributed to the degree of dissection of an arc. The essential absence of andesite clasts in the upper sections of the alluvial-fluvial assemblage shows that such rocks were removed by erosion. This may explain the absence of calc-alkaline volcanic rocks immediately north of the alluvial-fluvial assemblage (Fig. 1).

Timing of sedimentation

Quartz-feldspar porphyry clasts collected by Corfu et al. (1991) have yielded ages of 2682 - 2685 Ma. These ages overlap the age of the Bidgood granodiorite porphyry (2685 ± 3 Ma; Corfu et al., 1991), which is comagmatic with the diorite intrusions. The Dufault pluton which

is 75 km ENE of Kirkland Lake, is akin to the diorite intrusions in mineralogy (Rive et al., 1989) and chemistry (Feng and Kerrich, 1992) and has an age of 2690 ± 2 Ma (Mortensen, 1993), similar to ages of quartz porphyries of the Timmins area (2688 - 2691 Ma; Corfu et al., 1989) and felsic porphyries of the Val d'Or area (2685 - 2694 Ma; Wong et al., 1989; Zweng and Mortensen, 1989). Such porphyry intrusions may have been exposed during sedimentation and later removed by erosion. Calc-alkaline porphyry clasts may be the only indication that porphyry intrusions of that time period were also common in this area.

The presence of QPP2 clasts in basal conglomerates also indicates that the quartz porphyries were exposed during alluvial-fluvial sedimentation and that deposition started after 2685 Ma. An age of 2677 ± 2 Ma for a trachytic agglomerate (Corfu et al., 1991) may provide a minimum age of sedimentation, because it overlies alluvial-fluvial sedimentary rocks.

Nature of the LLCF

The LLCF has been interpreted as a suture zone between two tectonic blocks: the Round Lake (south) and the Blake River (north)(e.g., Ludden et al., 1986; Kerrich and Feng, 1992). The similarity in compositions of sandstones and clast populations of conglomerates of the alluvial-fluvial assemblage north and south of the LLCF indicates that these rocks had similar sources and were probably deposited at the same time. Therefore sedimentation of the alluvial-fluvial assemblage appears to have started after juxtaposition of the Round Lake and Blake River blocks. The presence of trachyte clasts only in conglomerates near the LLCF indicates that alkaline magmatism was areally restricted to the vicinity of the fault, and that movement along the LLCF may have created conduits for post-accretion magmatism.

Tectonic setting

The alluvial-fluvial assemblage may have formed during arc volcanism before major deformation (e.g., Hyde, 1980; Dimroth et al., 1983), in a pull-apart basin along the LLCF (e.g., Thurston and Chivers, 1990; Card, 1990) or as a fault-scarp deposit that accumulated during oblique thrusting along the LLCF (e.g., Hodgson and Hamilton, 1989).

The models of Hyde (1980) and Dimroth et al. (1983) are not consistent with the distribution on both sides of the LLCF. It also appears to discount deposition in a fault-scarp basin. Minor occurrences of the alluvial-fluvial assemblage south of the LLCF may be attributed to post-Timiskaming uplift of the south side along the fault (e.g., Hamilton and Hodgson, 1989; Jackson and Sutcliffe, 1990). Such movements would have caused rocks of the alluvial-fluvial assemblage on the south side of the LLCF to be mostly removed by erosion while preserving the same rocks on the north-side.

The presence of clasts derived from both north and south of the LLCF appears to favor a pull-apart basin model because fault scarp sediments in footwall troughs would contain clasts derived from only one side of the fault (e.g., Girard, 1992). The recognition of the Round Lake batholith and diorite/quartz diorite intrusions as source rocks for the alluvial-fluvial assemblage indicates that clasts were derived from both sides of the LLCF. The presence of chert (including jasper) and magnetitite also supports derivation of detritus from the south since magnetite banded-iron formations have only been observed in the Round Lake block (e.g., Jensen and Langford, 1985). Deposition of the alluvial-fluvial assemblage in a pull-apart basin is also consistent with recent sedimentological and volcanological studies on the alluvial-fluvial assemblage (Mueller et al., 1992).

Our results favor sedimentation in a pull-apart basin after juxtaposition of tectonic blocks, although horizontal movements along the LLCF during and after sedimentation appear to have been small. This is consistent with structural observations on the LLCF by Wilkinson and Cruden (1992) which indicate that any large-scale transcurrent movement must have occurred prior to deposition of the alluvial-fluvial assemblage. On the basis of the present study, the sources for the igneous clasts are all within 15 km of their depositional site, and so no exotic source is required, eliminating the need for large strike-slip displacements of the two sides during and/or after deposition of the Timiskaming Group.

CONCLUSIONS

1. Conglomerates and sandstones north and south of the LLCF are similar, indicating that sedimentation started after juxtaposition of tectonic blocks along the LLCF.
2. Coarse-grained holocrystalline clasts are trondhjemitic. Trace element contents, mineralogy and texture of clasts suggest their derivation from the marginal phase of the Round Lake batholith.
3. Andesitic clasts are common in basal conglomerates, but their abundances decrease up the stratigraphic section; tholeiitic basalt and porphyry clasts are predominant in upper sections. This change of clast populations suggests an increase in dissection of an arc during sedimentation.
4. Alkalic clasts were derived from Timiskaming trachytic volcanic rocks and associated hypabyssal phases. The presence of these clasts only in proximity to the LLCF indicates that alkaline magmatism was not widespread, and that the displacement along the fault may have

created conduits for alkaline magmatism.

5. Calc-alkaline porphyry clasts, the predominant clast in most outcrops, were not derived from the late feldspar porphyry intrusions which are now abundant in the area. The porphyry clasts are related to early diorites/quartz diorites and granodiorite porphyries, and calc-alkaline volcanic rocks of the Blake River Group. The predominance of these clasts suggests their derivation from a dissected island arc. Ages of early and late porphyry intrusions bracket sedimentation of the alluvial-fluvial assemblage between 2677 - 2685 Ma.

6. The occurrence of both the alluvial-fluvial assemblage and inferred source rocks on both sides of the LLCF suggests deposition in a pull-apart basin. However, proximity of the clasts to their sources indicates that only minor strike-slip movement occurred during and/or after sedimentation.

ACKNOWLEDGEMENTS

We thank Wulf Mueller of Université du Québec à Chicoutimi for his advice in the field, Ron Hartree of the University of Ottawa and Richard Rousseau of the Geological Survey of Canada for XRF analyses, John Loop of the University of Ottawa for ICP-AES and Greg Kennedy of Université de Montréal for INAA, Peter Jones of Carleton University for his patient assistance with microprobe analysis and Zoran Mador at the Drill Core Library of the Ministry of Northern Development and Mines at Swastika for supplemental samples. Helpful comments and unpublished data from Timiskaming porphyry intrusions were provided by Guy Levesque. The manuscript benefited from comments by Randy Rice and J. Allan Donaldson. The project was

funded by a Natural Sciences and Engineering Research Council of Canada grant to K.H..

REFERENCES

Arculus, R.J. and Powell, R., 1986. Source component mixing in the regions of arc magma generation. J. Geophys. Res., 91: B5913-B5926.

Capdevila, R., Goodwin, A.M., Ujike, O. and Gorton, M.P., 1982. Trace element geochemistry of Archean volcanic rocks and crustal growth in SW Abitibi belt, Canada. Geology, 10: 418-422.

Card, K.D., 1990. A review of the Superior Province of the Canadian Shield: a product of Archean accetion. Precambrian Res., 48: 99-156.

Cawthorne, R.G., 1976. Some chemical controls on igneous amphibole compositions. Geochim. Cosmochim. Acta, 40: 1319-1328.

Condie, K.C., 1993. Chemical composition and evolution of the upper continental crust: Contrasting results from surface samples and shales. Chem. Geol., 104: 1-37.

Condie, K.C. and Hunter, D.R., 1976. Trace element geochemistry of Archean granitic rocks from the Barberton region, South Africa. Earth Planet. Sci. Lett., 29: 389-400.

Cooke, D.L. and Moorhouse, W.W., 1969. Timiskaming volcanism in the Kirkland Lake area, Ontario, Canada. Can. J. Earth Sci., 6: 117-132.

Corfu, F., Krogh, T.E., Kwok, Y.Y. and Jensen, L.S., 1989. U-Pb zircon geochronology in the southwestern Abitibi greenstone belt, Superior Province. Can. J. Earth Sci., 26: 1747-1763.

Corfu, F., Jackson, S.L. and Sutcliffe, R.H., 1991. U-Pb ages and tectonic significance of late Archean alkalic magmatism and nonmarine sedimentation: Timiskaming Group, southern

Abitibi belt, Ontario. Can. J. Earth Sci., 28: 489-503.

De La Roche, H., Leterrier, J., Grandclaude, P. and Marchal, M., 1980. A classification of volcanic and plutonic rocks using R1R2-diagram and major-element analyses - its relationships with current nomenclature. Chem. Geol., 29: 183-210.

Dimroth, E., Imreh, L., Goulet, N. and Rocheleau, M., 1983. Evolution of the south-central segment of the Archean Abitibi belt, Quebec. Part III: Plutonic and metamorphic evolution and geotectonic model. Can. J. Earth Sci., 20: 1374-1388.

Dodge, F.C.W., Papike, J.J. and Mays, R.E., 1968. Hornblendes from granitic rocks of the Sierra Nevada batholith, California. J. Petrol., 9: 378-410.

Ermanovics, I.F., McRitchie, W.D. and Houston, W.N., 1979. Petrochemistry and tectonic setting of plutonic rocks of the Superioir Province in Manitoba. In: F. Barker (Editor), Trondhjemites, dacites, and related rocks. Elsevier. Developments in Petrology, 6: 323-362.

Feng, R. and Kerrich, R., 1990. Geochemistry of fine-grained clastic sediments in the Archean Abitibi greenstone belt, Canada: implications for provenance and tectonic setting. Geochim. Cosmochim. Acta, 54: 1061-1081.

Feng, R. and Kerrich, R., 1992. Geochemical evolution of granitoids from the Archean Abitibi Southern Volcanic Zone and the Pontiac subprovince, Superior Province, Canada: Implications for tectonic history and source regions. Chem. Geol., 98: 23-70.

Fowler, A.D. and Jensen, L.S., 1989. Quantitative trace-element modelling of the crystallization history of the Kinojevis and Blake River groups, Abitibi greenstone belt, Ontario. Can. J. Earth Sci., 26: 1356-1367.

Girard, R., 1992. Le Groupe de la Hutte Sauvage: sédimentation alluvionnaire épi-orogénique dans l'arrière-pays de la fosse du Labrador (Protérozoique inférieur, Nouveau-Québec). Can. J. Earth Sci., 29: 2571-2582.

Glikson, A.Y., 1979. Early Precambrian tonalite-trondhjemite sialic nuclei. Earth Sci. Rev., 15: 1-73.

Hammarstrom, J.M. and Zen, E., 1986. Aluminum in hornblende: an empirical igneous geobarometer. Am. Mineral., 71: 1297-1313.

Hewitt, D.F., 1963. The Timiskaming Series of the Kirkland Lake area. Can. Mineral., 7: 497-522.

Hicks, K.D. and Hattori, K., 1988. Magmatic-hydrothermal and wall rock alteration petrology at the Lake Shore gold deposit, Kirkland Lake, Ontario. Ont. Geol. Surv. Misc. Paper, 140: 192-204.

Hodgson, C.J., 1986. Place of gold ore formation in the geological development of Abitibi greenstone belt, Ontario. Inst. Min. Metall. Trans., 95B: BI83-BI94.

Hodgson, C.J. and Hamilton, J.V., 1989. Gold mineralization in the Abitibi greenstone belt: End-stage result of Archean collisional tectonics?. Econ. Geol. Monograph, 6: 86-100.

Hyde, R.S., 1980. Sedimentary facies in the Archean Timiskaming Group and their tectonic implications, Abitibi greenstone belt, northeastern Ontario, Canada. Precambrian Res., 12: 161-195.

Irvine, T.N. and Baragar, R.A., 1971. A guide to the chemical classification of the common volcanic rocks. Can. J. Earth Sci., 8: 523-548.

Jackson, S.L. and Fyon, J.A., 1991. The Western Abitibi Subprovince. In: P.C. Thurston, H.R.

Williams, R.H. Sutcliffe, and G.M. Stott (Editors), Geology of Ontario. Ont. Geol. Surv. Spec. Vol., 4: 405-482.

Jackson, S.L. and Sutcliffe, R.H., 1990. Central Superior Province: evidence for an allochthonous, ensimatic, southern Abitibi greenstone belt. Can. J. Earth Sci., 27: 582-589.

Jakes, P. and White, A.J.R., 1972. Hornblendes from calc-alkaline volcanic rocks of island arc and continental margins. Am. Mineral., 57: 887-902.

Jensen, L.S. and Langford, F.F., 1985. Geology and petrogenesis of the Archean Abitibi belt in the Kirkland Lake area, Ontario. Ont. Geol. Surv. Misc. Pap.: 123.

Jolly, W.T., 1980. Development and degradation of Archean lavas, Abitibi area, Canada, in light of major element geochemistry. J. Petrol., 21: 323-363.

Kerrich, R. and Feng, R., 1992. Archean geodynamics and the Abitibi-Pontiac collision: implications for advection of fluids at transpressive collisional boundaries and the origin of giant quartz vein systems. Earth Sci. Rev., 32: 33-60.

Kerrich, R. and Watson, G.P., 1984. The Macassa Mine Archean lode gold deposit, Kirkland Lake, Ontario: Geology, patterns of alteration, and hydrothermal regimes. Econ. Geol., 79: 1104-1130.

Lafleur, P.J., 1986. The Archean Round Lake batholith, Archean greenstone belt: a synthesis. M.Sc. Thesis, University of Ottawa, Ottawa, Ont. (Canada).

Lameyre, J. and Bowden, P., 1982. Plutonic rock types series: discrimination of various granitoid series and related rocks. J. Volcanol. Geotherm. Res., 14: 169-186.

Leake, B.E., 1978. Nomenclature of amphiboles. Am. Mineral., 63: 1023-1052.

Legault, M.I. and Hattori, K., in press. Late Archaean geological development recorded in the Timiskaming Group sedimentary rocks, Kirkland Lake area, Abitibi greenstone belt, Canada. Precambrian Res..

Levesque, G.S., Cameron, E.M. and Lalonde, A.E., 1991. Duality of magmatism along the Kirkland Lake - Larder Lake fault zone, Ontario. Geol. Surv. Can. Pap., 91-1C: 17-24.

Ludden, J., Hubert, C. and Gariépy, C., 1986. The tectonic evolution of the Abitibi greenstone belt of Canada. Geol. Mag., 123: 153-166.

Martin, H., 1987. Petrogenesis of Archean trondhjemites, tonalites, and granodiorites from eastern Finland: Major and trace element geochemistry. J. Petrol., 28: 921-953.

McCall, G.W., Nabelek, P.I., Bauer, R.L. and Glascock, M.D., 1990. Petrogenesis of Archean lamprophyres in the southern Vermilion Granitic Complex, northeastern Minnesota, with implications for the nature of their mantle source. Contrib. Mineral. Petrol., 104: 439-452.

Mortensen, J.K., 1993. U-Pb geochronology of the eastern Abitibi Subprovince. Part 2: Noranda - Kirkland Lake area. Can. J. Earth Sci., 30: 29-41.

Mueller, W., Donaldson, J.A., Dufresne, D. and Rocheleau, M., 1991. The Duparquet Formation: sedimentation in a late Archean successor basin, Abitibi greenstone belt, Quebec, Canada. Can. J. Earth Sci., 28: 1394-1406.

Mueller, W. and Donaldson, J.A., 1992. Development of sedimentary basins in the Archean Abitibi belt, Canada: an overview. Can. J. Earth Sci., 29: 2249-2265.

Mueller, W., Doucet, P., Desgagné, J. and Donaldson, J.A., 1992. The Kirkland Basin: volcanism and sedimentation in a late orogenic successor basin. Lithoprobe, project

Abitibi-Grenville, Abstracts, Report, 33: 41-46.

Ontario Geological Survey, 1986. Rock chemical data catalogue. Ont. Geol. Surv. Open File Rep. 5570.

Paradis, S., Ludden, J. and Gélinas, L., 1988. Evidence for contrasting compositional spectra in comagmatic intrusive and extrusive rocks of the late Archean Blake River Group, Abitibi, Quebec. Can. J. Earth Sci., 25: 134-144.

Pearce, J.A., Harris, N.B.W. and Tindle, A.G., 1984. Trace element discrimination diagrams for the tectonic interpretation of granitic rocks. J. Petrol., 25: 956-983.

Pringle, G.J., 1989. EDDI - a fortran computer program to produce corrected microprobe of minerals using an energy dispersive x-ray spectrometer. Geol. Surv. Can., Open File Rep. 2127.

Reid, J.B., Jr. and Hamilton, M.A., 1987. Origin of Sierra Nevadan granite: evidence from small scale composite dikes. Contr. Mineral. Petrol., 96: 441-454.

Rice, R.J. and Donaldson, J.A., 1992. Sedimentology of the Archean Doré metasediments, Arliss Lake area, southern Michipicoten greenstone belt, Superior Province. Can. J. Earth Sci., 29: 2558-2570.

Rive, M., Melancon, M. and Savage, R., 1989. Carte de compilation géologique (32D). Ministère Energie et Ressources, Secteur Mines, echelle 1:125 000.

Rock, N.M.S., 1987. The nature and origin of lamprophyres: an overview. In: J.G. Fitton and B.G.J. Upton (Editors), Alkaline igneous rocks. Geol. Soc. Spec. Publ., 30: 191-226.

Rock, N.M.S., Gaskarth, J.W., Henney, P.J. and Shand, P., 1988. Late Caledonian dyke-swarms of northern Britain: some preliminary petrogenetic and tectonic implications of their

province-wide distribution and chemical variation. Can. Mineral., 26: 3-22.

Seiders, V.M. and Blome, C.D., 1988. Implications of upper Mesozoic conglomerate for suspect terrane in western California and adjacent areas. Geol. Soc. Am. Bull., 100: 374-391.

Shegelski, R.J., 1980. Archean cratonization, emergence and red bed development, Lake Shebandowan area, Canada. Precambrian Res., 12: 331-347.

Smith, A.R. and Sutcliffe, R.H., 1988. Plutonic rocks of the Abitibi subprovince. Ont. Geol. Surv. Misc. Pap., 141: 188-196.

Stern, R.A. and Hanson, G.N., 1992. Origin of Archean lamprophyre dykes, Superior Province, Canada: rare earth element and Nd-Sr isotopic evidence. Contrib. Mineral. Petrol., 111: 515-526.

Sun, S.S. and McDonough, W.F., 1989. Chemical and isotopic systematics of oceanic basalts: implications for mantle composition and processes. In: A.D. Saunders and M.J. Norry (Editors), Magmatism in the ocean basins. Geol. Soc. Spec. Publ., 42; 313-345.

Sutcliffe, R.H., Smith, A.R., Doherty, W. and Barnett, R.L., 1990. Mantle derivation of Archean amphibole-bearing granitoid and associated mafic rocks: evidence from the southern Superior Province, Canada. Contrib. Mineral. Petrol., 105: 255-274.

Suzuki, K. and Shiraki, K., 1980. Chromite-bearing spessartites from Kasuga-mura, Japan, and their bearing on possible mantle origin andesite. Contr. Mineral. Petrol., 71: 313-322.

Taner, M.F. and Trudel, P., 1989. Bourlamaque batholith and its gold potential, Val d'Or, Quebec. Can. Inst. Min. Mettall. Bull., 82 (February): 33-42.

Tarney, J., Weaver, B. and Drury, S.A., 1979. Geochemistry of Archean trondhjemitic and tonalitic gneisses from Scotland and east Greenland. In: F. Barker (Editor),

Trondhjemites, dacites, and related rocks. Elsevier. Developments in Petrology, 6: 275-299.

Thomson, J.E., 1946. The Keewatin-Timiskaming unconformity in the Kirkland Lake district. Transactions of the Royal Society of Canada, Section 4, 40: 113-124.

Thomson, J.E., 1948. Geology of Teck Township and the Kenogami Lake area, Kirkland Lake Gold Belt. Ont. Dept. Mines, Annu. Rep., 57-5: 1-53.

Thurston, P.C. and Chivers, K.M., 1990. Secular variation in greenstone sequence development emphasizing Superior Province, Canada. Precambrian Res., 46: 21-58.

Ujike, O., 1985. Geochemistry of Archean alkalic volcanic rocks from the Crystal Lake area, east of Kirkland Lake, Ontario, Canada. Earth Planet. Sci. Lett., 73: 333-344.

Wilkinson, L. and Cruden, A.R., 1992. Post-Timiskaming structural history of the Kirkland Lake area. Lithoprobe, project Abitibi-Grenville, Abstracts, Report, 33: 61-64.

Wilson, M.E., 1956. Early Precambrian rocks of the Timiskaming region, Quebec and Ontario, Canada. Bull. Geol. Soc. Am., 67: 1397-1430.

Wong, L., Davis, D.W., Hanes, J.A., Archibald, D.A. and Hodgson, C.J., 1989. An integrated U-Pb and Ar-Ar geochronological study of the Archean Sigma gold deposit, Val d'Or, Quebec. Geol. Assoc. Can., Min. Assoc. Can., Prog. with Abstracts, 14: A45.

Wyman, D.A. and Kerrich, R., 1989. Archean lamprophyre dikes of the Superior Province, Canada: distribution, petrology, and geochemical characteristics. J. Geophys. Res., 94B: 4667-4696.

Zweng, P.L. and Mortensen, J.K., 1989. U-Pb age constraints on Archean magmatism and gold mineralization at the Camflo mine, Malartic, Quebec. Geol. Soc. Am., Prog. with

Abstracts, 21: A351.

Appendix I: Carbon and oxygen isotopic compositions of carbonate-bearing igneous clasts

SUMMARY

Carbonates in 17 igneous clasts from the alluvial-fluvial assemblage and turbidite south unit and 1 lamprophyre were analyzed for C and O isotopes. Carbonates are mostly calcite with minor dolomite and ankerite. Values for $\delta^{13}C$ and $\delta^{18}O$ for carbonates from clasts of the alluvial-fluvial assemblage show a remarkable similarity and are indistinguishable from values for carbonates associated with the lamprophyre intrusion. Values for carbonates in clasts from the turbidite south unit are more enriched in ^{18}O, but depleted in ^{13}C compared to carbonates in clasts from the alluvial-fluvial assemblage. All isotope compositions, however, fall within the range of disseminated and vesicle-filling carbonates of the Blake River Group.

ANALYTICAL METHODS

Samples of clasts were collected during the summers of 1991 and 1992. Over 90 thin sections were made, and 18 of these samples showed different degrees of carbonatization (see Appendix 1a for sample descriptions). These samples were stained to distinguish calcite, ankerite and dolomite using Alizarin Red S and potassium ferricyanide.

Isotope compositions for carbonates were determined on CO_2 released from whole-rock powders or hand-picked vein fillings, after reaction with 100% H_3PO_4 at 25°C (McCrea, 1950). For samples containing calcite and dolomite/ankerite, extractions of CO_2 were timed at 2 h to obtain CO_2 only from calcite. The isotopic compositions of CO_2 were determined by the triple-collector VG-SIRA mass spectrometer at the University of Ottawa. Isotopic ratios are reported in the standard δ notation, relative to PDB for carbon and to SMOW for oxygen (Table 1).

OCCURRENCE OF CARBONATES

Staining of samples indicate that the main carbonate present in veins and alteration is ferroan calcite. Dolomite and ankerite are minor constituents. This is in contrast with carbonate minerals found along the LLCF where ferro-dolomite and siderite are the predominant carbonates (W. Zhan, unpub. data; Kerrich et al., 1987).

Host rocks vary in their lithologies. They range from mafic and trachytic volcanic rocks to tuffs, plagioclase ± quartz porphyries and trondhjemites (see Appendix 1a). Occurrences of carbonates are of 3 types: 1) vesicle-filling carbonates; 2) carbonates associated

Table 1. Oxygen and carbon isotope data from alluvial-fluvial assemblage and turbidite unit clasts. See Appendix 1a for description of occurrence of carbonates.

Sample	*Clast type**	*delta 18O SMOW per mil*	*delta 13C PDB per mil*
1j	FP	10.7	-2.8
1k	QFP	10.9	-2.7
1n	MV	10.4	-2.1
1s	FP	10.4	-2.0
1w	MV	10.6	-3.0
2c	FP	10.0	-2.1
2l	S	9.8	-1.8
3k	H	11.7	-2.7
3o	QFP	10.9	-2.5
3v	T	10.3	-1.9
3x	T	10.3	-1.9
1m	H	10.8	-2.7
1c	KFP	10.9	-2.3
15g	FP	10.3	-2.4
15l	KFP	10.5	-1.9
30d	FP	12.2	-3.6
30ep	S	10.6	-4.2
47b	M#	10.2	-2.4

* FP - Feldspar porphyry; QFP - Quartz-feldspar porphyry;
S - Spessartite; MV - Mafic volcanic; H - Holocrystalline;
T - Tuff; KFP - K-feldspar porphyry.
M - Minette dyke

with alteration of plagioclase and mafic minerals; and 3) carbonates in veinlets. Carbonates of the third occurrence generally occur together with quartz in the veins and in some cases epidote. Sulfide and oxide minerals in the veins are rare and are restricted to pyrite and hematite.

Two types of alteration associated with carbonate-bearing veins are recognized: quartz + epidote + sericite ± albite and quartz + sericite + chlorite ± albite (see Appendix 1a). These assemblages imply that the carbonate veining took place under the conditions equivalent to prehnite-pumpellyite to middle greenschist facies metamorphic grade. Estimated temperatures of formation for the epidote-bearing assemblage are from ~350°C, based on the stability of epidote (Liou, 1973). The absence of biotite as a metamorphic mineral provides a maximum temperature for the formation of the epidote-bearing assemblages. The appearance of biotite is considered to be ~450°C (Nitsch, 1971). Minimum temperatures of formation for the quartz + sericite + chlorite assemblage is ~300°C at which clay minerals are no longer stable (Hower et al., 1976). Maximum temperatures for this assemblage may be constrained by the absence of epidote which forms at ~350 °C.

ISOTOPIC COMPOSITIONS

Values for $\delta^{18}O$ and $\delta^{13}C$ for calcite are very consistent within the clasts of the alluvial-fluvial assemblage ($\delta^{18}O$ = +10.6 ± 0.4 ‰; $\delta^{13}C$ = -2.3 ± 0.4 ‰; n=17; all uncertainties expressed as ± 1 σ)(Table 1). These values are indistinguishable from calcite associated with a lamprophyre intrusion ($\delta^{18}O$ = +10.2 ‰; $\delta^{13}C$ = -2.4 ‰; sample 47b). Two clasts from conglomerates of the turbidite unit south of the LLCF have calcite-bearing

veins and their compositions are slightly different from calcite from alluvial-fluvial assemblage ($\delta^{18}O$ = +11.4 ± 0.8 ‰; $\delta^{13}C$ = -3.9 ± 0.3 ‰; n=2).

DISCUSSION

The consistency of the $\delta^{18}O$ and $\delta^{13}C$ values of veins indicates that all calcite may have been precipitated from fluids of similar origin. This consistency is remarkable considering the values are from clasts of various source rocks.

The high values of $\delta^{18}O$ (> +10.0 ‰) of calcite from the clasts indicate that calcite may have undergone isotopic exchange with present day surface waters ($\delta^{18}O$ ~ -15 ‰). $\delta^{18}O$ for calcite in equilibrium with the surface waters at low temperatures (25°C) gives a value of ~ +13 ‰. In surface waters, $\delta^{13}C$ is mostly controlled by $\delta^{13}C_{HCO3-}$, because of the neutral to slightly alkaline nature of the water. The area is underlain by igneous rocks, especially alkaline rocks. $\delta^{13}C_{HCO3-}$ in the water is ~ 0 ‰ because it is likely buffered by atmospheric CO_2, -7 ‰. At 25°C, isotope fractionation factors are small between calcite and HCO_3^- (~ +3 ‰) and therefore isotopic re-equilibrium of calcite with present-day surface water (~ 0 ‰) would have expected values of ~ +3 ‰, which are much higher than what is observed (~ -3 ‰). It appears that the calcite from the clasts has not undergone extensive isotopic re-equilibrium with present-day surface waters.

The low $\delta^{18}O$ values compared to Archean greenstone belt limestone ($\delta^{18}O$ = +21 to +24 ‰; Veizer et al., 1989) suggest that they are not a low temperature product. Therefore, carbonates have retained the original isotopic ratios of the fluids and a hydrothermal origin for these fluids is consistent with alteration envelopes.

Values reported here are compared with results for dolomites from Au deposits located in the Kirkland Lake - Larder Lake area. Isotopic fractionation factors between calcite and dolomite are small (Bottinga, 1968) and therefore, the difference between the calcite and dolomite data is negligible. Compared to the data reported by Kerrich et al. (1987), calcites from the clasts of the alluvial-fluvial assemblage are lower in ^{18}O and higher in ^{13}C than ferro-dolomites from the Au deposits (Fig. 1). Clasts from the turbidite unit have carbonates with similar values to those associated with the mineralization.

Isotope data from the clasts fall within the field of calcite from metavolcanic rocks of the calc-alkalic Blake River Group (Kerrich, 1990) located just north of the LLCF (Fig. 1). Calcite from tholeiitic basalts of the Malartic Group (~100 km ENE of Kirkland Lake) have similar isotopic compositions (Kerrich, 1990). They are also distinct from disseminated carbonates in sedimentary rocks of the Kewagama and Cadillac groups (Fig. 1), ~ 90 km E of Kirkland Lake, which are believed to be of similar age as the Timiskaming Group (Davis, 1991).

Figure 1. Isotopic compositions of calcite from clasts of the alluvial-fluvial (solid triangles) and turbidite south (solid squares) assemblages. Open circles = values for carbonates associated with gold mineralization along the LLCF (W. Zhan, unpubl. data; Kerrich et al., 1987). Fields are for the Blake River Group (thick solid line), Kewagama Group (thin solid line), and Cadillac Group (thin dashed line)(Kerrich, 1990); Archean limestone (thick dashed line)(Veizer et al., 1989).

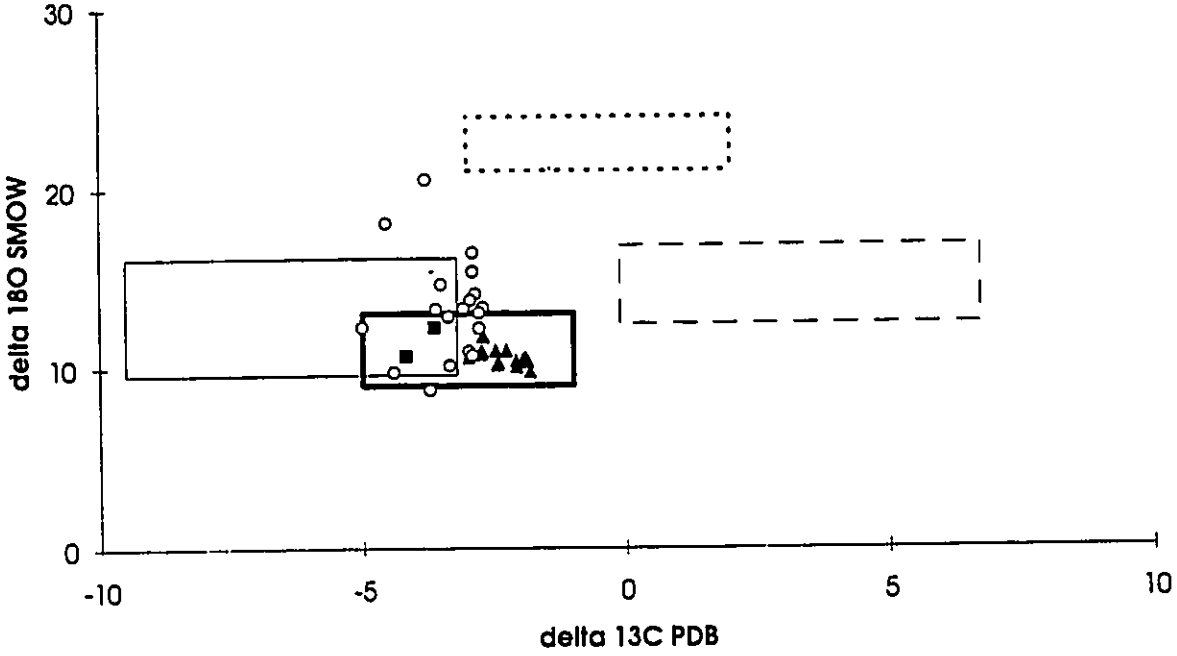
30
20
10
0
delta 18O SMOW
-10
-5
0
5
10
delta 13C PDB

REFERENCES

Bottinga, Y., 1968. Calculation of fractionation factors for carbon and oxygen isotopic exchange in the system calcite-carbon dioxide-water. J. Phys. Chem., 72: 800-808.

Davis, D.W., 1991. Age constraints on deposition and provenance of Archean sediments in the southern Abitibi and Pontiac subprovinces from U-Pb analyses of detrital zircons. Lithoprobe, project Abitibi-Grenville, Abstracts: 147-150.

Hower, J., Eslinger, E., Hower, M.E. and Perry, E.A., 1976. Mechanism of burial metamorphism of argillaceous sediments: I. Mineralogical and chemical evidence. Geol. Soc. Am. Bull., 87: 725-737.

Kerrich, R., 1990. Carbon-isotope systematics of Archean Au-Ag vein deposits in the Superior Province. Can. J. Earth Sci., 27: 40-56.

Kerrich, R., Fryer, B.J., King, R.W., Willmore, L.M. and van Hees, E., 1987. Crustal outgassing and LILE enrichment in major lithosphere structures, Archean Abitibi greenstone belt: evidence on the source reservoir from strontium and carbon isotope tracers. Contrib. Miner. Petrol., 97: 156-168.

Liou, J.G., 1973. Synthesis and stability relations of epidote, $Ca_2Al_2FeSi_3O_{12}(OH)$. J. Petrol., 14: 381-413.

McCrea, J.M., 1950. The isotopic chemistry of carbonates and a paleotemperature scale. J. Chem. Phys., 18: 849.

Nitsch, K.-H., 1971. Stability relations of parageneses containing prehnite and pumpellyite. Contrib. Mineral. Petrol., 30: 240-260.

O'Neil, J.R., Clayton, R.N. and Mayeda, T., 1969. Oxygen isotope fractionation in divalent

metal carbonates. J. Chem. Phys., 51: 5547-5558.

Rye, R.O. and Ohmoto, H., 1974. Sulfur and carbon isotopes and ore genesis: a review. Econ. Geol., 69: 826-842.

Veizer, J., Hoefs, J., Lowe, D.R. and Thurston, P.C., 1989. Geochemistry of Precambrian carbonates: II. Archean greenstone belts and Archean sea water. Geochim. Cosmochim. Acta, 53: 859-871.

APPENDIX 1A: Occurrence of carbonate minerals in clasts.

Clasts are from alluvial-fluvial conglomerates unless otherwise specified. The small size of the alteration minerals in the envelopes (< 0.5 mm) around carbonate veins prevents optical identification of all minerals. Therefore only those identified with certainty are indicated.

1c - K-feldspar porphyry. Calcite along cracks of orthoclase phenocrysts.

1j - Hornblende-plagioclase porphyry. Calcite is associated with alteration of plagioclase phenocrysts.

1k - Quartz-plagioclase porphyry. Quartz-calcite veinlets (~ 1mm) and calcite in recrystallized groundmass. Alteration envelope - quartz, sericite and chlorite.

1m - Trondhjemite. Quartz-calcite veinlets (~ 0.5 mm) and calcite associated with chlorite and iron-oxides. Alteration envelope - quartz, sericite and chlorite.

1n - Mafic volcanic rock. Calcite and dolomite in recrystallized groundmass.

1s - Hornblende-plagioclase porphyry. Calcite veinlets (~ 1 mm) and calcite associated with chlorite and iron-oxides. Alteration envelope - quartz, albite and sericite.

1w - Mafic volcanic rock. Quartz-dolomite-calcite veinlets (~ 0.5 mm) and calcite and dolomite in recrystallized groundmass.

2c - Hornblende-plagioclase porphyry. Epidote-quartz-calcite veinlets (~ 1 mm). Alteration envelope - epidote and quartz.

2i - Spessartite. Calcite veinlets (~ 0.5 mm) and calcite associated with altered hornblende phenocrysts. Alteration envelope - quartz, epidote and albite.

3k - Trondhjemite. Calcite veinlets (~ 2 mm). Alteration envelope - quartz, sericite and

chlorite.

3o - Quartz-plagioclase porphyry. Calcite veinlets (~ 5 mm). Alteration envelope - quartz and sericite.

3v - Crystal tuff. Calcite and dolomite in cavities.

3x - Crystal tuff. Calcite in cavities and associated with altered plagioclase phenocrysts.

15g - Hornblende-plagioclase porphyry. Calcite veinlets (~ 1 mm) and associated with chlorite and iron-oxides. Alteration envelope - quartz, sericite and chlorite.

15l - K-feldspar porphyry. Calcite along cracks in orthoclase phenocrysts.

30d - Feldspar porphyry from conglomerate of the turbidite assemblage south of LLCF. Calcite veinlets (~ 2 mm), calcite in recrystallized groundmass and associated with altered plagioclase phenocrysts. Alteration envelope - quartz, epidote and sericite.

30ep - Spessartite from conglomerate of the turbidite assemblage south of LLCF. Calcite veinlets (~ 1 mm) and calcite associated with altered hornblende phenocrysts. Alteration envelope - quartz, epidote and sericite.

47b - Minette intrusion. Calcite and specular hematite found at contact with turbidite assemblage. Alteration envelope - quartz, sericite and albite.

Appendix II: Field observations, gamma ray spectrometry and magnetic susceptibility measurements, and collected samples

The following notes are accompanied by schematic diagrams to facilitate locations of outcrops. On these diagrams, north is towards the top of the page. Major roads and power lines (dark lines) are shown as well as railway tracks (stippled lines). For general location of samples refer to geological map accompanying "Late Archaean geological development recorded in the Timiskaming Group sedimentary rocks, Kirkland Lake area, Abitibi greenstone belt, Canada". Point counting of clasts at outcrops 91-1, 91-2, 91-3 and 92-39 is shown in "Igneous activity recorded in the conglomerate clasts of the Late Archaean Timiskaming Group, Kirkland Lake area, Abitibi greenstone belt". Clast proportions in this appendix refer to conglomerates that were not point counted (i.e. estimated).

Classification scheme for Timiskaming conglomerate clasts of the Kirkland Lake area

Volcanic rock:	Trachytic (TVR) Felsic (FVR) Mafic (MVR) Ultramafic (UMVR) Tuff (VT)
Holocrystalline rock:	(HR)
Porphyritic rock:	Hornblende-feldspar (HFP) Quartz-feldspar (QFP) Feldspar (FP) Spessartite lamprophyre (SL)
Sedimentary rock:	Chert including jasper (CH) Sandstone (SS) Banded iron-formation (BIF)
Monomineralic rock:	Vein quartz (VQ) Magnetitite (MT)

Abbreviations:

MS - Magnetic susceptibility. Measurements of magnetic susceptibility and radio-element concentrations were made on flat surfaces in the field.

K - potassium

eU - equivalent uranium

eTh - equivalent thorium

Outcrop 91-1 (Chaput-Hughes outcrop on Hwy. 66)

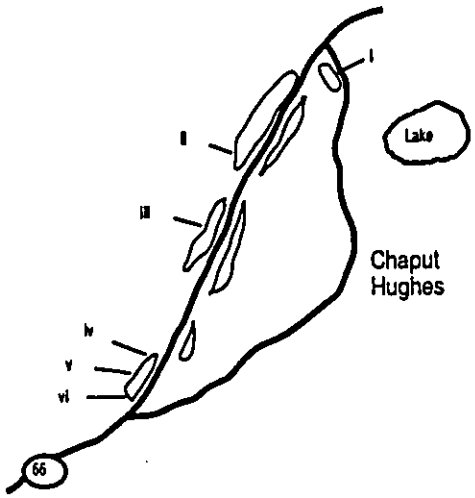

i) Clast-supported conglomerate with thin interbeds of sandstone
Largest clast: Holocrystalline (12 x 25 cm)
Remarks: Average clast size is about 5 cm. Clasts are rounded to well-rounded, poorly sorted and elongated clasts have a random orientation. Sandstone beds have an orientation of 095/47 S. They vary in thickness from 15 to 40 cm and are massive.
Matrix: 20%; greenish color, minor quartz and feldspar
Collected samples 91-1b HFP
91-1c FP
91-1d VT
91-1e VT
91-1f HR
91-1g MVR
91-1x MVR

ii) Clast-supported conglomerate with small lenses of sandstone
Largest clast: Quartz-feldspar porphyry (13 x 22 cm)
Remarks: Clasts have an average size of 5 cm. They are rounded to well-rounded, fairly well sorted, and the elongated clasts have a random orientation. Sandstone beds have an orientation of 093/52 S. The lenses of sandstone are about 20 cm thick and are massive.
Matrix: 16%; greenish color; minor quartz and feldspar
Collected samples 91-1h TVR
91-1i UMVR
91-1j SL
91-1k QFP
91-1l HFP
91-1m HR
91-1n MVR

91-1o HR
91-1a TVR

iii) Matrix-supported conglomerate with small lenses of sandstone in contact with sandstone bed with small lenses of conglomerate
Largest clast: Quartz-feldspar porphyry (12 x 23 cm)
Remarks: The clasts have an average size of 5 to 7 cm. They are subrounded to well rounded, fairly well sorted and elongated clasts appear to be parallel to the bedding. Lenses of sandstone are 10 to 30 cm thick while the lenses of conglomerate are 2 to 10 cm thick. Sandstone bed displays cross-bedding indicating that top is toward south. The contact between conglomerate and sandstone beds is parallel to both lenses of conglomerate and sandstone and was measured as 082/66 S.
Matrix: 20%; greenish color, minor quartz and feldspar
Collected samples 91-1p HR
91-1q SS
91-1r HFP
91-1s HFP
91-1t HR
91-1u TVR

iv) Interbedding of sandstone and conglomerate beds. Two argillite lenses are also present as well as a feldspar porphyry intrusion.
Largest clast: Quartz-feldspar porphyry (6 x 13 cm)
Remarks: The clasts have an average size of 1 to 2 cm. They are subrounded to well rounded and are poorly sorted.
Matrix: 77%

v) Clast-supported conglomerate
Largest clast: Quartz-feldspar porphyry (10 x 12 cm)
Remarks: The clasts have an average size of 3 to 4 cm. They are rounded to well rounded and are poorly sorted
Matrix: 24%

vi) Clast-supported conglomerate near altered zone
Remarks: Sandstone beds contains a few pebbles and the thicker beds are cross-stratified indicating top towards south. One of these thick beds of the sandstone beds also contains two narrow (15 and 25 cm) beds of argillite. Contact between sandstone and conglomerate is gradual. Conglomerate contains a few lenses of sandstone which are parallel to the conglomerate-sandstone contact, 087/56 S. Within the conglomerate, there is a wide (25 m) alteration zone which weathers a yellowish brown color and contains numerous crosscutting carbonate veins. This zone is highly deformed with foliation developed at 050.
Matrix: 32%
2.8 wt.% K, 2.0 ppm eU, 8.1 ppm eTh; MS = 9.0 x 10^{-3} SI units (porphyry intrusion)

1.1 wt.% K, 0.9 ppm eU, 6.0 ppm eTh; MS = 9.0 x 10^{-3} SI units (sandstone)
0.8 wt.% K, 1.6 ppm eU, 4.6 ppm eTh; MS = 1 to 10 x 10^{-3} SI units (argillite)
1.0 wt.% K, 0.7 ppm eU, 4.7 ppm eTh (conglomerate)
Collected samples 91-1v Feldspar porphyry intrusion
91-1w MVR
92-1x Sandstone bed
92-1y Argillite bed

Outcrop 91-2 (near Macassa Mine #3 Shaft)

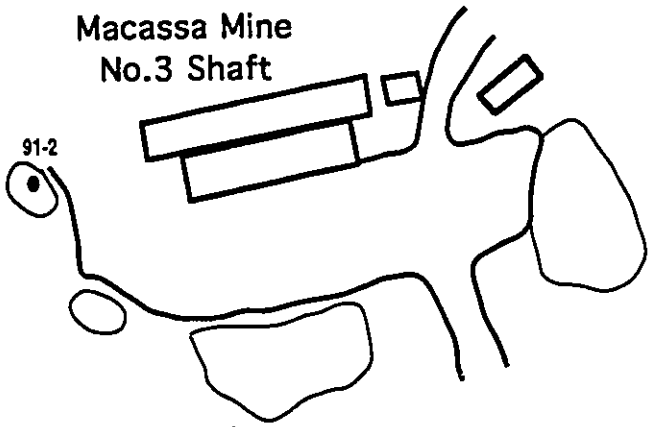

Clast-supported conglomerate
Largest clast: Quartz porphyry (30 cm x 45 cm)
Remarks: The clasts have an average size of 8 to 10 cm. They are subangular to well rounded and are poorly sorted. The conglomerate appears massive as no lenses of greywacke were observed.
Matrix: 17%; dark green color, minor quartz and feldspar
Collected samples 91-2a CH
91-2b MT
91-2c FP
91-2d SL
91-2e HFP
91-2f HFP
91-2g HR
91-2h HFP
91-2i SL

Outcrop 91-3 (End of Hwy. 568 at railway track)

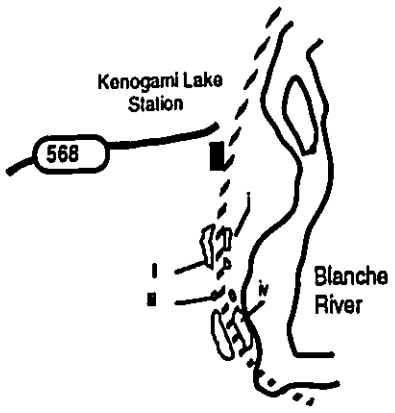

i) Clast-supported conglomerate underlain by tuff breccia and trachytic volcanic rock
Largest clast: Mafic volcanic rock (8 x 10 cm)
Remarks: The clasts have an average size of 3 to 5 cm. They are subangular to rounded and are poorly sorted. Elongated clasts have a random orientation. Spotty trachytic volcanic clasts are very similar to the underlying unit, suggesting their derivation from this unit. Contact between the conglomerate and the volcanic rocks is irregular and trends 050/78 NW. Thin sandstone lense (about 30 cm thick) is found at about 20 cm above the contact but only on western side of track. Lense is subparallel to contact.
4.2 wt.% K, 2.2 ppm eU, 33.4 ppm eTh; MS = 0.4 x 10^{-3} SI units (tuff breccia)
1.7 wt.% K, 0.7 ppm eU, 3.9 ppm eTh; MS = 0.4 x 10^{-3} SI units (sandstone)
0.9 wt.% K, 2.3 ppm eU, 8.3 ppm eTh (conglomerate ~10 m from breccia)
Matrix: 25%; dark green color
Collected samples 91-3a TVR
91-3b TVR
91-3c CH
91-3d TVR

ii) Clast-supported conglomerate with a thin lense of sandstone
Largest clast: Sandstone (15 x 28 cm)
Clasts: (estimated)
35% PR
30% TVR
10% VT
10% HR
10% MVR
Tr UMVR
Tr CH
Tr SS
Remarks: The clasts have an average size of 5 to 7 cm. They are well rounded and poorly sorted. Sandstone lens is 30 cm thick and has an

orientation of 035/77 NW, which is contrary to Hewitt's measurements in the area of south dipping beds. Clasts appear to be more altered here than at previous outcrop.
Matrix: 20%
Collected samples 91-3g HFP
91-3h TVR
91-3i MVR
91-3j SS
91-3k HR
91-3l FVR
91-3m MVR
91-3n QFP
91-3o QFP

iii) Clast-supported conglomerate
Largest clast: Hornblende-feldspar porphyry (20 x 30 cm)
Remarks: The clasts have an average size of 5 to 7 cm. They are rounded to well rounded, poorly sorted and elongated clasts appear to be randomly oriented. An conglomerate clast was observed and photographed.
Matrix: 26%
Collected samples 91-3p SS
91-3q QFP
91-3r HFP
91-3s HR
91-3t QFP
91-3u TVR

iv) Clast-supported conglomerate with lenses of sandstone in contact with a sandstone bed.
Largest clast: Holocrystalline (17 x 17 cm)
Remarks: The clasts have an average size of 3 to 5 cm. They are rounded to well rounded, fairly well sorted and elongated clasts are parallel to bedding. Sandstone lenses are more common towards the contact with the sandstone bed. Lenses are 20 to 30 cm thick and have a general orientation of 050/80 NW. Cross-bedding is found in the sandstone bed indicating top to the south. Contact between conglomerate and sandstone beds has a strike of 055. About 30 cm in the conglomerate from the contact, there appears to be a minor fault. It is only a few cm wide and contains euhedral quartz needles indicative of hydrothermal precipitation . The conglomerate near the fault is foliated.
Matrix: 23%
Collected samples 91-3v VT
91-3w HR
91-3x VT
92-3y Sandstone bed
92-3z QFP

Outcrop 91-14 (near Blanche River KL0724)

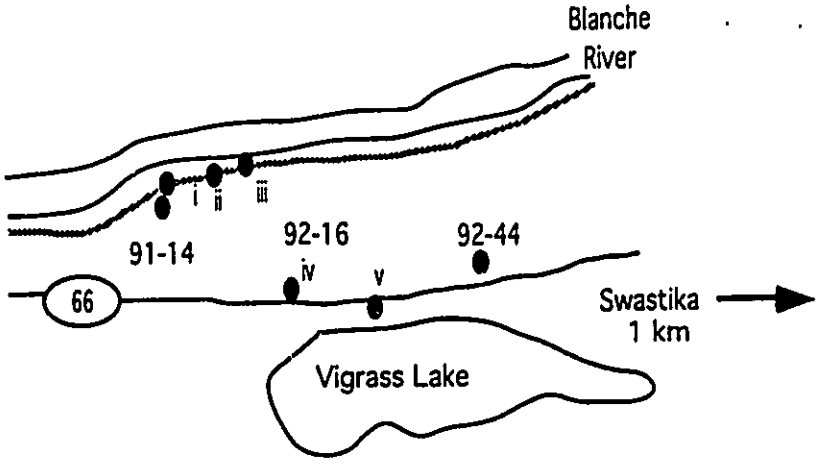

Matrix-supported conglomerate
Remarks: Pervasively altered and crosscutting quartz-carbonate veins (<1 cm wide). Some jasper clasts (< 1%). Holocrystalline rock clasts (1 to 2%). Matrix is about 70% of the conglomerate. Quartz-carbonate veins with or without pyrite (15-20%). Clasts larger than 5 cm are too altered to be identified with certainty.
Depth of examined core: 8 to 74.5 feet

Outcrop 91-15 (near Chaput-Hughes Kirkland Minerals No. 2 Shaft KL1959)

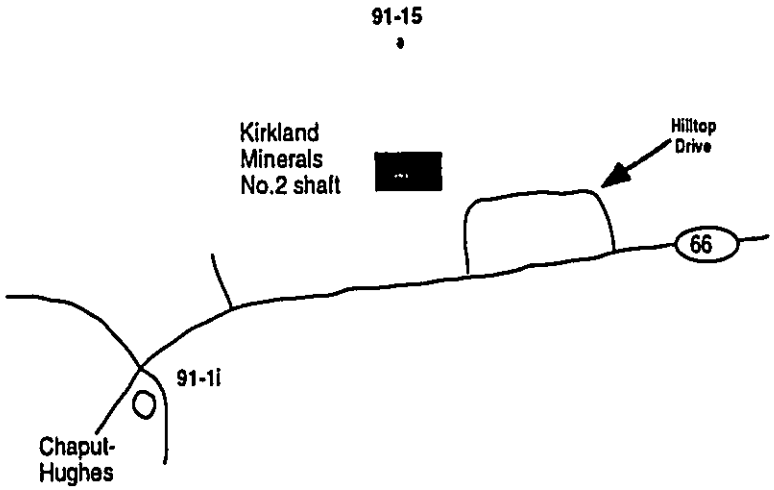

Clast-supported conglomerate
Largest clast: trachytic volcanic rock (> 15cm)
Remarks: Clasts appear to be mostly subangular to well rounded, and poorly sorted. Average size clasts varied from 2 to 5 cm in diameter. Samples are not weathered for the most part.
Matrix: green color (23%)
Depth of examined core: 543' - 737'
Collected samples 91-15a Feldspar porphyry dyke (538')
91-15b MVR (550')

91-15c FHP (570')
91-15d FHP (567')
91-15e VT (581')
91-15f TVR (584')
91-15g VT (585')
91-15h TVR (622')
91-15i HFP (635')
91-15j MVR (636')
91-15k HFP (637')
91-15l FP (680')
91-15m TVR (681')

Outcrop 92-16 (south shore of Blanche River; see 91-14)

i) Green spotted trachyte
Highly altered, containing numerous xenoliths
Similar to trachyte at 91-3
1.7 wt.% K, 2.6 ppm eU, 8.2 ppm eTh; MS = 0.3 x 10^{-3} SI units

ii) Same as i)
0.9 wt.% K, 1.9 ppm eU, 7.7 ppm eTh; MS = 30 x 10^{-3} SI units

iii) Feldspar porphyry
Highly sheared, containing numerous xenoliths
4.5 wt.% K, 3.0 ppm eU, 11.4 ppm eTh; MS = 0.4 x 10^{-3} SI units
Collected sample 91-16a

iv) Argillite (shale)
Thin bedded
1.9 wt.% K, 1.8 ppm eU, 5.7 ppm eTh; MS = 0.3 x 10^{-3} SI units

v) Syenite
Highly altered and foliated
Located on Larder Lake - Cadillac Fault (LLCF)
1.5 wt.% K, 1.5 ppm eU, 5.0 ppm eTh; MS = 1.2 x 10^{-3} SI units
Collected sample 91-16b

Outcrop 92-17 (along road to Macassa #3 shaft; south of 91-2)

Feldspar porphyry
Unaltered; containing common xenoliths
2.5 wt.% K, 2.5 ppm eU, 6.1 ppm eTh; MS = 4.5 x 10^{-3} SI units
2.4 wt.% K, 2.0 ppm eU, 6.6 ppm eTh (different location)
Collected sample 92-17a

Outcrop 92-18 (at power line on east side of road to Cheminis)

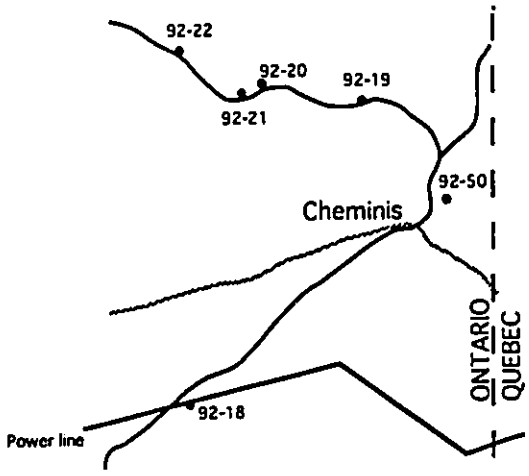

Argillite of Cobalt Group
Dark green
Fractures 050-230
Collected sample 92-18a

Outcrop 92-19 (NW of Cheminis; see 92-18)

i) Matrix-supported conglomerate (~70% matrix)
0.8 wt.% K, 1.9 ppm eU, 4.9 ppm eTh; MS = 37.0 x 10^{-3} SI units
0.5 wt.% K, 1.5 ppm eU, 4.8 ppm eTh (different location)

ii) Clast-supported conglomerate (~30% matrix)
Largest clast: Plagioclase-bearing mafic volcanic rock (20 x 38 cm)

Clasts:	60% MVR
(estimated)	20% FVR
	20% SS
	Tr HFP

Remarks: Clasts have an average size of 4 cm. They are subrounded to well rounded and are poorly sorted. Bedding is 120/40 SE. No jasper, chert or trachyte clasts are present. Mafic volcanic clasts (plagioclase-bearing volcanic rock) are not similar to any clasts observed in Timiskaming conglomerates.
0.2 wt.% K, 2.0 ppm eU, 5.2 ppm eTh
Collected samples 92-19a Matrix
92-19b&c MVR
92-19d&e HFP

Outcrop 92-20 (see 92-18)

i) Sandstone
Red coloration of sandstone is probably due to feldspar intrusion
Bedding 104/sub-vertical SE
1.5 wt.% K, 1.7 ppm eU, 5.8 ppm eTh; MS = 0.2 x 10^{-3} SI units

Collected sample 92-20a

ii) Feldspar porphyry
Large feldspar crystals (~5 mm)
Fractures 150/45 W
0.7 wt.% K, 2.7 ppm eU, 7.9 ppm eTh; MS = 6 to 30 x 10^{-3} SI units
Collected sample 92-20b

Outcrop 92-21 (see 92-18)

Sandstone
Light brown color
Thin bedded (~10 cm)
Bedding 070/sub-vertical S
2.2 wt.% K, 1.4 ppm eU, 3.2 ppm eTh; MS = 0.2 x 10^{-3} SI units
Collected sample 92-21a

Outcrop 92-22 (see 92-18)

Sandstone
Black color
Bedding 080/sub-vertical S
0.9 wt.% K, 0.8 ppm eU, 4.4 ppm eTh; MS variable
Collected samples 92-22a (MS = 0.4 x 10^{-3} SI units)
92-22b (MS = 30 x 10^{-3} SI units)

Outcrop 92-23 (north of Virginiatown at power line)

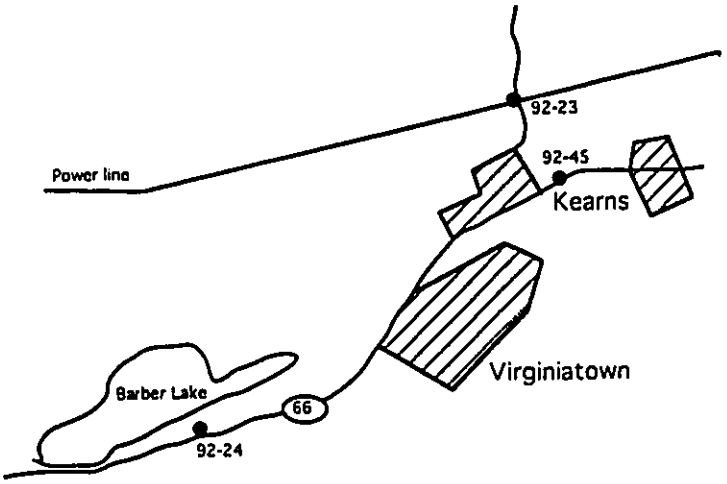

i) Turbidites (east of road)
Light brown color
Thin bedded (2 to 20 cm)
Bedding 105/90
2.6 wt.% K, 2.3 ppm eU, 9.7 ppm eTh (sandstone and shale)
2.8 wt.% K, 2.3 ppm eU, 11.4 ppm eTh (mostly shale)
2.9 wt.% K, 2.7 ppm eU, 13.6 ppm eTh (sandstone and shale)

2.2 wt.% K, 1.4 ppm eU, 8.5 ppm eTh (mostly sandstone)
2.4 wt.% K, 2.1 ppm eU, 9.8 ppm eTh (sandstone and shale)
MS = 0.2 x 10^{-3} SI units
Collected samples 92-23a Shale
92-23b Sandstone

ii) Tuff breccia (west of road)
Large white phenocrysts in matrix and clasts similar to matrix
Clasts are angular and fuchsite-bearing ultramafic clasts are present
Sheared 035/sub-vertical N
Folded turbidites at base of outcrop but contact was not observed
2.0 wt.% K, 2.4 ppm eU, 7.7 ppm eTh, MS = 0.2 x 10^{-3} SI units

Outcrop 92-24 (see 92-23)

Turbidites (mostly sandstone)
Thin bedded
Bedding 075/90
Foliation 100/90
2.7 wt.% K, 0.7 ppm eU, 5.7 ppm eTh; MS = 0.3 x 10^{-3} SI units
Collected sample 92-24a Shale

Outcrop 92-25 (east of Bear Lake)

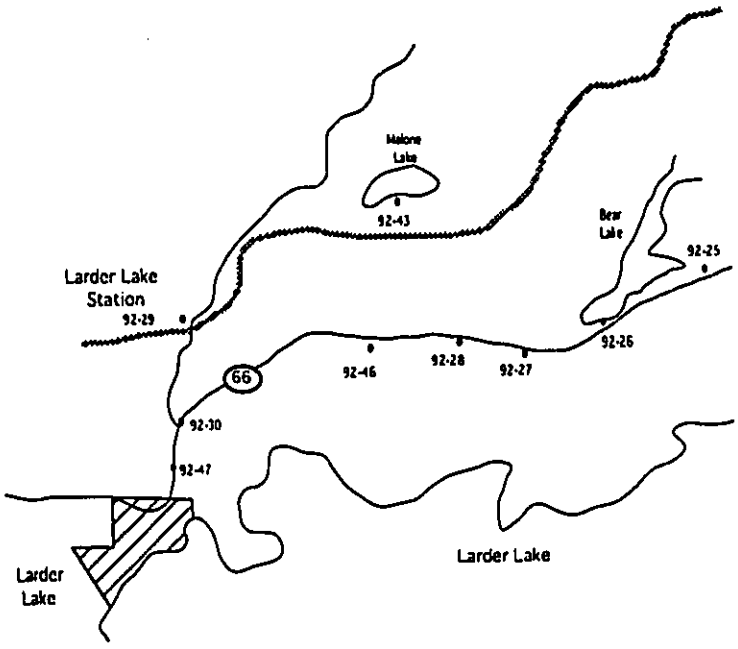

i) Turbidites
Light brown color
Thin bedded
Bedding 075/90
1.5 wt.% K, 1.9 ppm eU, 5.6 ppm eTh; MS = 0.3 x 10^{-3} SI units

Collected sample 92-25a sandstone

ii) Clast-supported conglomerate
Seperated by fault trending 330
Similar to conglomerates at Chaput-Hughes (i.e. outcrop 91-1)
1.4 wt.% K, 2.7 ppm eU, 6.8 ppm eTh; MS = 2.0 x 10^{-3} SI units

Outcrop 92-26 (see 92-25)

Turbidites (mostly shale)
Altered
Thin bedded
Iron-rich layers contain abundant hematite
Bedding 075/sub-vertical S
2.2 wt.% K, 0.8 ppm eU, 2.1 ppm eTh; MS = 0.5 x 10^{-3} SI units
Collected sample 92-26a Shale

Outcrop 92-27 (see 92-25)

Turbidites (mostly sandstone)
Folded
Bedding 030/sub-vertical S
0.9 wt.% K, 1.3 ppm eU, 2.2 ppm eTh; MS = 0.6 x 10^{-3} SI units
Collected sample 92-27a Shale

Outcrop 92-28 (see 92-25)

Turbidites
Altered and folded
Containing folded quartz veins
Iron-rich bed (~20 cm) with abundant magnetite
Bedding 070/sub-vertical S
1.7 wt.% K, 1.6 ppm eU, 1.2 ppm eTh; MS = 0.6 x 10^{-3} SI units
Collected sample 92-28a Shale

Outcrop 92-29 (south of Larder Lake Station; see 92-25)

Argillite
Very thinly laminated (<1 cm)
Iron-rich lamellae with abundant magnetite
Quartz veining
Euhedral pyrite in argillite
Bedding 080/60 S
2.5 wt.% K, 1.5 ppm eU, 3.2 ppm eTh; MS = 0.2 x 10^{-3} SI units
Collected sample 92-29a

Outcrop 92-30 (north of Larder Lake; see 92-25)

i) Sheared clast-supported conglomerate
Mostly ultramafic volcanic clasts with spinifex texture
No jasper clasts
Intensely quartz veined
Bedding 055/sub-vertical S
Foliation 095/sub-vertical S
1.0 wt.% K, 0.4 ppm eU, 0.5 ppm eTh; MS = 80 to 120 x 10^{-3} SI units
Collected samples 92-30a UMVR
92-30b Red aphanitic dyke

ii) Sheared matrix-supported conglomerate
Clasts: 60% MVR
(estimated) 15% FVR
15% SS
10% CH
Tr QFP
Minor jasper was observed
Bedding 045/80S
1.3 wt.% K, 0.7 ppm eU, 2.3 ppm eTh; MS = 0.4 x 10^{-3} SI units
Collected sample 92-30c Sandstone

ii) Clast-supported conglomerate
Undeformed
Clasts: 75% MVR
(estimated) 10% SL
10% HFP
Tr VQ
Tr SS
Bedding 050/sub-vertical S
Collected samples 92-30d HFP
92-30em MVR
92-30ep SL

iv) Highly sheared conglomerate
Clasts: 80% MVR & UMVR
(estimated) 10% FVR
10% QFP
0.2 wt.% K, 0.4 ppm eU, 0.1 ppm eTh; MS = 20 to 30 x 10^{-3} SI units
Collected sample 92-30f Conglomerate

Outcrop 92-31 (north of Kirkland Lake Airport)

Clast-supported conglomerate
Very altered
Clasts < 2 cm
0.4 wt.% K, 0.4 ppm eU, 0.2 ppm eTh
Collected samples 92-31a Underlying mafic volcanic rock
92-31b&c Conglomerate

Outcrop 92-32 (north of Gull Lake)

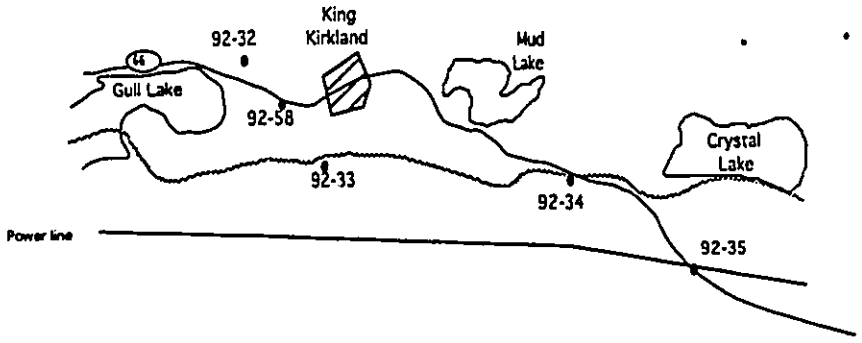

Clast-supported conglomerate

Clasts:	25% MVR
(estimated)	25% HFP
	20% QFP
	5% CH
	5% TVR
	2% HR
	Tr UMVR
	Tr VQ
	Tr SS

Remarks: Clasts are flattened, fairly well sorted and rounded. Average clast size is 5 cm.
1.6 wt.% K, 1.3 ppm eU, 3.7 ppm eTh
Collected samples 92-32a QFP
92-32b VQ

Outcrop 92-33 (south of King Kirkland on railway track; see 92-32)

Argillite
White to black (rust stained)
Thinly laminated
Altered and folded
Coarser grained beds boudinaged
Bedding 070/80 S
2.7 wt.% K, 4.0 ppm eU, 7.1 ppm eTh; MS = 0.3 x 10^{-3} SI units
Collected sample 92-33a Argillite

Outcrop 92-34 (east of King Kirkland; see 92-32)

Turbidites
Thin bedded (<10 cm)
Highly sheared and altered
Bedding 070/sub-vertical S
Foliation 090/sub-vertical S
2.2 wt.% K, 1.8 ppm eU, 5.3 ppm eTh: MS = 0.2 x 10^{-3} SI units
Collected sample 92-34a Shale

Outcrop 92-35 (east of 92-34; see 92-32)

i) Volcanic agglomerate
2.6 wt.% K, 2.9 ppm eU, 8.2 ppm eTh; MS = 1.5 x 10^{-3} SI units

ii) Mafic trachyte
2.0 wt.% K, 4.1 ppm eU, 26.3 ppm eTh; MS = 50 to 75 x 10^{-3} SI units
Collected sample 92-35a Mafic trachyte

Outcrop 92-36 (south of Perron Lake)

i) Clast-supported conglomerate
Similar to conglomerate at Chaput-Hughes (i.e. 91-1)
Bedding 062/85 S
1.7 wt.% K, 9.0 ppm eU, 5.9 ppm eTh
Collected sample 92-36e Conglomerate

ii) Pillowed basalt of Kinojevis Group
Collected sample 92-36d Basalt

iii) Hyaloclastites and associated sedimentary rocks
Unconformably overlain by Timiskaming conglomerate
1.0 wt.% K, 2.5 ppm eU, 6.7 ppm eTh (92-36a)
0.7 wt.% K, 2.1 ppm eU, 4.5 ppm eTh (92-36b)
1.3 wt.% K, 2.3 ppm eU, 6.6 ppm eTh (92-36c)
Collected samples 92-36a,b&c Volcaniclastic sedimentary rocks

Outcrop 92-37 (east of Gami Lake; north of Kirkland Lake)

Clast-supported conglomerate
Unconformably overlying pillow basalts
Clasts: 80% QFP
(estimated) 20% MVR
Clasts are angular to subangular
This conglomerate bed was point counted by W. Mueller
Collected samples 92-37a Conglomerate
92-37b QFP

Outcrop 92-38 (between Larder Lake and Southwest Arm)

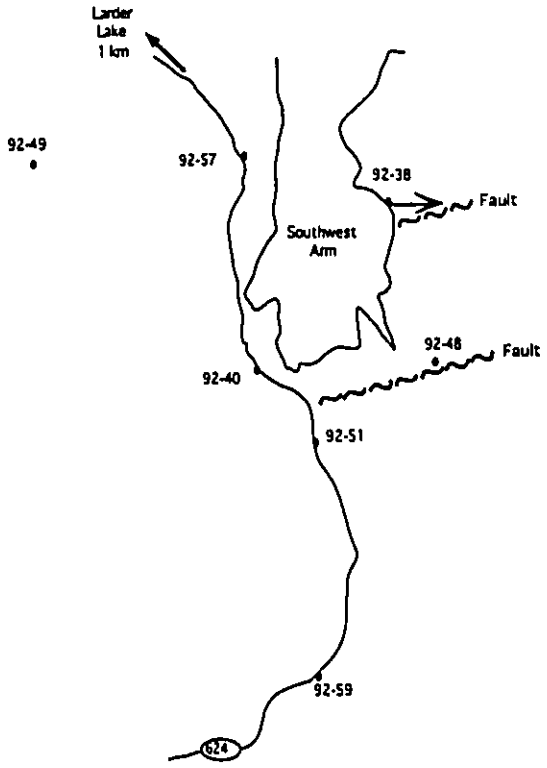

Mapped as Timiskaming sedimentary rocks by Hyde (1978)
Distance in meters from Southwest Arm along E-W cut-line (see arrow above)

80 Basalt
90 Hyaloclastites
130 Conglomerate associated with hyaloclastites
140 Sandstone
150 Sandstone
155 Conglomerate
160 Minette lamprophyre dyke
South of line Quartz-feldspar porphyry

These outcrops are located north of a large NE-trending fault (see above). Sedimentary rocks are in gradational contact with Keewatin volcanic rocks and are therefore not of Timiskaming age.

Collected sample 92-38a Basalt
92-38b Sandstone
92-38c Conglomerate
92-38d Quartz-feldspar porphyry intrusion
92-38e Minette lamprophyre dyke

Outcrop 92-39 (intersection of Hwy. 11 and 66; east of Kenogami Lake)

Clast-supported conglomerate
Interbedded with sandstone lenses

Largest clast: Quartz-feldspar porphyry (40 x 60 cm)
Remarks: The clasts are subrounded and very poorly sorted. Bedding is 050/80 S. Conglomerate is approximately 200 metres from underlying basalts (S_0 = 335/sub-vertical).
1.0 wt.% K, 1.1 ppm eU, 1.4 ppm eTh (conglomerate)
1.5 wt.% K, 1.3 ppm eU, 3.3 ppm eTh (sandstone)
Collected samples 92-39a MT
92-39b BIF
92-39c HFP
92-39d SS
92-39e HFP
92-39f VT
92-39g MVR
92-39h VT
92-39i Sandstone
92-39j HFP
92-39k QFP

Outcrop 92-40 (west of Southwest Arm on highway 624; see 92-38)

Matrix-supported conglomerate
Interbedded with sandstone and shale
Clasts: (estimated)
50% MVR
20% FVR
10% UMVR
5% CH
5% SS
5% HR
Tr QFP
Euhedral pyrite was observed in matrix of conglomerate and in sandstone
1.5 wt.% K, 0.5 ppm eU, 1.3 ppm eTh; MS = 0.4 x 10^{-3} SI units
Collected samples 92-40a Sandstone
92-40d Sandstone
92-40e Conglomerate
92-40f Sheared conglomerate

Outcrop 92-43 (south of Malone Lake; see 92-25)

Interbedded clast-supported conglomerate and sandstone
Unconformably overlying pillowed basalt
Similar conglomerate to Chaput-Hughes (i.e. outcrop 91-1) (however fuchsite-bearing argillite clasts are present and have not been observed in other conglomerates)
Point counted by W. Mueller
Collected samples 92-43a QFP
92-43b MVR
92-43c Sandstone
92-43d Sandstone
92-43e QFP

Outcrop 92-44 (east of outcrop 92-16v; see 91-14)

i) Interbedded matrix-supported conglomerate and sandstone
1.5 wt.% K, 0.9 ppm eU, 3.8 ppm eTh (conglomerate)
Collected sample 92-44a Conglomerate

ii) Argillite
Thin lamellae
Similar to outcrops 92-29 and 92-33
1.9 wt.% K, 1.2 ppm eU, 3.4 ppm eTh
Collected sample 92-44b Argillite

Outcrop 92-45 (Kearns; see 92-23)

Turbidites (mostly sandstone)
Altered and foliated
1.5 wt.% K, 2.2 ppm eU, 5.5 ppm eTh; MS = 0.2 x 10^{-3} SI units
Collected sample 92-45a Sandstone
92-45b Shale

Outcrop 92-46 (east of outcrop 92-30; see 92-25)

Argillite
Thin lamellae
Bedding 100/sub-vertical S
0.8 K%, 0.1 ppm eU, 0.0 ppm eTh; MS = 0.3 x 10^{-3} SI units
Collected sample 92-46a Argillite

Outcrop 92-47 (see 92-25)

i) Minette lamprophyre dyke
Carbonate and specular hematite at its margins
Collected samples 92-47a Pink aphanitic dyke
92-47b Minette

ii) Matrix-supported conglomerate
Clasts: 65% MVR & UMVR
(estimated) 30% BIF
5% HR
Sheared 000
0.2 wt.% K, 0.5 ppm eU, 0.0 ppm eTh
Collected samples 92-47c BIF
92-47d HR
92-47e Matrix of conglomerate
92-47f Minette

Outcrop 92-48 (south east of Southwest Arm; see 92-38)

i) Sandstone
Cross-bedded
North of fault (see diagram at 92-38)
1.3 wt.% K, 1.8 ppm eU, 4.5 ppm eTh; MS = 0.4 x 10^{-3} SI units
Collected sample 92-48a

ii) Sandstone (50 metres SE of i)
South of fault
1.1 wt.% K, 0.4 ppm eU, 1.2 ppm eTh; MS = 1.5 x 10^{-3} SI units
Collected sample 92-48b

iii) Gabbro dyke?
1.2 wt.% K, 1.1 ppm eU, 1.6 ppm eTh; MS = 1.0 x 10^{-3} SI units
Collected sample 92-48c

Outcrop 92-49 (see 92-38 - drill core KL1875)

Interbedded argillite(black, shaly) and sandstone (light to medium grey, massive)
Carbonate veins
Collected samples 92-49b Sandstone
92-49c Argillite

Outcrop 92-50 (see 92-18 - drill core KL1361)

Interbedded dark grey sandstone and argillite
Collected samples 92-50a Argillite
92-50b Sanstone

Outcrop 92-51 (south of Larder Lake; see 92-38)

Minette lamprophyre dyke
Specular hematite and carbonate along margins
Strike 170
0.6 wt.% K, 0.7 ppm eU, 0.0 ppm eTh; MS = 160 x 10^{-3} SI units
Collected sample 92-51a

Outcrop 92-52 (~1 km west of Larder Lake - north of Hwy. 66)

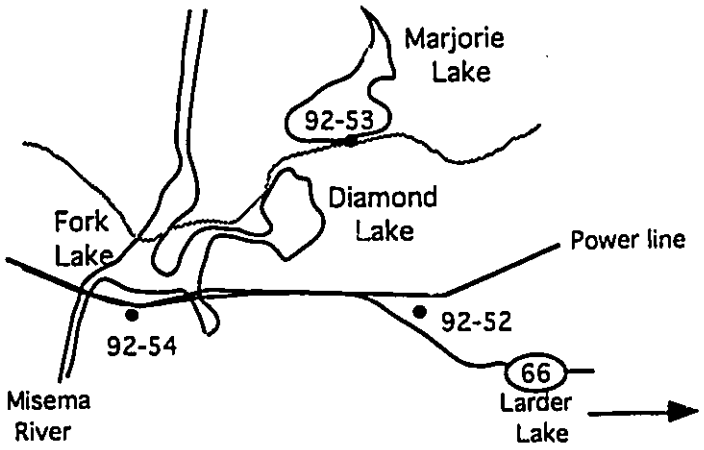

Clast-supported conglomerate
Flattening of clasts increases towards the north
Clasts of leucite-bearing trachyte and K-feldspar porphyry are present along with jasper clasts indicating this is a Timiskaming conglomerate. This is the third occurence of alluvial-fluvial assemblage rocks south of the LLCF (others are west of Larder Lake and east of Kenogami Lake).
0.7 wt.% K, 1.2 ppm eU,. 3.1 ppm eTh
Collected sample 92-52a Conglomerate

Outcrop 92-53 (east of Fork Lake along railway track; see 92-52)

Turbidites
Thin bedded
Bedding 085/72 S
2.4 wt.% K, 1.5 ppm eU, 5.0 ppm eTh; MS = 0.2 x 10^{-3} SI units (sandstone)
2.5 wt.% K, 3.1 ppm eU, 6.1 ppm eTh; MS = 0.2 x 10^{-3} SI units (shale)
Collected samples 92-53a Shale
92-53b Sandstone

Outcrop 92-54 (south of Fork Lake on LLCF; see 92-52)

i) Matrix-supported conglomerate interbedded with sandstone
Mostly mafic and ultra-mafic volcanic clasts
Highly sheared
1.1 wt.% K, 0.5 ppm eU, 0.4 ppm eTh; MS = 40 x 10^{-3} SI units (conglomerate)
Collected samples 92-54a Conglomerate
92-54b Sandstone

ii) Feldspar porphyry
Foliated
Small veinlets of quartz and carbonates
1.4 wt.% K, 1.1 ppm eU, 0.9 ppm eTh; MS = 3.0 x 10^{-3} SI units
Collected sample 92-54c

Outcrop 92-55 (east of Dobie)

i) Clast-supported conglomerate
Highly sheared (clasts elongated more than 10:1)
Jasper clasts were observed; lithology of other clasts were impossible to identify
2.3 wt.% K, 1.3 ppm eU, 2.3 ppm eTh
1.6 wt.% K, 1.1 ppm eU, 3.0 ppm eTh
Collected sample 92-55a Conglomerate

ii) Sandstone
Light green and brown bands
Foliated and crenulated
1.7 wt.% K, 2.5 ppm eU, 3.1 ppm eTh; MS = 0.2 x 10^{-3} SI units
1.9 wt.% K, 1.6 ppm eU, 4.2 ppm eTh; MS = 0.3 x 10^{-3} SI units
Collected sample 92-55b&c Sandstone

Outcrop 92-56 (south-west of Kirkland Lake - trenches perpendicular to gas line)

i) Sandstone (200 m south of gas line)
Light brown color
Minor clasts (< 5%); mostly fuchsite-carbonate, jasper and argillite
2.1 wt.% K, 3.6 ppm eU, 3.1 ppm eTh; MS = 0.2 x 10^{-3} SI units
Collected sample 92-56a Sandstone

ii) Sandstone (100 m south of gas line)
Same as i)
2.2 wt.% K, 3.4 ppm eU, 4.5 ppm eTh; MS = 0.2 x 10^{-3} SI units
Collected sample 92-56b Sandstone

iii) Clast-supported conglomerate (at gas line)
Clasts include jasper, fuchsite-carbonate, porphyry, holocrystalline and leucite-bearing trachyte
Collected sample 92-56c Conglomerate

Outcrop 92-57 (see 92-38)

Mafic/ultramafic volcanic rocks and associated sedimentary rocks
Foliated
Bedding 050
0.8 wt.% K, 1.0 ppm eU, 0.9 ppm eTh; MS = 0.6 x 10^{-3} SI units (sandstone)
Collected sample 92-57a Sandstone

Outcrop 92-58 (west of King Kirkland on highway 66; see 92-32)

i) Interbedded clast-supported conglomerate and cross-bedded sandstone (found both north and south of road)

Clasts include chert and jasper, fuchsite-carbonate, felsic volcanic rock, mafic volcanic rock, quartz-feldspar porphyry, holocrystalline and porphyry
Bedding 250/60 N
Clast elongation 080
3.0 wt.% K, 1.9 ppm eU, 5.3 ppm eTh; MS = 0.3 x 10^{-3} SI units (sandstone)
0.4 wt.% K, 2.5 ppm eU, 4.3 ppm eTh; MS = 14 x 10^{-3} SI units (conglomerate)
Collected samples 92-58a Sandstone
92-58c QFP
92-58d MVR
92-58e MVR
92-58f QFP

ii) Argillite (as at outcrops 92-29, 92-33 and 92-44)
Thin lamellae
Occurs only on south side of road
Fault (254/66N) contact with conglomerate
Bedding 130/70 S
1.6 wt.% K, 2.5 ppm eU, 4.7 ppm eTh; MS = 0.4 x 10^{-3} SI units
Collected sample 92-58b Argillite

Outcrop 92-59 (south of 92-40; see 92-38)

i) Argillite
Thin lamellae (<2 cm)
Collected sample 92-59b

ii) Quartz porphyry intrusion
Skead Group
Collected sample 92-59c

Outcrop 92-QP (north of Gami Lake)

Quartz porphyry
Refered to as the Goodfish porphyry
Collected sample 92-QP

Appendix III: Major and minor element concentrations of clasts and rocks which are not included in the manuscripts

Abbreviations for clasts: HPP - hornblende-pagioclase porphyry; QPP - quartz-plagioclase porphyry; MV - mafic volcanic rock; HR - holocrystalline rock; SL - spessartite lamprophyre. Clasts from the alluvial-fluvial assemblage are highly altered and some are carbonatized. Clasts from the turbidite assemblage south of the LLCF (i.e. outcrop 92-30 & 92-47) are fresh.

Abbreviations for rocks: Intrusion - feldspar porphyry (92-47a & 92-54c), quartz-feldspar porphyry (92-38d) and quartz porphyry (92-59c & 92-QP); Sst - sandstone.

Clasts	2c	1j	3v	15i	15k	1k	47d	30em	30ep	30d
SiO2 wt.%	64.0	49.8	66.0	53.8	59.9	69.2	58.9	62.6	56.9	54.2
Al2O3	15.1	15.7	14.5	15.0	13.5	14.2	17.9	17.2	13.9	16.5
Fe2O3(tot)	5.19	7.42	2.92	9.06	7.90	4.13	1.00	6.06	9.90	4.45
MgO	2.03	2.95	1.27	2.02	4.74	1.58	0.79	4.14	3.75	2.17
CaO	3.42	7.66	2.88	6.19	1.35	1.29	6.84	0.24	4.89	11.0
Na2O	4.79	5.35	4.05	7.59	3.02	3.43	8.71	3.03	4.22	4.81
K2O	2.28	1.71	2.81	0.29	3.00	2.77	1.09	2.54	1.07	2.63
TiO2	0.53	0.78	0.34	0.62	0.51	0.36	0.19	0.70	1.79	0.41
P2O5	0.12	0.56	0.06	0.35	0.25	0.13	0.06	0.21	0.15	0.11
S	0.00	0.01	0.01	0.00	0.06	0.01	0.15	0.09	0.07	0.07
MnO	0.08	0.19	0.07	0.13	0.12	0.04	0.07	0.01	0.21	0.14
Ba ppm	931	640	412	369	8508	522	604	686	571	834
Cr	45	158	33	278	286	32	n.d.	265	26	16
Zr	81	167	82	133	85	149	72	134	109	141
Sr	887	621	159	606	1041	246	276	113	145	1085
Rb	94	67	99	<10	83	112	18	88	23	17
Y	12	28	<10	20	15	10	n.d.	19	36	n.d.
Nb	<10	<10	<10	<10	<10	<10	n.d.	n.d.	n.d.	n.d.
Zn	52	88	41	57	109	45	n.d.	50	111	n.d.
Ni	32	81	43	102	84	29	n.d.	79	90	28
Cu	n.d.	n.d.	n.d.	n.d.	n.d.	n.d.	n.d.	n.d.	n.d.	n.d.
Pb	n.d.	n.d.	n.d.	n.d.	n.d.	n.d.	n.d.	n.d.	n.d.	n.d.
V	72	212	27	204	198	22	n.d.	n.d.	n.d.	n.d.
LOI wt.%	2.54	7.89	4.22	5.26	4.3	2.71	4.6	3.6	4	4.1
Total %	100.36	100.33	99.29	100.54	99.88	100.05	100.31	100.48	100.9	100.76
	HPP	HPP	QPP	HPP	HPP	QPP	HR	MV	SL	HPP

Non-clasts	54c.	47b	47a	38e	36d	38d	CP	48c	59c	31a	38a
SiO2 wt.%	64.2	57.6	70.9	62.6	46.5	68.3	70.9	52.6	75.8	41.6	51.5
Al2O3	16.4	17.5	15.0	13.4	14.1	14.4	16.3	13.6	12.9	12.7	17.1
Fe2O3(tot)	3.30	6.64	1.21	7.41	9.96	3.29	1.52	13.8	0.95	10.0	9.29
MgO	2.28	3.34	0.42	5.19	6.59	1.98	0.79	5.16	0.33	6.65	6.92
CaO	1.70	0.54	1.08	1.66	8.29	1.98	0.84	8.42	1.29	11.6	3.25
Na2O	6.90	2.73	6.19	4.13	0.89	6.05	3.78	2.25	6.34	2.07	6.54
K2O	1.68	3.03	3.68	1.43	2.25	2.94	3.11	1.51	0.82	0.03	0.36
TiO2	0.33	0.65	0.12	0.68	0.71	0.34	0.26	1.16	0.24	0.76	0.78
P2O5	0.12	0.15	0.04	0.18	0.06	0.15	0.14	0.11	0.07	0.05	0.56
S	0.04	0.15	0.08	0.11	0.09	0.08	0.05	0.11	0.09	0.32	0.17
MnO	0.04	0.04	0.01	0.06	0.16	0.04	0.00	0.23	0.02	0.20	0.13
Ba ppm	385	739	1508	643	198	1011	1150	319	85	21	261
Cr	92	135	63	430	300	40	n.d.	27	n.d.	280	352
Zr	107	118	121	113	52	123	104	81	89	35	100
Sr	559	125	316	362	161	429	194	231	149	246	260
Rb	27	84	64	24	72	58	69	57	27	n.d.	n.d.
Y	n.d.	16	n.d.	19	20	12	n.d.	24	n.d.	13	17
Nb	n.d.	n.d.	n.d.	n.d.	n.d.	n.d.	n.d.	11	13	n.d.	n.d.
Zn	13	83	n.d.	69	53	14	n.d.	55	22	58	50
Ni	n.d.	121	n.d.	99	102	n.d.	n.d.	24	n.d.	87	73
Cu	n.d.	n.d.	n.d.	n.d.	n.d.	n.d.	n.d.	121	n.d.	18	n.d.
Pb	n.d.	n.d.	n.d.	n.d.	n.d.	n.d.	n.d.	n.d.	n.d.	n.d.	n.d.
V	n.d.	n.d.	n.d.	n.d.	n.d.	n.d.	n.d.	n.d.	n.d.	n.d.	n.d.
LOI wt.%	3	7.5	1	3.5	11.4	2.2	2.4	2.3	1.5	14.5	5.2
Total %	100.09	99.99	99.92	100.44	101.06	101.82	100.28	101.29	100.27	100.38	101.77
	Intrusion	Minette	Intrusion	Minette	Basalt	Intrusion	Intrusion	Gabbro?	Intrusion	Basalt	Basalt

Non-clasts	36b	19a	26a	36c	36a	20a	24a	54b	18a	28a	53a	57a
SiO2 wt.%	52.5	54.7	61.3	62.3	57.4	56.0	60.4	51.4	59.7	57.9	63.7	53.1
Al2O3	11.1	14.9	15.5	11.9	14.0	13.7	18.2	13.9	16.9	16.2	15.6	13.8
Fe2O3(tot)	7.10	7.26	9.87	4.46	5.67	8.27	6.91	10.9	7.51	12.90	4.70	9.65
MgO	4.77	5.96	4.98	2.69	5.29	6.02	3.53	3.48	3.84	4.45	2.44	5.49
CaO	8.10	4.01	0.27	5.46	4.05	6.17	0.56	3.65	2.85	0.20	1.51	7.75
Na2O	2.19	5.92	4.38	2.31	4.49	3.70	3.01	5.35	4.98	4.47	3.99	5.91
K2O	1.30	0.54	0.34	1.97	1.27	3.69	3.16	1.61	1.77	0.23	2.05	0.84
TiO2	0.47	0.55	0.78	0.41	0.53	0.72	0.67	2.01	0.66	0.73	0.53	0.66
P2O5	0.09	0.30	0.13	0.10	0.24	0.41	0.16	0.17	0.15	0.13	0.16	0.24
S	0.44	0.12	0.07	0.11	0.12	0.09	0.17	0.10	0.15	0.09	0.16	0.13
MnO	0.25	0.15	0.02	0.13	0.07	0.14	0.04	0.14	0.11	0.05	0.05	0.17
Ba ppm	253	828	363	427	1271	2110	788	343	505	85	730	223
Cr	110	133	315	180	248	243	150	17	155	179	170	34
Zr	74	137	104	108	135	218	123	121	109	106	126	116
Sr	183	1355	60	168	588	1299	125	181	478	134	431	261
Rb	39	22	21	53	48	105	90	19	56	11	65	13
Y	16	17	16	11	15	32	12	40	16	13	14	17
Nb	n.d.	n.d.	15	n.d.	n.d.	n.d.	n.d.	n.d.	n.d.	n.d.	n.d.	n.d.
Zn	12	67	95	11	51	93	87	102	54	43	30	15
Ni	n.d.	n.d.	144	39	107	102	84	55	31	81	46	102
Cu	n.d.	n.d.	35	n.d.	n.d.	36	n.d.	n.d.	n.d.	n.d.	n.d.	86
Pb	n.d.	12	n.d.	n.d.	n.d.	n.d.	n.d.	n.d.	n.d.	n.d.	n.d.	n.d.
V	n.d.	n.d.	n.d.	n.d.	n.d.	n.d.	n.d.	n.d.	n.d.	n.d.	n.d.	n.d.
LOI wt.%	12.4	5.8	3.6	8.5	7.8	1.6	3.5	8.6	2.5	3.6	5.4	2.7
Total %	100.58	100.45	101.31	100.45	101.16	100.95	100.41	101.31	101.16	100.99	100.38	100.46
	Sst	Sst	Shale	Sst	Sst	Sst	Shale	Sst	Shale	Shale	Shale	Sst

Appendix IV: Average microprobe analyses of amphiboles and plagioclases which are not included in manuscripts

Amphibole compositions are calculated on the basis of 24 oxygen following the recommended procedure of Leake (1978) and are from a feldspar porphyry intrusion (92-17a) and a spessartite clast (92-30ep) from the turbidite assemblage south of the LLCF. Ferric and ferrous iron were calculated by stoichiometry. Plagioclase compositions are calculated on the basis of 8 oxygen and are from holocrystalline rock clasts (91-1m, 91-3k & 91-3s) and hornblende-plagioclase porphyry clasts (92-39e & 92-39i) from the alluvial-fluvial assemblage.

Amphiboles

	17a	30ep
n	9	7
SiO2 wt.%	44.88	41.92
Al2O3	8.16	12.18
TiO2	1.28	1.57
FeO*	15.00	15.28
MnO	0.26	0.17
Cr2O3	0.02	0.00
MgO	12.83	11.79
CaO	10.92	11.20
K2O	0.79	0.88
Na2O	2.08	2.18
Cl	0.00	0.00
Total	96.22	97.17
Si	6.78	6.31
Al IV	1.22	1.69
T site	8.00	8.00
Al VI	0.23	0.46
Ti	0.15	0.18
Cr	0.00	-
Mg	2.89	2.64
Fe +2	1.73	1.71
M1,2,3	5.00	5.00
Fe +2	0.17	0.21
Mn	0.03	0.02
Ca	1.77	1.77
Na	0.03	-
M4 site	2.00	2.00
Ca	-	0.03
Na	0.58	0.64
K	0.15	0.17
A site	0.73	0.84

Total iron expressed as FeO
"n" refers to the number of
measurements on each thin section

Plagioclases

	1m	3k	3s	39e	39i
n	8	6	6	2	3
SiO2 wt.%	65.13	63.42	63.88	67.33	63.63
Al2O3	21.57	22.73	22.29	20.07	22.95
CaO	2.84	4.28	3.75	0.69	3.93
Na2O	9.56	8.83	9.07	10.66	8.47
K2O	0.43	0.41	0.53	1.56	1.60
FeO*	0.12	0.13	0.09	0.15	0.15
Total	99.65	99.80	99.61	100.46	100.73
Si	2.88	2.81	2.83	2.95	2.81
Al	1.12	1.19	1.16	1.04	1.19
	4.00	4.00	3.99	3.99	4.00
Ca	0.13	0.20	0.18	0.03	0.19
Na	0.82	0.76	0.78	0.91	0.72
K	0.02	0.02	0.03	0.09	0.09
	0.97	0.98	0.99	1.03	1.00

Total iron expressed as FeO
"n" refers to the number of
measurements on each thin section

Appendix V: Comparison of gamma ray spectrometry and instrumental neutron activation analysis (INAA) measurements

Shale and argillite samples in which both gamma ray spectrometry and INAA measurements were made on uranium and thorium are shown. The objective is to show the validity of gamma ray spectrometry in measuring eU and eTh in the field.

Correlation coefficients were calculated based on the assumption that gamma ray spectrometry measurements should be equal to INAA measurements. A slope of 1 and an intercept at y of 0 were therefore taken to represent this relationship. Coefficients are equal to +0.92 in both cases indicating measurements by gamma ray spectrometry are a very good approximation of contents of U and Th in the rock.

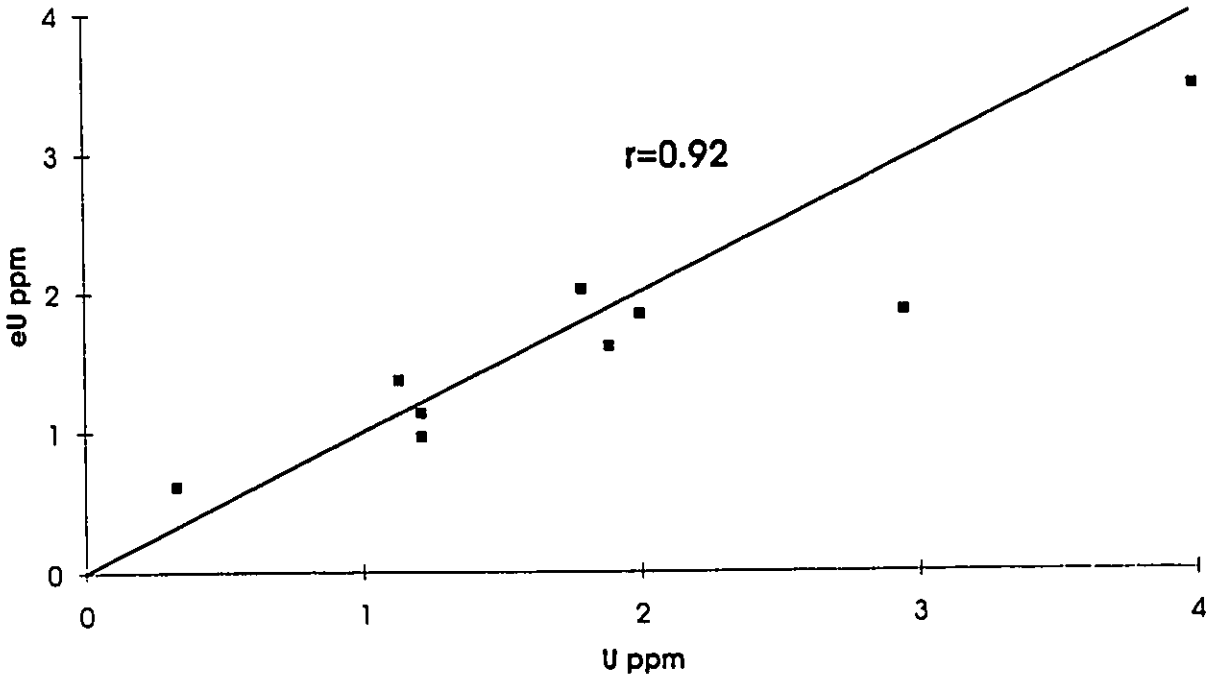
r=0.92
eU ppm
U ppm
0
1
2
3
4

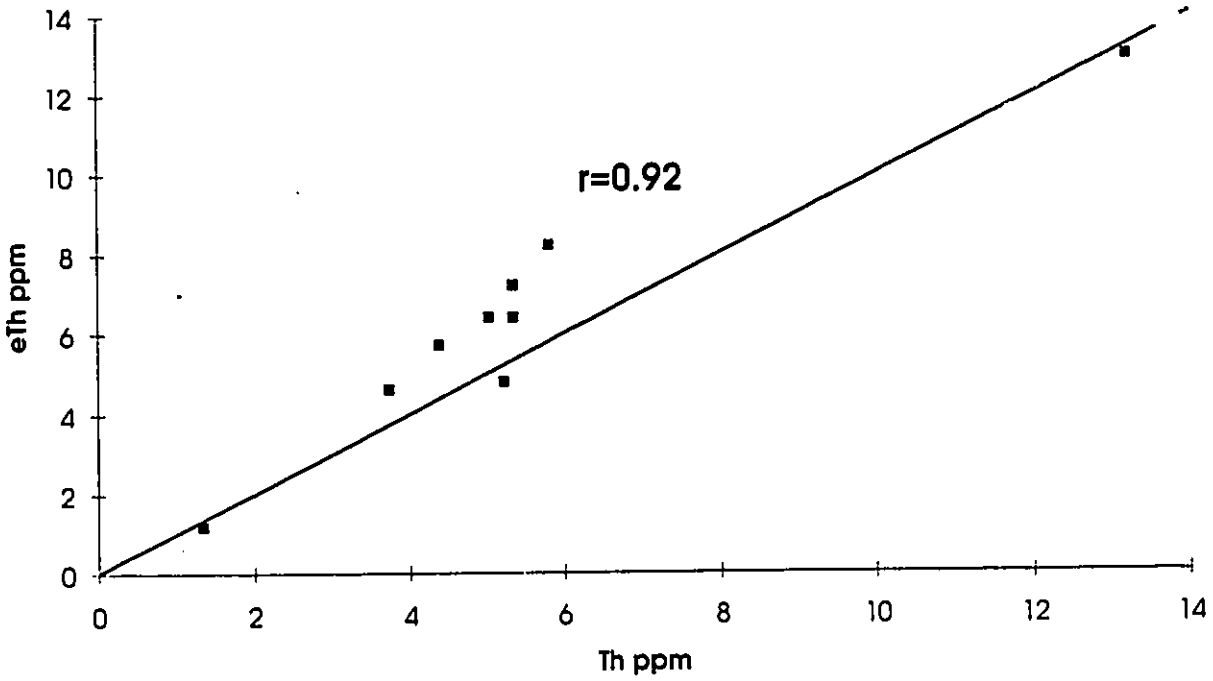
r=0.92
eTh ppm
Th ppm
0
2
4
6
8
10
12
14